THE EFFECT OF RESIDUAL STRESSES ON WELD FATIGUE LIFE

by

J. D. Burk

F. V. Lawrence, Jr.

Department of Metallurgical Engineering

ABSTRACT

In this investigation a model was developed which predicts the influence of residual stress and stress ratio on the total fatigue life of a weld. The total fatigue life of a weld was considered to be composed of both crack initiation and crack propagation. Residual stresses were considered to influence the crack initiation life but not the crack propagation life.

The crack initiation life was estimated by a damage integral method developed from cummulative damage concepts. Actual weld material properties (weld metal and heat affected zone) were considered in the initiation life estimation. Neuber's rule was used to determine the local cyclic stress-strain behavior at the weld toe, and the fatigue notch factor was evaluated using Peterson's equation. Residual stresses were introduced into the analysis as a simulated prestressing of the weld. Cyclic relaxation of the mean stress established during the set-up cycle was modeled by a power function and allowed relaxation to be considered in life estimates.

Fatigue tests of ASTM A514 grade F/E110 and ASTM A36/E60S-3 steel weldments and ASTM 5083-0/5183 aluminum butt welds having tensile and compressive residual stresses were conducted to verify the analytically predicted total fatigue life predictions. Agreement between analytical predictions and experimental results were quite good in most cases. The total fatigue life model was extended to investigate the influence of stress relief and stress ratio on fatigue life for the three different welded material considered.

A Report of the

FRACTURE CONTROL PROGRAM

College of Engineering, University of Illinois
Urbana, Illinois 61801

January 1978

ACKNOWLEDGEMENT

The authors wish to acknowledge the advice and help of Professor JoDean Morrow, Department of Theoretical and Applied Mechanics. Both Professor Morrow and Professor R. A. Yeske, Department of Metallurgy and Mining, kindly allowed the use of their laboratory facilities. The funds for this study were provided mostly by the University of Illinois Fracture Control Program. The portions of the study relating to aluminum were funded by the U. S. Navy - Naval Ship Systems Command under the grant N00024-75-4504.

The authors thank Mr. Ron Zweigoron and Mr. Glen Lafenhagen for their assistance in the operation of testing equipment. The help and assistance of the late Mr. James Sterner during this and many previous studies is gratefully acknowledged.

TABLE OF CONTENTS

LIST OF TABLES

LIST OF FIGURES

LIST OF SYMBOLS

A	Parameter depending on weld geometry (ϕ, θ)
a, a_I, a_{th}	Crack length, initial crack length, threshold crack length
a	Material constant
β	Sign function
C, C_R, m	Crack growth rate material constants
c_f, c_f $(R=0)$, c_f (R)	Crack opening factor, crack opening factor for zero to tension loading, crack opening factor for any stress ratio
D_i, $D_{i,p}$, $D_{i,E}$, $D_{i,m}$	Total, plastic, elastic, and mean stress damage per reversal
$\Delta\varepsilon_p/2$, $\Delta\varepsilon_E/2$, ε_a	Plastic, elastic, and total strain amplitude
ε_{tr}, ε_m, ε_T	Transition, mean, and total strain
ε_p (σ_{max}), ε_p (σ_{min})	Plastic strain range as a function of maximum or minimum stress
$\Delta\varepsilon$, Δe, ε	Local and remote strain range, strain
H_B	Brinnell Hardness or BHN
ΔK	Range in stress intensity
K_{open}, K_{min}	Crack opening and minimum stress intensity factor
ΔK_{eff}, ΔK_{th}	Effective and threshold range in stress intensity factor
K_t, K_ε, K_σ	Theoretical, strain, and stress concentration factors
k	Relaxation exponent
k_ε, k_N	Strain control and Neuber control relaxation exponent

K_f	Fatigue notch factor
$K_{f\ max}$	Maximum fatigue notch factor
K, K'	Monotonic and cyclic strength coefficient
n, n'	Monotonic and cyclic strain hardening exponent
E	Young's modulus
ϵ_f, σ_f	True strain and stress at fracture
ϵ_f', σ_f'	Fatigue ductility and strength coefficients
c, b	Fatigue ductility and strength exponent
$2N_f$, $2N_{tr}$, 2N	Reversals to failure, transition fatigue life, reversals
N, N_I, N_p, N_T	Cycles, initiation, propagation, and total fatigue life
σ_o, S_m	Local and remote mean stress
$\sigma_{o,i}$, $\sigma_{o,2N}$	Initial and current mean stress
ΔS, $\Delta\sigma$	Remote and local stress range
σ_a, σ	Local stress amplitude, local stress
σ_y', S_y	Cyclic and Monotonic yield stress
S_{YBM}	Monotonic yield stress of base metal
S_u	Ultimate strength
σ_r, σ_r^*	Initial and post set-up cycle residual stress at weld toe
R	Stress ratio
r, t, ϕ, θ	Weld toe root radius, weld plate thickness, and edge preparation and flank angle of weld
r_{crit}	Critical value of r corresponding to $K_{f\ max}$

1. INTRODUCTION

1.1 GENERAL

The fatigue resistance of a welded structure is most often controlled by its welds. Welds are complex; and to predict their fatigue resistance,one must consider many variables (1-6): weld geometry; weld defects (porosity, incomplete fusion, incomplete penetration, and slag inclusions); variable weld zone material properties of heat affected zone (HAZ), weld metal (WM), and base metal (BM), and residual stresses.

Residual stresses are often cited as the cause of scatter in fatigue life data and other anomalous aspects of weld fatigue behavior. The influence of weld residual stresses on fatigue life has proven difficult to predict, and economically important questions (such as when to stress relieve, when to give special treatments to the weld, or even which material to select) badly need clarification. This study is an attempt to predict or at least bound the influence of residual stresses on the fatigue life of welds.

1.2 CRACK INITIATION AND PROPAGATION LIFE ESTIMATES

For a weld or any metal component, the fatigue failure process is composed of three periods (7):

1) Crack nucleation.

2) Crack growth on crystallographic planes (Stage I).

3) Crack growth normal to the maximum tensile stress (Stage II).

Unfortunately, no single theory for predicting fatigue life is available. Fatigue life predictions require a model that considers the total fatigue life (N_T) to be composed of the cycles to develop an active Stage II fatigue crack (N_I), and the cycles to propagate that crack to final failure (N_p).

$$N_T = N_I + N_p \tag{1}$$

Concepts based on cummulative fatigue damage and material strain-life properties are used to estimate the initiation life (N_I), while fracture mechanics theory is used to estimate the propagation life (N_p).

Fatigue crack initiation life estimates are based on knowledge of the material fatigue properties and the Palmgren-Miner linear damage summation rule (8, 9). The initiation life (N_I) for a notched member (weldment) may be estimated by knowing the stress-strain response for an element of material at the critical location (weld toe) and by assuming that element has a life identical to that of a smooth specimen of similar material subjected to the same stress-strain history (10). When the total sum of damage for the element of material or smooth specimen exceeds unity, a crack is considered to be present, and the initiation life (N_I) is considered to be over.

$$\sum_{1}^{2N_I} D_i = 1 \tag{2}$$

The damage per reversal (D_i) for the element of material at the notch root is the reciprocal of life of a smooth specimen under the same strain and

mean stress conditions. This initiation life analysis does not specify the size of the element at the critical location in which the crack has initiated and, therefore, does not define the crack length after the end of the estimated N_I portion of life. The assumptions required to overcome this deficiency in the model will be discussed subsequently.

Fatigue crack propagation life (N_p) estimates may be made using the power law suggested by Paris and Erdogan (11) which relates the crack growth rate (da/dN) to the range in stress intensity (ΔK) and the material constants (C and m).

$$\frac{da}{dN} = C\,(\Delta K)^m \tag{3}$$

The cycles required to propagate a crack of initial size (a_I) to a final crack length (a_f) are then:

$$N_p = N_T - N_I = \int_{N_I}^{N_T} dN = \int_{a_I}^{a_f} \frac{da}{C(\Delta K)^m} \tag{4}$$

The propagation life is extremely sensitive to the initial crack length (a_I) but insensitive to the final crack length (a_f) (12). The initial crack length (a_I) is taken as the crack size when the initiation life (N_I) is complete. For welds, the initial crack length may be taken as the length of some pre-existent weld defect; but a_I should not be smaller than the threshold crack size (a_{th}) which may be estimated from the threshold stress intensity factor (ΔK_{th}) and the stress range (ΔS):

$$a_{th} \gtrsim \frac{1}{\pi} \left(\frac{\Delta K_{th}}{\Delta S}\right)^2 \tag{5}$$

When failure originates at a blunt notch (weld toe or porosity), the value of a_I is unclear. One common assumption which enables the estimation of the total fatigue life from propagation theory only is that some small defect, resulting from the fabrication process, exists at the weld toe; however, such a strategy may require a_I to be less than a_{th}, especially at long lives.

1.3 PREVIOUS WORK ON THE INFLUENCE OF RESIDUAL STRESSES ON FATIGUE LIFE AND WELD FATIGUE LIFE ESTIMATES

The influence of residual stress on the fatigue life of mild steel and aluminum butt and fillet welds has been reviewed and summarized by Gurney (1), Munse (2), Pollard and Cover (4), and Kelsey (5). Tensile residual stresses at the weld toe decrease the fatigue resistance of the weld. Stress relief (no residual stresses) was found to improve weld fatigue resistance. Moreover, the improvement in fatigue resistance by stress relief was found to be less effective for short weld lives or more negative stress ratios. No analytical models were proposed which would estimate the fatigue life in a weld or predict residual stress influence.

Subsequently, Harrison (13), Maddox (14), Frank (15), and Zettlemoyer (16) used fracture mechanics concepts to predict the fatigue behavior of mild steel fillet welds. It was hypothesized that welds are fabricated with small, crack-life defects at the weld toe (17). The initiation life was therefore assumed to be short or nonexistent.

However, in studies by Lawrence and Munse (18) and Burk and Lawrence (19), the fatigue life in butt welds with incomplete penetration

(which is a crack-like defect) could not be explained solely by crack propagation, and the initiation life was found to occupy as much as half the total life. Investigations by Lawrence (12) and Burk and Lawrence (20) on ASTM 36 butt welds showed that a significant portion of fatigue life was spent in initiating a 0.01 in. (.25 mm) fatigue crack at the weld toe and that unrealistically small values of a_I below a_{th} would be required, especially in the long life regime, to account for total fatigue life.

Mattos (21) studied the crack initiation life (N_I) of ASTM A36 butt welds and considered the influence of base metal material properties, weld geometry, and residual stress on the fatigue life. The weld geometry was found to have an influence on the initiation life which was similar to the influence of geometry on the propagation life (N_p) in butt or fillet welds (12-16, 20, 21). Also, Mattos found that welds of different materials spent different proportions of their total fatigue life in crack initiation or propagation when an initial crack length (a_I) of 0.01 in. (.25 mm) and base metal properties were assumed. The influence of residual stress on the crack initiation life (N_I) was also considered. Mattos (21) found that residual stresses had no effect on the initiation life of a weld for lives of less than 10^6 cycles. Subsequently, Lomacky et al. (22) and Smith et al. (23) considered the crack initiation and propagation lives in an analysis of butt weld fatigue life.

The crack growth rate constants for Eq. 3 and strain-life fatigue properties of heat affected zone (HAZ) and weld metal (WM) in butt welds have been studied by numerous researchers (24-28). The crack growth rates

for high-strength low alloy and mild steel (24-27) and 5000 series Al-Mg alloy (28) heat affected zone and weld metal materials were found to group in the scatter band for the base metal behavior. Higashida (29) determined the strain-life fatigue properties of heat affected zone (HAZ) and weld metal (WM) in ASTM A36 and A514 grade F steels. The strain-life fatigue properties were found to differ significantly from the base metal properties (29), especially at longer lives (> 10^4 cycles), but were shown to vary systematically with hardness. Relaxation rates of mean stress, an important material property which governs the influence of residual stress on fatigue life (21), was also found to be significantly different from that of the base metal.

1.4 SCOPE

In this study, the model suggested by Mattos (21) for estimating the crack initiation life was extended and applied to estimate the residual stress influence on the fatigue crack initiation life of welds. Both weld material properties and stress ratio effects were considered. The total fatigue life was estimated as a sum of the crack initiation and propagation life.

The crack initiation life for a weld with residual stresses at the weld toe was calculated using cummulative damage concepts and a computer simulation of stress-strain response under Neuber control conditions. Residual stresses were introduced into the simulation as a prestress. The initial mean stress after the second load reversal was estimated along with the stress and strain amplitude at the weld toe. The relaxation

of the mean stress after the second reversal (set-up cycle) was shown to decay according to a power function. Crack initiation life estimates were made by approximating the Palmgren-Miner damage summation rule as an integral and solving for the upper limit of integration.

The crack propagation life was estimated using crack propagation theory. The a_I used in N_p calculations was 0.01 in. (.25 mm). The influence of residual stresses on crack propagation was ignored, but stress ratio effects were taken into account by the crack opening factor (c_f) for a given stress ratio and by modifying the crack growth rate constant C in Eq. 3.

Strain-life fatigue properties of aluminum 5083-0 base and 5183 weld metal (WM) were determined. Cyclic relaxation tests of mean stress behavior under constant amplitude strain control and under Neuber control were also conducted to verify that the relaxation behavior was the same in both cases. Fatigue tests of weldments of A514F/E110, A36/E60S-3 and 5083-0/5183 with tensile and compressive residuals under zero to tension loading were carried out. The results of these tests were compared with predictions.

2. THEORY

2.1 CRACK INITIATION LIFE ESTIMATES

Estimation of the crack initiation life in a weld or notched member subjected to fatigue requires (10):

1) A mechanics analysis that relates the remote and local (weld toe or notch root) stresses and strains.
2) Knowledge of the notch root cyclic stress-strain behavior.
3) The strain-life fatigue properties of the notch root material.
4) A damage summation expression for the material.

Notch Analysis - Local Stresses and Strains

For a elasto-plastic material, Neuber (30) found that the geometric mean of the actual stress (K_σ) and the strain (K_ε) concentration factors are related to the theoretical stress concentration factor (K_t):

$$K_t = (K_\sigma \cdot K_\varepsilon)^{1/2} \tag{6}$$

Topper et al.(10) have shown that Eq. 6 is useful in solving the fatigue notch problem if the fatigue notch factor (K_f) is substituted for K_t and the remote (S, e) and local (σ, ε) stresses and strains are expressed as ranges.

$$K_f = \left(\frac{\Delta\sigma}{\Delta s}\,\frac{\Delta\varepsilon}{\Delta e}\right)^{1/2} \tag{7}$$

When elastic conditions are assumed for the bulk of the weld or notched body away from the critical location (weld toe), then Eq. 7 can be expressed as:

$$\frac{(K_f \Delta S)^2}{E} = \Delta\sigma\Delta\epsilon \qquad (8)$$

For smooth specimens that were forced to undergo the stress-strain behavior imposed by Eq. 8, Topper et al (10) found that the fatigue life of the smooth specimen may be used to estimate the initiation life of the notched specimen.

The fatigue notch factor (K_f) is defined as the ratio of the fatigue strength at long life of notched and unnotched specimens. The fatigue notch factor may be estimated by an empirical relationship known as Peterson's equation (31):

$$K_f = 1 + \frac{K_t - 1}{1 + a/r} \qquad (9)$$

where K_t is the theoretical stress concentration factor, r the notch root radius (weld toe) and a is a material parameter which for steels may be estimated based on the ultimate strength of the material (S_u) (32):

$$a = 0.001 \left(\frac{300 \text{ ksi}}{S_u}\right)^{1.8} \text{(in.)} \qquad (10)$$

Values of "a" for aluminums range between 0.002 in. (.51 mm) and 0.02 in. (5.1 mm) depending on the alloy and finishing treatments (32). The theoretical stress concentration (K_t) for welds has been shown to be a function of the external macro- and micro-geometry (21) and may be described by an equation of the form:

$$K_t = 1 + A\sqrt{t/r} \qquad (11)$$

Figures 1 and 2 show results of finite element analyses of butt welds (21) to determine K_t as a function of t/r. From the figures, it can be seen that Eq. 11 fits the results well. Similarly, both K_t and K_f are a function of r and t for the weld toe or any other notches in a weld (porosity or incomplete penetration). It can be shown (21,29) from Eq. 11 that K_f goes through a maximum ($K_{f\ max}$) when r is equal to "a" as shown schematically in Fig. 3.

$$K_{f\ max} = 1 + \frac{A}{2}\sqrt{t/a}, \text{ at } r = a \tag{12}$$

Since $K_{f\ max}$ depends on the Peterson "a" value, $K_{f\ max}$ will be a function of material and weld geometry.

Fatigue and Cyclic Stress-Strain Properties

The smooth specimen fatigue behavior of a metal under reversed strain control is characterized by four material parameters that relates the strain amplitude to the failure life (33,34).

$$\varepsilon_a = \varepsilon_f' (2N_f)^c + \frac{\sigma_f'}{E} (2N_f)^b \tag{13}$$

In the presence of a mean stress (σ_o) Eq. 13 may be corrected (32) to give:

$$\varepsilon_a = \varepsilon_f' (2N_f)^c + \frac{(\sigma_f' - \sigma_o)}{E} (2N_f)^b \tag{14}$$

where ε_f' and c are the fatigue ductility coefficient and exponent, and σ_f' and b are the fatigue strength coefficient and exponent. The failure

$$D_{i,m} = \left(\frac{\sigma_f' - \sigma_o}{\sigma_a}\right)^{\frac{-1}{b}} \quad (21)$$

In Eq. 21 the mean stress is considered to remain constant during cycling.

2.2 CRACK INITIATION LIFE OF A WELD WITH RESIDUAL STRESSES

Residual stresses from the welding process may be treated as a mechanical prestressing as suggested by Morrow et al. (39, 40) and applied by Mattos (21), Lomacky et al. (22) and Smith et al. (23). The residual stress acting in a transverse direction on an element of material at the weld toe for a butt weld may be assumed to be equal to the yield strength of the base metal.

$$\sigma_r = S_{YBM} \quad (22)$$

This assumption is suggested by a numerical analysis of the problem by Friedman (41) and the fact that the HAZ and WM (which are often of higher strength than the base metal) cannot be subjected to residual stresses higher than S_{YBM}.

The residual stress at the weld toe may be simulated as shown in Fig. 4. A remote stress of σ_r/K_f is then applied to produce a local stress equal to the residual stress (σ_r) from welding. The normally applied remote stress range (ΔS) is then added to give $\Delta S + \sigma_r/K_f$ which is equivalent to the remote stress range (ΔS) in Eq. 8. The local and remote stress-strain behavior then may be bounded by Neuber's Rule (Eq. 8) as shown in Fig. 4. The first reversal (O-A) is bounded by:

$$(K_f \frac{\Delta S}{1-R} + \sigma_r)^2/E = \Delta\sigma\Delta\varepsilon \quad (23)$$

and the subsequent reversals are bounded by:

$$(K_f \Delta S)^2/E = \Delta\sigma\Delta\varepsilon \quad (24)$$

For constant amplitude situations (neglecting hardening or softening and mean stress relaxation), the first few reversals set up an initial mean stress ($\sigma_{o,i}$) and a stress and strain amplitude. The first two reversals for the set-up cycle (O-A-B) in Fig. 5 establish a residual stress (σ_r*) at point B which is different in sign and magnitude than the initial residual stress (σ_r). Compressive residuals may be simulated as an overload followed by remote stress cycling. To simulate compressive residual stresses, the weld as shown in Fig. 5 is loaded from (O-A-B) for a ΔS such that at B the local stress is equal to the desired residual stress of $\sigma_r = -S_{YBM}$. The set-up cycle and resulting mean stress (σ_o) and stress amplitude (σ_a) are then established by the patch (B-C-D) for subsequent remote loading.

The crack initiation life of a butt weld with residual stress at the weld toe depends on the stress amplitude and the mean stress. The mean stress has been shown to relax according to the following power function for constant strain amplitude tests (21, 29, 42).

$$\sigma_{o,2N} = \sigma_{o,i} (2N-1)^k \quad (25)$$

life ($2N_f$) is given in reversals (2 reversals = 1 cycle). Typical values of the fatigue properties in Eq. 13 for various materials and their definitions are given in the literature (35). An additional useful index of fatigue resistance is the transition fatigue life ($2N_{tr}$). The transition fatigue life ($2N_{tr}$) is the life of a smooth specimen under strain control at which the elastic ($\Delta\varepsilon_E/2$) and plastic ($\Delta\varepsilon_p/2$) strain amplitudes are identical.

$$2N_{tr} = \left(\frac{\varepsilon_f' E}{\sigma_f'}\right)^{\frac{1}{b-c}} \tag{15}$$

The monotonic and cyclic stress-strain properties of a material may be partitioned into elastic and plastic strain components expressed as:

Monotonic

$$\varepsilon = \frac{\sigma}{E} + \left(\frac{\sigma}{K}\right)^{\frac{1}{n}} \tag{16}$$

Cyclic

$$\varepsilon_a = \frac{\sigma_a}{E} + \left(\frac{\sigma_a}{K'}\right)^{\frac{1}{n'}} \tag{17}$$

where K and n are the monotonic or cyclic strength coefficient and exponent. The monotonic and cyclic responses in Eqs. 16 and 17 are not usually the same. Typical values for numerous materials are listed in the literature (35).

Cummulative Damage Analysis

Fatigue crack initiation life calculations are based on the rule of linear damage summation (Eq. 1). The damage per reverals (D_i) may be expressed in terms of the material fatigue properties and either the stress or strain amplitudes:

$$D_{i,e} = \left(\frac{\sigma_a}{\sigma'_f}\right)^{-1/b} \qquad \text{(stress)} \qquad (18)$$

or

$$D_{i,p} = \left(\frac{\varepsilon_a}{\varepsilon'_f}\right)^{-1/c} \qquad \text{(plastic strain)} \qquad (19)$$

The damage due to the mean stress (σ_o) then may be estimated (36) by:

$$D_{i,o} = \varepsilon'_f{}^{1/c} \left(\frac{\sigma_a}{K}\right)^{-1/n'c} \left[\left(1 - \frac{\sigma_o}{\sigma_f}\right)^{1/n'c} - 1\right] \qquad (20)$$

Equations 1 and 18-20 prove very valuable in the computer simulation models for determining the stress-strain response and calculating damage (36, 37). In the simple case of constant load history, the damage (for longer life and strains that are predominantly elastic) is given by modifying Eq. 18 to also consider mean stress (σ_o) damage as suggested by Morrow (32).

From Eq. 25 the mean stress at any reversal ($\sigma_{o,2N}$) is given by the initial mean stress ($\sigma_{o,i}$) as a function of the reversals (2N-1). The relaxation exponent (k) is dependent on the strain amplitude (σ_a). Given the strain and stress amplitudes, and the initial mean stress ($\sigma_{o,i}$), then the crack initiation life may be estimated by combining Eqs. 1, 21 and 25 to give:

$$\sum_{1}^{2N_I} \left\{\frac{\sigma_f' - \sigma_{o,2N}\,(2N-1)^k}{\sigma_a}\right\}^{-1/b} = 1 \qquad (26)$$

For long lives, the sum of Eq. 26 may be approximated as an integral with little error for lives in excess of the transition fatigue life ($2N_{tr}$).

$$\int_{1}^{N_I} \frac{1}{2} \left\{\frac{\sigma_f' - \sigma_{o,i}\,(2N-1)^k}{\sigma_a}\right\}^{-1/b} dN = 1 \qquad (27)$$

The upper limit of integration (N_I) may be determined by expansion of the integral in a power series, integrating, and solving numerically for N_I. The initial mean stress ($\sigma_{o,i}$) with appropriate residual stresses is estimated by a set-up cycle from a rheological simulation (21, 36, 37) of the first loading reversals. The stress amplitude is then computed based on the Neuber parameter (Eq. 8) using stabilized cyclic stress-strain response. The value of k is determined by the stabilized strain amplitude after the material hardens or softens. Equation 27 considers only the effect of mean stress relaxation. The influences of hardening or softening on $\sigma_{o,2N}$ was found to be small and therefore neglected. A typical life prediction for an A36 butt weld which will be discussed more fully in subsequent sections is shown in Fig. 7 with upper and lower bounding curves.

2.3 CRACK PROPAGATION LIFE FOR A WELD

The fatigue crack propagation life (N_p) for a butt weld can be estimated by using the Paris power law (Eq. 3). The stress intensity factor for a butt weld with remote axial or bending stress has been determined and is expressed as:

$$\Delta K = \Delta S \sqrt{\pi a}\, f\,(a/t, \phi, \theta) \tag{28}$$

The function, $f\,(a/t, \phi, \theta)$, appearing in Eq. 28 is a correction factor for weld geometry and thickness (12, 20). The influence of stress ratio on crack growth rate (Eq. 3) can be accounted for by expressing the range in stress intensity as an effective stress intensity factor (ΔK_{eff}) as (38, 43-45):

$$\Delta K_{eff} = c_f\, \Delta K \tag{28a}$$

where c_f is the cracking open factor and is expressed as:

$$c_f = \frac{\Delta K - \Delta K_{open}}{\Delta K} \tag{29}$$

when $\Delta K_{open} > \Delta K_{min}$. If $\Delta K_{open} < \Delta K_{min}$ then $c_f = 1$. The crack growth rate constant C must be modified (38) in Eq. 3 as:

$$C_R = C\,[c_f(R)/c_f(R=0)]^m \tag{30}$$

where $c_f(R=0)$ is the crack opening factor for R=0 loading and $c_f(R)$ is the crack opening factor for any stress ratio. Equation 3 then becomes:

$$\frac{da}{dN} = C_R(\Delta K)^m \tag{31}$$

Equation 31 takes into account stress ratio or mean stress effects. Approximate trends of c_f with R for several materials are shown in Fig. 8. (Based on the analytical results of Socie (38), crack opening factor may be a function of geometry as well as load and material.)

2.4 THE TOTAL LIFE MODEL

The total fatigue life of a butt weld containing residual stresses was estimated based on the partitioning of the crack initiation (N_I) and crack propagation life (N_p) as given by Eq. 1. Residual stresses were considered to influence only the crack initiation life (N_I) and were accounted for by a set-up cycle model that produced an initial mean stress which then relaxed with cycling according to Eq. 25. The initiation life was estimated based on the damage integral given in Eq. 27, which allowed the damage during cycling to vary as the mean stress relaxed. Cyclic hardening or softening influence on mean stress was ignored in the calculations. The crack propagation life was estimated using Eq. 4 and assumed a_I = 0.01 in. (.25 mm). Residual stresses were assumed to be approximately equal to the monotonic yield stress (S_{YBM}) of the base metal (Eq. 22).

3. EXPERIMENTAL PROCEDURES

3.1 MATERIAL CHARACTERIZATION OF ASTM 5083-O ALUMINUM AND ASTM 5183 WELD METAL

Measurement of strain-life fatigue properties for the weld microstructures of A36 and A514 F welds was carried out by Higashida (29). However, the strain-life fatigue properties of the 5083-O base and 5183 filler metal were not available.

Base and Weld Metal Specimens

Base metal specimens of 5083-O aluminum were machined from 1-in. (25.4 mm) thick plate with the axis parallel to the plate rolling direction. After machining, all specimens were polished using successively finer grades of emery paper to the final dimensions shown in Fig. 9.

Weld metal specimens were machined from a single pass of deposited weld metal from a 1-in. (25.4-mm) aluminum butt weld. Hourglass-shaped, smooth-specimens were used since the amount of deposited weld metal limited the gage section of the specimen. Radiographs were made of the deposited weld metal to allow for the selection of a defect free specimen. All specimens were taken transverse to the welding axis. Final dimensions of the specimens after mechanical polishing with emery paper are given in Fig. 9. An additional weld metal specimen was machined with its axis parallel to the welding axis for monotonic tension tests.

Monotonic Tension and Fatigue Tests

Monotonic tension tests of base and filler metal specimens were conducted using a 20,000 lb (89 kN) MTS hydraulic test system similar to that described by Feltner and Mitchell (45). A 0.5 in. (12.7 mm) gage length clip-on extensometer was used for both base and weld metal specimens to measure and control strain prior to necking; thereafter, stroke was controlled to failure.

Fatigue tests of the base metal (5083-0) and filler metal (5183) were conducted under strain control using the same equipment employed for monotonic tension tests. A sine-wave function generator was employed to control the strain signal and the test frequencies varied from 0.1 to 20 Hz. Stress-strain hysteresis loops were recorded at logarithmically spaced intervals. Strains were measured for the base metal (5083-0) tests using the same extensometer as in the monotonic tension tests. Weld metal specimens were hourglass in shape and required an analog computer to convert diametrical to axial strain (29). Axial strain control was thus achieved.

Cyclic tests of weld metal (5183) specimens were conducted under strain control, employing various strain amplitudes at constant mean strain, to study mean stress relaxation effects for the 5183 material. Prior to testing, the material was cyclically stabilized to eliminate cyclic hardening interactions with the mean stress relaxation response. Mean stress relaxation data were obtained by straining the material to a predetermined mean strain and then recorded at logarithmic intervals as the mean stress relaxed. After the mean stress relaxed or if the test lasted 10^3 - 10^4 reversals, the

stress and strain were returned to zero. A stabilizing, mean-stress washout-block was then employed which allowed further mean stress relaxation testing with the same specimen. The block strain history used is shown in Fig. 10.

3.2 NEUBER CONTROL TESTS OF A36 WELD HEAT AFFECTED ZONE (HAZ) AND 5183 WELD METAL (WM)

Neuber control tests of A36 HAZ material and 5183 WM were run to confirm that the behavior of residual stresses and resulting mean stress relaxation behavior could be described by Eq. 25. Tests were conducted on A36 HAZ specimens both in the uncycled (virgin) state and in the cyclically stabilized condition. A single test of uncycled (virgin) 5183 WM material was made.

Specimen Preparation

Simulated A36 weld HAZ specimens were produced from ASTM A36 base metal (chemical composition in Table 1) using the resistance heating technique described by Higashida (29). All specimens underwent the thermal history measured at the weld toe for a single pass A36 weld having a heat input of 1.20 kJ/mm. After thermal simulation, specimens were machined and mechanically polished to the dimensions in Fig. 9. The 5183 WM specimens used were the same as shown in Fig. 9 for the fatigue testing.

Neuber Testing

A 20,000 lb (89 kN) computer controlled MTS hydraulic testing apparatus was used for testing. The computer controlled apparatus was required to control the product of local (notch root) stress and strain ($\Delta\sigma\Delta\varepsilon$), i.e. where $\Delta\sigma\Delta\varepsilon = K_f^2\,\Delta S\Delta e$ (the Neuber parameter) during a reversal. Strain was measured using a 0.3 in. (7.6 mm) gage length extensometer. Further details of the apparatus and methods are described by Donaldson et al.(47).

Specimens were tested both in the virgin and cyclically stabilized state (similar to the prior treatment given a material before mean stress relaxation tests under strain control). Control limits given by the Neuber parameter were computed for a given nominal stress range and a tensile residual stress of 35 ksi (240 MPa). The value of K_f was assumed to be 2 for convenience in calculations. A constant strain rate of 0.0010 per second was used to maximize testing speed, while remaining within computational response limits imposed by the computer and analog/digital converter. Tests were limited to 5,000 to 10,000 reversals because of frequent machine failure after 24 to 48 hours of continuous operation. Cyclic hysteresis loops were periodically plotted, and the stress and strain amplitudes and means were computed and recorded.

3.3 WELD PREPARATION AND FATIGUE TESTING

Weld Test Specimens

Butt weld fatigue specimens were machined from weldments of A36, A514 F and 5183 materials. The gas metal arc (GMA) process and Linde 82

(AWS E60S-3), Mureloy 110 (AWS E110) and AWS 5183 electrodes were used to weld the respective plates. The aluminum 5083-0/5183 welds were fabricated as double-vee butt welds. The A36 and A514 F weldments were made by simply depositing a weld bead on the appropriate steel plate after mill scale removal (i.e. bead on plate). Chemical composition of the base and filler metals and the welding parameters employed are given in Tables 1 and 2. All specimens were sawed out in strips from the welded plates and then machined to a reduced section of the dimensions shown in Fig. 11.

TIG Dressing

Several of the A514 F weldments were TIG dressed to explore the effect of weld toe geometry modification on the fatigue life. The process involved the remelting of the weld metal at the toe thus producing a more generous weld toe radius. The welding parameters are listed in Table 2.

Tensile Preloading - Generation of Compressive Residual Stresses

All weldments test specimens were presumed initially to contain tensile residual stresses at the weld toe equal to the base metal monotonic yield strength (41). To verify by experiment the fatigue life predictions made for welds with initial compressive residuals, it was necessary to induce a compressive residual in the material at the weld toe. Compressive yield stresses at the weld toe in the welded specimens can be produced by shot peening or tensile preloading. Tensile preloading was used for most weld specimens because it produced the least amount of change or damage to the material located at the weld toe.

The tensile preloading causes a compressive residual by the following mechanism. First due to the stress concentration, loading the specimen to below the yield stress of the net section causes the material at the weld toe to become plastic and undergo large non-recoverable strains. The material becomes permanently stretched while the total section remains elastic. Then, upon unloading, the material becomes compressed as the specimen returns to its original shape (or nearly so) as the load is returned to zero. The weld toe then contains a compressive residual stress roughly equal to the base metal monotonic yield stress (see Fig. 6).

Both A36 and A514 welds were loaded to slightly less than the monotonic yield strength of the base metal (36 ksi (250 MPa) and 118 ksi (815 MPa)). To verify that the weld remained elastic away from the weld toe, two strain gages were fixed to the specimen in the reduced section and load strain plots made during the preloading.

Fatigue Testing

All specimens were fatigue tested to failure under load control using a haversine wave form (R=0) in a MTS 50,000 or 100,000 lbs (220 or 440 kN) hydraulic testing apparatus described by Burk and Lawrence (20). Tests were conducted under ambient laboratory conditions (22°C, 50 percent RH) at frequencies ranging from 3 to 15 Hz. Nominal stress ranges were selected on the basis of prior fatigue life predictions made using the theories and concepts discussed previously. The stresses were chosen to produce fatigue lives in the 10^4 - 10^7 cycles life range.

4. RESULTS

4.1 PROPERTIES OF ASTM 5083-0 AND 5183 ALUMINUM BASE AND WELD METAL

Monotonic and Cyclic Stress-Strain Behavior

The monotonic and cyclic stress-strain properties for both the 5083-0 base and 5183 weld metals are listed in Tables 3 and 4, respectively. Monotonic and cyclic stress-strain and fatigue properties are listed in Tables 5 through 8 for the A514 and A36 weld materials (29). The monotonic and cyclic true stress-strain response are reproduced in Fig. 12. Comparison of the monotonic response of the base and weld metals shows that the two materials are almost identical. The 5183 weld metal appears to be only slightly stronger and more ductile. Hardness measurements (Table 3) of both materials also would indicate similar mechanical strengths and behavior.

The cyclic stress-strain curves of the two materials (see Fig. 12) are similar in shape, but the weld metal has greater strength and a higher cyclic yield stress than the 5083-0 base metal. Both materials obviously cyclically harden and exhibit extremely large increases in the yield stress and stress amplitude (approximately a factor of 2). The variation of stress amplitude with reversals (at constant reversed strain amplitude) is shown for both materials in Figs. 13 and 14. The hardening response of both the 5083-0 base metal and 5183 weld metal is quite rapid. Both materials seem to cyclically stabilize after 10^3 reversals.

Fatigue Behavior

The results of the strain controlled fatigue tests for the 5083-0 and 5183 base and weld metals are summarized in Table 9. The fatigue strength coefficient (σ_f') and exponent (b) and the fatigue ductility coefficient (ε_f') and exponent (c) were calculated by a least squares fit to the elastic or plastic strain-life results. Figures 15 and 16 show the resulting total strain-life plot for 5083-0 and 5183 materials. Extrapolation of the elastic and plastic strain-life curves gives intercepts above the measured monotonic values (ε_f', σ_f'/E). This difference is due to the large amount of cyclic hardening that occurs for both materials. Comparison of the total strain-life curves for 5083-0 and 5183 in Fig. 17 shows that the 5083-0 base metal has a greater fatigue resistance at short and intermediate lives (10^1 - 10^5) and is similar to 5183 at longer lives ($> 10^5$) even though the hardness of 5083-0 and 5183 are the same and the 5183 weld metal is superior in strength. Additionally, the transition fatigue life ($2N_{tr}$) of the 5183 WM is less than the $2N_{tr}$ of 5083-0 (205 versus 640) yet the materials exhibit a similar resistance at long lives. This result is in contrast to the behavior observed for steels.

Cyclic Mean Stress Relaxation

Figure 18 shows the results for tests conducted on 5183 WM at a constant value of mean strain (ε_m = 0.003) and variable strain amplitudes. The results were plotted by normalizing the mean stress at any reversal ($\sigma_{0,2N}$) by the initial mean stress ($\sigma_{0,i}$) to fit the power function (Eq. 25)

discussed earlier. Test results were then curve-fit to obtain k, the mean stress relaxation exponent for a given test at a constant strain amplitude. The more negative k is the more rapidly the mean stress diminishes with reversals (2N-1). From Fig. 19 it can be seen that the relaxation exponent (k) varies parabolically with the strain amplitude for the amplitude considered. Additionally, the data show that at strains which are less than the strain at the cyclic yield stress of the material that there is an appreciable amount of mean stress relaxation below the proportional limit (see Fig. 19). The strain amplitude at which no relaxation would occur (k = 0) is approximately $\sigma_y'/2E$ or corresponds to half the cyclic yield stress and proportional limit of the material.

4.2 NEUBER CONTROL TESTS OF A36 HAZ AND 5183 WM SMOOTH SPECIMENS

Test results of the mean stress relaxation behavior under Neuber control with a simulated tensile residual of 35 ksi (242 MPa) and 18 ksi (125 MPa) for A36 HAZ and 5183 WM smooth specimens are summarized in Table 10 and plotted in Figs. 20 through 25. A typical stress-strain response for a test (A36 HAZ 107-1) is shown in Fig. 20. The Neuber parameter $(K_f \Delta S)^2/E$ for all tests was calculated for a K_f of 2 and zero to tension (R=0) remote loading. Computer simulation of the smooth specimen response was carried out to predict the initial mean stress ($\sigma_{o,i}$) for the set-up cycle discussed previously. Predicted and experimental results are listed in Table 10 and plotted in Figs. 21 and 22 for A36 HAZ and 5183 WM.

The relaxation behavior of virgin, uncycled A36 HAZ and 5183 WM smooth specimens is shown in Figs. 23 and 24. The normalized mean stress ($\sigma_{o,2N}/\sigma_{o,i}$) for the first group of three tests can be described by the power function as shown in Fig. 23. Values of the relaxation exponent for a Neuber control test (k_N) correspond very favorably for these tests with the relaxation exponent k_ε given by the strain amplitude ε_a for strain control relaxation data (k_ε). The two relaxation exponents, k_N and k_ε are listed in Table 10.

The relaxation behavior of normalized mean stress ($\sigma_{o,2N}/\sigma_{o,i}$) for the second group of uncycled, virgin A36 HAZ material under Neuber control shown in Fig. 24 shows a nonlinear behavior of the data in contrast to the first group shown in Fig. 23. In Fig. 24 the expected curves based on the power function (Eq. 25) are shown in the figure for the relaxation exponents that correspond to the strain amplitude for strain control relaxation data (k_ε). The data in Fig. 24 conform to the linear curve for the first few hundred reversals but then deviate from the power function.

The Neuber control tests of cyclically stabilized A36 HAZ material in Fig. 25 show an excellent agreement with the assumed power function (Eq. 25) for normalized mean stress relaxation behavior. Best fit lines were computed and the relaxation exponents (k_N) calculated for each test. Comparison of k_ε with the k_N in Table 10 shows an excellent agreement in the relaxation exponents.

4.3 FATIGUE LIFE OF WELDMENTS WITH TENSILE AND COMPRESSIVE RESIDUAL STRESSES

Fatigue lives of A514F/E110, A36/E60S-3, and 5083-0/5183 weldments were estimated by the model discussed previously. Values of $K_{f\ max}$ were computed based on weld geometry (Eq. 12) and are listed in Table 11. The crack propagation lives (N_p) for the butt welds were predicted using Eqs. 4 and 28. Crack growth rate constants for the A514 HAZ, A36 HAZ, and 5183 WM were assumed to be the same as A514, A36, and 5083-0 base metals which are reported by Pary et al. (24), Barsom (48), and Nordmark (49) and are listed in Table 12 along with the material constant "a" used in Peterson's equation for the materials.

ASTM A514F/E110 Bead on Plate Weldments

Results for the fatigue tests of the A514F weldments are listed in Table 13 and plotted in Fig. 26, which show that there is a factor of four difference in life for welds with tensile (σ_r = 120 ksi (830 MPa)) and compressive (σ_r = -120 ksi (-830 MPa)) residual stresses at the weld toe for a 55 ksi (380 MPa) remote stress range. For the same life (400,000 cycles), the data show that the stress range may be increased 60 percent for welds with compressive residuals instead of tensile residuals at the weld toe. The use of TIG dressing process at the weld toe and induced compressive residuals definitely improves the fatigue resistance of the weldments at 10^5 cycles as shown in Fig. 26.

Predicted total life curves, based on the sum of the calculated initiation and propagation lives are shown with the experimental data in Fig. 26. There was a surprisingly good correlation between the predicted and experimental values. The curves were calculated prior to the mechanical tests. Material properties used in the initiation calculations were those determined for heat affected zone material (A514F HAZ) listed in Tables 5, 6, and 11. The $K_{f\ max}$ value is given in Table 12. After failure, the crack initiation site was confirmed as being in HAZ at the weld toe using optical microscopy.

Prediction of the fatigue life for the TIG dressed weldments was not as good, being non-conservative by a factor of four in life for TIG weldments with tensile residual stresses and 100 for compressive residual stresses. The discrepancy between the experimental data and predicted result could result from a modification of material properties at the weld toe by the additional heat input of the TIG dressing or an incorrect value of K_f which was calculated (Table 12) as 1.42 based on the TIG dressed notch root radius of 0.2 in. (5 mm). Moreover, an examination of the fracture surfaces revealed that crack initiation was found to be from a crater crack for three of the welds caused by stopping and starting the torch during TIG dressing. The fourth TIG dressed weld fracture surface revealed that the crack had initiated from a surface worm-hole porosity.

ASTM A36/E60S-3 Bead On Plate Weldments

Fatigue test results for the A36 weldments are recorded in Table 14 and shown in Fig. 27. The data show a much larger amount of

scatter than for the A514 weldments. From the results, it is apparent that compressive residuals at the weld toe increase the life by a factor of 2 to 4 at a stress range of 30 ksi (208 MPa). The large amount of scatter in the data for welds with compressive residuals at the weld toe is thought to result from the two methods employed to induce the residual stresses as discussed in Section 3. Due to the maximum value of K_f being 2.51 and the maximum possible applied remote stress being 36 ksi (248 MPa), a compressive residual stress of only -20 ksi (-138 MPa) could be induced by overloading. The other weldments with compressive residuals were hammer peened which caused some work hardening and weld toe radius modification of the material where crack initiation occured. Residuals for peened welds were assumed to be -35 ksi (-242 MPa).

Prediction of total life was made for the A36 weldments with tensile and compressive residuals prior to testing. Crack initiation was assumed to occur in A36 HAZ material at the weld toe and the fatigue properties used to calculate life are listed in Tables 7, 8, and 11. The assumed failure location was verified by optical microscopy of the failed sections. The predictions and the experimental results were found to be in good agreement for A36 weldments with tensile residual stresses as shown in Fig. 27. Calculations of total life (N_T) were made for compressive residual stresses at the weld toe of both full -35 ksi (-242 MPa) and partial -20 ksi (-135 MPa) residual stresses.

Aluminum 5083-O/5183 Butt Welds

Test results for the aluminum 5083-O butt welds are tabulated in Tables 15 and 16 and shown in Figs. 28 and 29. A comparison of the data in both figures shows that a large amount of scatter is associated with the results for both weld thicknesses. The scatter is thought to be associated with variations in weld bead shape from specimen to specimen and resulting $K_{f\ max}$ value variations due to weld geometry (ϕ, θ) fluctuations: see Tables 15 and 16. All welds were fabricated as double-vee butt welds, causing possible compressive as well as tensile residuals at the weld toe. (Residual stress at the weld toe was estimated by x-ray diffraction techniques for one weld and found to be 15 ksi (104 MPa) on one side at the weld toe and -11 (-76 MPa) on the other.) The welds were all assumed to contain tensile residuals of 18 ksi (125 MPa), at the failure location. Tests with compressive residuals were not performed. Previous work by Hill (50) and Nordmark (51) and analytical predictions made prior to any testing of welds with initial compressive residuals which suggested that they would have little influence on total life.

Predictions using material properties given in Tables 3, 4, and 11 were made for the total life of the 5083-O/5183 butt welds for both tensile and compressive residuals of 18 ksi (125 MPa) and -18 ksi (-125 MPa) and are shown in Figs. 28 and 29. Agreement in both cases seems good when considering the relative amounts of scatter. The predictions indicate that residual stresses influence life at lives in excess of 10^6 cycles, but neither sign nor magnitude have much influence at shorter fatigue lives.

4.4 COMPARISON OF PREDICTED BEHAVIOR WITH PUBLISHED DATA

Crack Initiation Life for A36 Butt Welds

Predictions of crack initiation life for A36/E60S-3 butt welds for which the crack initiation life was measured (defined as the cycles required to initiate a 0.010 in. (.25 mm) crack) were made based on the previous work of Burk and Lawrence (20). Welds of two thicknesses, 3/8 in. (10 mm) and 5/8 in. (16 mm), were considered with the corresponding values of $K_{f\ max}$ being 2.19 and 2.51 (Table 12). Both full tensile residual and no residual stress were considered and should bound the data. A comparison of the predictions and the data is shown in Figs. 30 and 31. The data agrees with the predicted curve with tensile residual stresses. This agreement would be expected since the as-weld condition of the butt welds would suggest the existance of full tensile residuals (41). Also, the data in Fig. 31 for the 3/8 in. (10 mm) butt welds seem to exhibit the curvature suggested by the predicted line of the 10^5 - 10^6 cycles region.

Canadian CSA G40.1/E7018 Mild Steel Butt Welds

Smith et al. (23) conducted tests on mild steel butt welds for completely reversed cycling (R=-1) and cycling about a 10 ksi (69 MPa) remotely applied mean stress. In the study, the researchers reported a K_f value for the butt weld of 1.45 determined from the actual test data for fully reversed loading. Analysis was made of the weld geometry of actual failed sections to calculate $K_{f\ max}$ for the weld. A value of 2.10 (Table 12)

was calculated and a prediction of crack initiation life was then made for the butt welds under fully reversed conditions. A comparison of the prediction of N_I and N_p using A36 HAZ properties given in Tables 7, 8, and 11 to the experimental results of Smith et al. (23) is shown in Fig. 32 and indicates an over-prediction in life by a factor of 3 to 4 (at 10^5 - 10^6 cycles).

5. DISCUSSION

5.1 OBSERVATIONS ON THE USE OF THE TOTAL LIFE MODEL

The total life model applied in this study was found to predict accurately the fatigue behavior of butt welds with residual stresses for most of the cases considered. Two rather basic and major assumptions were made in the total life model: (1) the initial crack length at the end of the crack initiation life was assumed to be 0.01 in. (.25 mm) and (2) the crack propagation portion of fatigue life was considered to not be affected by residual stress distributions. These assumptions were made for lack of better approximations.

Theoretical work being conducted by Chen (52) based on a damage rate model proposed by Socie (53) indicates that a_I is in the range of 0.01 in. (.25 mm) for plates of aluminum and mild steel with holes as crack initiation sites.

The assumption that residual stresses from welding do not influence the crack propagation life is justifiable because of the redistribution of the residual stresses after cyclic, notch-root yielding or due to the presence of a crack at the weld toe. Moreover, the crack propagation life is an important portion of total fatigue life only for the higher stress ranges or more positive stress ratios which cause larger amounts of plasticity at the notch root and a considerable redistribution of residual stresses during cycling.

Another aspect of the total life model which should be discussed is the application of Neuber's Rule (Eq. 23 and 24) which assumes that the

notched body (weld) remains mostly elastic. For the A36/E60S-3 butt welds considered, the weld metal and heat affected zone properties greatly overmatched the base metal which causes general yielding of the weld net-section at higher stress ranges and ratios. The application of Neuber's Rule was assumed valid in these instances, and it was assumed that the undermatched base metal would simply work harden and thereafter respond elastically to the remote loading.

The mean stress relaxation behavior was successfully modeled by a power function (Eq. 25) which was shown to be valid for most mean stress relaxation tests under Neuber control conditions. Those few tests of A36 HAZ material which did not conform to the power function, shown in Fig. 24, occurred for A36 HAZ material tests in which the strain amplitudes were between 0.0026 and 0.0030. These amplitudes correspond to short crack initiation lives between 20,000 and 60,000 cycles--a life regime for A36/E60S-3 butt welds in which mean stress has little influence on crack initiation life.

Fatigue crack initiation life predictions using Eq. 27 were found to be sensitive to the relationship between the relaxation exponent (k) and the strain amplitude (ε_a) for the A36 HAZ. The behavior of the relaxation exponent (k) with strain amplitude (ε_a) for A514, A36, and 5083-O weld materials is shown in Fig. 33. The relationship between k and ε_a for the A514 and 5083-O weld materials rises smoothly from zero with increasing the strain amplitude, while those of the A36 weld materials rise abruptly from zero with increasing the strain amplitude. The abrupt rise is probably an artifact resulting from limited data in the low k region near the

proportional limit (σ'_y/E). If an abrupt rise is assumed for the k versus ε_a relationship (see Fig. 34 curve A), then Eq. 27 predicts a crack initiation life curve that becomes multi-valued as shown in Fig. 34, curve A. However, if a smooth rise is assumed (see Fig. 34, curve B) which is suggested by the data shown, then the predicted life (Fig. 34, curve B) results which conforms to the expected behavior. The smooth rise of curve B, however, requires that the mean stress relaxation exponent be non-zero for strains below the proportional limit of the cyclic stress-strain curve (σ'_y/E). This condition would contradict the finding of Martin (36) and Mitchell and Wetzel (54) who found no relaxation to occur below the cyclic yield stress (σ'_y). This point will be discussed subsequently.

5.2 THE INFLUENCE OF RESIDUAL STRESSES ON WELDS OF DIFFERENT MATERIALS

Based on the damage integral method of initiation life estimation, the influence of residual stresses on fatigue crack initiation life in welds is seen to be principally controlled by two factors:

1) The sign and magnitude of the initial mean stress ($\sigma_{o,i}$) after the set-up cycle.
2) The rate with which the mean stress ($\sigma_{o,i}$) relaxes with continued cycling.

For the three welded materials studied (A514 HAZ, A36 HAZ, 5183 WM), quite different behavior results.

Initial Mean Stress

The set-up cycle response for the A514 HAZ, A36 HAZ, and 5183 WM materials with yield-point, tensile residual stresses is shown in Fig. 35.

For the purpose of discussion, the first reversal of the three set-up cycles is bound by one Neuber parameter ($\Delta\sigma\Delta\varepsilon = 1$). The figure shows that different values of mean stress ($\sigma_{o,i}$) are established for each of the three materials. The response of the "strong" A514 HAZ material shows that little weld notch root yielding occurs which produces a large initial mean stress ($\sigma_{o,i}$) at the weld toe. Conversely the "ductile" 5183 WM material responds such that only a negligible, slightly negative mean stress ($\sigma_{o,i}$) results. The negative value is in part due to a high rate of cyclic work hardening in this material. The response of the "tough" A36 HAZ material shows appreciable weld notch root yielding like the 5183 WM material, but, as with the A514 HAZ material, a significant mean stress ($\sigma_{o,i}$) is established.

The initial residual stress (σ_r) at the weld toe does not remain constant, but changes in sign and/or magnitude to a new value (σ_r*) after the set-up cycle, as shown in Fig. 35. The value of σ_r* remains high and positive for the A514 HAZ material; but, becomes negative for the A36 HAZ and 5183 WM materials. Initial residual stresses, therefore, change after the set-up cycle due to weld toe notch root plasticity.

Welds of materials that are strong or tough like the A514 and A36 HAZ materials may be influenced by initial residual stresses at the weld toe, since there is an initial mean stress ($\sigma_{o,i}$) after the set-up cycle. However, the fatigue life of welds fabricated from the materials like 5083-O aluminum would not be influenced by residual stresses, since the residual stresses produce a negligible initial mean stress ($\sigma_{o,i}$) after the set-up cycle.

Mean Stress Relaxation Behavior of Several Materials

The mean stress relaxation behavior of any metal is dependent on the plastic strain accummulated during a reversal (39, 42). Morrow (39) found that mean stress relaxation behavior depends on the nonclosure of cyclic hysteresis loops and the resulting nonsymmetric loop shape. Based on this observation, Morrow (39) developed a mean stress relaxation rate equation which was developed from the diagram shown in Fig. 36.

$$\frac{\partial \sigma_{o,2N}}{\sigma_{2N}} = \frac{\beta E}{2} \{\varepsilon_p (\sigma_{max}) - \varepsilon_p (\sigma_{min})\} \quad (32)$$

where the value of β is given as:

β	$\partial\sigma/\partial\varepsilon$	$\sigma_{o,2N}$
+1	positive	positive
-1	negative	positive
-1	positive	negative
+1	negative	negative

Equation 32 states that for a tensile mean stress on the nth reversal, the plastic strain ($\varepsilon_p (\sigma_{max})$) is larger on the path to σ_{max} than the plastic strain ($\varepsilon_p (\sigma_{min})$) on the path to σ_{min}. From this equation two factors affecting the mean stress relaxation are apparent: (1) relaxation depends on plastic strain which is controlled by the magnitude of the mean stress ($\sigma_{o,2N}$), and (2) that the modulus of the material is important. By differentiation of the mean stress relaxation power function (Eq. 25), the relaxation rate is given as:

$$\frac{\partial \sigma_{o,2N}}{\partial 2N} = \frac{k\sigma_{o,2N}}{(2N-1)} \tag{33}$$

Based on Eqs. 32 and 33 one may deduce that mean stress relaxation depends on the mean stress ($\sigma_{o,2N}$) and the plastic strain ($\Delta\varepsilon_p/2$) during a reversal, and the elastic modulus (E) of the material. Thus, from Eqs. 32 and 33 the relaxation exponent (k) in Eq. 25 should be a function of plastic strain ($\Delta\varepsilon_p/2$) and the elastic modulus (E) of the material.

From a trial and error approach, a material parameter was found which was linearly related to the relaxation exponent (k). To obtain this relationship the plastic strain amplitude ($\Delta\varepsilon_p/2$) was normalized by the transition strain (ε_{tr}) which corresponds to the strain on the cyclic stress curve where the elastic ($\Delta\varepsilon_E/2$) and plastic ($\Delta\varepsilon_p/2$) strains are equal (see Fig. 37). Figures 38 and 39 show the results of plotting the material parameters, ($\Delta\varepsilon_p/2$ / ε_{tr}) and ($\Delta\varepsilon_p/2$ / $E\varepsilon_{tr}$), versus the relaxation exponent (k). Both figures suggest a linear relationship for the relaxation exponent with the corresponding material parameters, but the consideration of both elastic modulus (E) and transition strain (ε_{tr}) produce the better correlation shown in Fig. 39. The relationship is given as:

$$k = -4625\ [\Delta\varepsilon_p/2\ /\ E\varepsilon_{tr}]/\text{ksi} \tag{35}$$

The correlation found for Eq. 35 is surprising, however, in light of Higashida's (29) finding that the relaxation exponent (k) was a function of Brinell Hardness (H_B) for the A514 group of weld materials but not for the A36 group of weld materials as shown in Fig. 40. Based on Eq. 35, one

would expect materials with high modulus and yield strength or large transition strains (ε_{tr}) and small transition fatigue lives ($2N_{tr}$) to relax the least, and materials with low modulus and yield strength or small transition strains (ε_{tr}) and large transition fatigue life ($2N_{tr}$) to relax the most for a specific strain amplitude (ε_a).

5.3 INFLUENCE OF RESIDUAL STRESSES AND STRESS RATIO ON WELD FATIGUE LIFE

The influence of stress relief on the tensile residual stresses and the effect of stress ratio on butt weld fatigue life was investigated. Hypothetical welds of A514, A36, and 5083-0 base materials having a common weld shape (ϕ = 90°, θ = 60°, t = 1/2 in. (13 mm)) were considered. Cracks were assumed to initiate in HAZ material of the A514 and A36 butt welds and the (5183) WM of the 5083-0 butt welds. The crack size (a_I) at the end of the initiation life (N_I) was again assumed to be 0.01 in. (.25 mm). The initial residual stress distribution (which changes during the set-up cycle) was considered not to influence the crack propagation life (N_p); but the influence of stress ratio (R) on crack propagation life was accounted for by using Eq. 31 to modify the crack growth coefficient in Eq. 3. The required value of the crack opening factor (c_f) were estimated for the A514 HAZ, A36 HAZ, and 5183 WM weld materials from averaged analytical and experimental values for RQC100, Manten, and 2219-T851 materials: see Fig. 8.

A514F/E110 Butt Welds

The predicted influence of stress relief and stress ratio for A514 butt welds is shown in Figs. 41 to 43. The S-N diagram in Fig. 41 shows that, irrespective of the stress ratio, the fatigue life of A514 butt welds may be greatly improved by stress relieving the weld when the fatigue life is greater than 10^5 cycles. The modified Goodman diagram shown in Fig. 42 also indicates that stress relief should improve the fatigue resistance of a A514 butt weld. Moreover, the diagram shows that stress ratio (R) or mean stress (S_m) affects the fatigue strength of a A514 butt weld and should be greater for more negative stress ratios or decreasing amounts of mean stress.

Averaged fatigue strength data for A514 butt welds (55) are seen to be in excellent agreement with the predicted curves for lives of 10^5 and 10^6 cycles and 1/2, 0, and -1 stress ratios (see Fig. 42).

The predicted percentage of total life spent in crack initiation for the A514 butt weld is plotted as a function of total life (N_T) for as-welded and stress relieved welds in Fig. 43. For lives less than 10^5 cycles, the figure shows that the total life is dominated by crack propagation life while for lives greater than 10^6 cycles,crack initiation life dominates for both the stress relieved and as-welded butt welds at stress ratios of 1/2, 0, and -1. In the life regime of 10^5 to 10^6 cycles, both stress relief and increasing the stress ratio of the butt weld increases the amount of life spent in crack initiation at a given total fatigue life. It should be noted that the fraction of life spent in initiation is rather sensitive to the initial crack size (a_I) and its definition.

A36/E60S-3 Butt Welds

The predicted influence of stress relief and stress ratio is shown in Figs. 44 to 46 for A36 butt welds with a crack initiating in HAZ weld material. From the S-N diagram in Fig. 44, it can be seen that, like the A514 butt welds, both stress relief and stress ratio have a marked influence on A36 butt weld fatigue life for lives greater than 10^5 cycles. The modified Goodman diagram of Fig. 45 also shows that stress relief improves the fatigue life of A36 butt welds for lives greater than 10^5 cycles; moreover, from the diagram it can be seen that the stress ratio (R) or mean stress (S_m) only influences the fatigue life for positive stress ratios. This result is contrary to the predicted trend found for A514 butt welds.

Averaged fatigue strength data for mild steel butt welds (2) for 10^5 and 10^6 cycles at a stress ratio of zero are also plotted in Fig. 45 which shows fair agreement with the predicted result for the A36 butt weld.

The predicted percentage of total life spent in crack initiation for the A36 butt welds as a function of total life (N_T) is shown in Fig. 46 for both as-welded and stress relieved cases and stress ratios of 0 and -1. From this diagram, it is seen that the percentage of crack initiation life should dominate for total fatigue lives that are greater than 10^5 cycles which is a factor of 10 less than that for the A514 butt weld. Also, like the A514 butt welds, the percentage of life spent in crack initiation was increased by stress relief for lives greater than 10^5 cycles; and, as stress ratio increased, the percentage of life spent in crack initiation also increased for the A36 butt welds.

5083-O/5183 Butt Welds

The predicted influence of stress relief and stress ratio on 5083-O butt welds is shown in Figs. 47 to 49. The crack initiation site was assumed to be 5183 WM material. From the S-N diagram in Fig. 47, it is apparent that neither stress relief nor stress ratio should have much influence on fatigue life (in the life regime of 10^5 to 10^6 cycles). The modified Goodman diagram of Fig. 48 also bears this out, showing no influence of stress relief or stress ratio (mean stress) on the 5083-O butt welds.

Averaged fatigue strength data (3), shown in Fig. 48, are also found to be in excellent agreement with the predicted lives for fatigue lives of 10^5, 10^6, and 10^7 cycles and stress ratios of 0, 1/4, and 1/2.

The predicted percentage of crack initiation life as a function of total fatigue life for the 5083-O butt welds is shown in Fig. 49 from which it is apparent that stress relief has no influence on the amount of life spent in crack initiation (for lives greater than 10^4 cycles). Also, the diagram shows that crack initiation life dominates the total fatigue life (N_T) for the 5083-O butt welds for lives greater than 10^4 cycles and that, like the A514 and A36 butt welds, the amount of life spent in crack initiation increases as the stress ratio increases.

The predicted insensitivity of the 5083-O butt welds to stress relief or stress ratio is due to the ductility and initial low strength of the 5183 WM as evidenced in the set-up cycles of Fig. 35 as discussed in the previous section. The weld would become sensitive to stress ratio

however, if the weld was precycled causing the material to cyclically harden (see Fig. 14). A larger yield stress results (see Fig. 12) and the set-up cycle would produce significant initial mean stress at the weld toe and influence the crack initiation (N_I) and total fatigue life (N_T). The predicted influence of stress ratio for a cyclically hardened 5083-0 butt weld is shown in Fig. 50. Contrasted to results of Fig. 47, it is apparent that for a precycled 5083-0 butt weld stress ratio should have a significant influence on life.

6. CONCLUSIONS

1. The residual stress influence on weld fatigue life may be treated by the set-up cycle model which establishes a mean stress and the damage integral which allows the mean stress relaxation to be considered in the prediction of fatigue life. Residual stresses were neglected in the prediction of crack propagation life. The resulting total life predictions were in good agreement with experimental results for A514, A36, and 5083-0 weldments containing residual stresses.

2. Material properties of the A514, A36, and 5083-0 butt welds were found to influence significantly the effect of residual stresses on weld fatigue life. High strength materials like the A514 welds were found to be influenced by residual stresses while low strength 5083-0 welds were not. A36 weld fatigue life was also found to be influenced by residual stresses but not as greatly as A514 welds.

3. Mean stress relaxation was found to depend on the plastic strain amplitude and transition fatigue life of a material. Materials with small $2N_{tr}$ had low relaxation rates for a given strain amplitude, while materials with a large $2N_{tr}$ had high relaxation rates.

4. Stress relief of A514 and A36 butt welds was predicted to give large improvements for lives exceeding 10^5 cycles in fatigue resistance with the greatest improvement for the A514 butt welds. Little improvement, except at long lives (10^7 cycles), was found for the fatigue life of 5083-0 welds.

VII REFERENCES

1. Gurney, T. R., Fatigue of Welded Structures, Cambridge University Press, London, 1968.

2. Munse, W. H., Fatigue of Welded Steel Structures, Welding Research Council, New York, 1964.

3. Sanders, W. W., "Fatigue Behavior of Aluminum Alloy Weldments," Welding Research Council, Bulletin No. 171, 1972.

4. Pollard, B. and Cover, R. J., "Fatigue of Steel Weldments," Weld. J., 51, 11, p. 544s, 1972.

5. Kelsey, R. A., "Fatigue and Fracture Characteristics of Al-Mg Butt Welds," Alcoa Laboratories, Report No. 57-77-18, 1977.

6. Francis, P. H., Lankford, J, and Lyle, F. F., "A Study of Subcritical Crack Growth in Ship Steels," Report No. SSC-251, Ship Structure Committee, Washington, D. C., 1975.

7. Forsyth, P. J. E., The Physical Basis of Metal Fatigue, American Elsevier, New York, 1969.

8. Palmgren, A., "Die Lebensdauer von Kygellagern," Verein Deutscher Ingenieure Zeitschrift, 68, p. 339, 1924.

9. Miner, M. A., "Cummulative Damage in Fatigue," J. Appl. Mech., 12, p. A159, 1945.

10. Topper, T. H., Wetzel, R. M., and Morrow, JoDean, "Neuber's Rule Applied to Fatigue of Notched Specimens," J. Mat., 4, p. 200, 1969.

11. Paris, P. C. and Erdogan, "A Critical Analysis of Crack Propagation Laws," J. Basic Eng., 85, p. 528, 1963.

12. Lawrence, F. V., "Estimation of Fatigue Crack Propagation Life in Butt Welds," Weld. J., 52, p. 212s, 1973.

13. Harrison, J. D., "An Analysis of the Fatigue Behavior of Cruciform Joints," Brit. Weld. Inst., Report No. E/21/12/68, Cambridge, England, 1968.

14. Maddox, S. J., "An Analysis of Fatigue Cracks in Fillet Welded Joints," Int. J. Frac. Mech., 11, 2, p. 221, 1975.

15. Frank, K. H., "The Fatigue Strength of Fillet Welded Connections," Ph.D. Thesis, Lehigh University, 1971.

16. Zettlemoyer, N., "Stress Concentration and Fatigue of Welded Details," Ph.D. Thesis, Lehigh University, 1976.

17. Signes, E. G., Baker, R. G., Harrison, J. D., and Buidekin, F. M., "Factors Affecting the Fatigue Strength of Welded High Strength Steels," Brit. Weld. J., 14, p. 108, 1967.

18. Lawrence, F. V., and Munse, W. H., "Fatigue Crack Propagation in Butt Welds Containing Joint Penetration Defects," Weld. J., 52, p221s, 1973.

19. Burk, J. D., and Lawrence, F. V., "Effects of Lack-of-Penetration and Lack-of-Fusion on the Fatigue Properties of 5083 Aluminum Alloy Welds," To be published, Weld. Res. Council Bull., 1978.

20. Burk, J. D., and Lawrence, F. V., "Influence of Bending Stresses on Fatigue Crack Propagation Life in Butt Joint Welds," Weld. J., 56, p. 43s, 1977.

21. Mattos, R. J., "Estimation of the Fatigue Crack Initiation Life in Welds Using Low Cycle Fatigue Concepts," Ph.D. Thesis, University of Illinois, Urbana-Champaign, 1975.

22. Lomacky, O., Ellingwood, B., and Gifford, L. N., "Analysis of Low Cycle Fatigue Performance of Welded Structural Joints," Trans. 3rd Int. Conf. on Structural Mechanics in Reactor Technology, 5 Part L, L6/6, 1975.

23. Smith, K. N., El Haddad, M., and Martin, J. F., "Fatigue Life and Crack Propagation Analyses of Welded Components Containing Residual Stresses," J. Mat. and Eval., 5, No. 4, p. 327, 1977.

24. Parry, M., Norberg, H. and Hertzberg, R. W., "Fatigue Crack Propagation in A514 Base Plate and Welded Joints," Weld. J., 51, p. 485s, 1972.

25. Maddox, S. J., "Fatigue Crack Propagation Data Obtained from Parent Plate, Weld Metal, and HAZ in Structural Steels," Brit. Weld. Inst. Report No. E/48/72, 1972.

26. Kapadia, B. M. and Imhof, E. J., "Fatigue Crack Propagation in Electroslag Weldments," Pub. Symposium Proceedings, 10th National Symposium on Fracture Mechanics, 1976.

27. Bucci, R. J., Clark, W. G. and Paris, P. C., "Fatigue Crack Propagation Growth Rates under Wide Variation of ΔK for an ASTM A517 Grade F (T-1) Steel," ASTM STP 513, American Society for Testing and Materials, 1972.

28. Kelsey, R. A., Nordmark, G. E. and Clark, J. W., "Fatigue Crack Growth in Aluminum Alloy 5083-0 Thick Plates and Welds for Liquified National Gas Tanks," ASTM STP 556, American Society for Testing and Materials, 1974.

29. Higashida, Y., "Strain Controlled Fatigue Behavior of Weld Metal and Heat-Affected Base Metal in A36 and A514 Steel Welds," Ph.D. Thesis, University of Illinois, Urbana-Champaign, 1976.

30. Neuber, H., "Theory of Stress Concentration for Shear Strained Prismatical Bodies with Arbitrary Non-Linear Stress-Strain Law," J. App Mech., p. 544, 1961.

31. Peterson, R. E., Notch Sensitivity," Chap. 13, Metal Fatigue, Sines and Waisman (ed.), McGraw-Hill, New York, 1959.

32. Morrow, JoDean, (ed.) Graham, J. A., Sec. 3.2, SAE Fatigue Design Handbook, Society of Automotive Engineers, 1968.

33. Morrow, JoDean, "Cyclic Plastic Strain Energy and Fatigue of Metals," ASTM STP 378, American Society for Testing and Materials, 1965.

34. Raske, D. T., and Morrow, JoDean, "Mechanics of Materials of Low Cycle Fatigue Testing," ASTM STP 465, American Society for Testing and Materials, 1969.

35. Tucker, L. E., Landgraf, R. W., and Brose, W. R., "Proposed Technical Report on Fatigue Properties for the SAE Handbook," Paper No. 740279, Society of Automotive Engineers, 1974.

36. Martin, J. F., "Fatigue Damage Analysis for Irregular Shaped Structures Subject to Representative Loads," Fracture Control Program Report No. 10, University of Illinois College of Engineering, Urbana-Champaign, 1973.

37. Wetzel, R. M., "A Method of Fatigue Damage Analysis, "Metallurgy Department, Technical Report No. SR71-107, Ford Motor Co. Scientific Research Staff, 1974.

38. Socie, D. F., "Estimating Fatigue Crack Initiation and Propagation Lives in Notched Plates under Variable Loading Histories, "TAM Report No. 417, University of Illinois, Urbana-Champaign, 1977.

39. Morrow, JoDean, Ross, A. S., and Sinclair, G. M., "Relaxation of Residual Stresses Due to Fatigue Loadings," TAM Report No. 568, University of Illinois, Urbana-Champaign, 1959.

40. Morrow, JoDean and Sinclair, G. M., "An Analysis of Cyclic Stress Strain Behavior for Conditions of Controlled Strain," TAM Report No. 543, University of Illinois, Urbana-Champaign, 1957.

41. Friedman, E. "Thermomechanical Analysis of the Welding Process Using the Finite Element Method," J. Pressure Vessel Tech., 97, 3, p. 206, 1975.

42. Jhansale, H. R. and Topper, T. H., "Engineering Analysis of the Inelastic Response of a Structural Metal under Variable Cyclic Strains," ASTM STP 519, American Society for Testing and Materials, 1973.

43. Barsom, J. M., "Fatigue-Crack Growth Under Variable Amplitude Loading in ASTM A514 Grade B Steel," ASTM STP 536, American Society For Testing and Materials, 1973.

44. Elber, W., "The Significance of Fatigue Crack Closure," ASTM STP 595, American Society for Testing and Materials, 1971.

45. Bell, P. D., and Wolfman, A., "Mathematical Modeling of Crack Growth Interaction Effects," ASTM STP 595, American Society for Testing and Materials, 1976.

46. Feltner, C. E. and Mitchell, M. R., "Basic Research on the Cyclic Deformation and Fracture Behavior of Materials," ASTM STP 465, American Society for Testing and Materials, 1976.

47. Donaldson, K. H., Dittmer, D. F., and Morrow, JoDean, "Fatigue Testing Using a Digital Computer-Based System," ASTM STP 613, American Society for Testing and Materials, 1976.

48. Barsom, J. M., Fatigue-Crack Propagation in Steels of Various Yield Strengths, J. Eng. Ind., 93, 4, 1971.

49. Nordmark, G. E., "Peening Increases Fatigue Strength of Welded Aluminum," Metal Progress, 4, No. 5, p. 101, 1963.

50. Hill, H. N., "Residual Welding Stresses in Aluminum Alloys," Metal Progress, 80, No. 2, p. 92, 1961.

51. Nordmark, G. E., Private Communication, Alcoa Research Labs, Alcoa, Pennsylvania, 1975.

52. Chen, Wen-Ching, Private Communication, Department of Metallurgy and Mining, University of Illinois, Urbana-Champaign, 1977.

53. Socie, D. F., "Nonarbitary Crack Initiation Length," Paper presented at SAE Fatigue Design and Evaluation Committee meeting, April, 1977.

54. Mitchell, M. and Wetzel, R. M., "Cummulative Fatigue Damage Analysis of a Light Truck Frame," Scientific Research Staff, Ford Motor Co..

55. Radziminski, J. B., Srinivasan, R., Moore, D., Thrasher, C., and Munse, W. H., "Fatigue Data Bank and Data Analysis Investigation," SRS No. 405, University of Illinois Department of Civil Engineering, Urbana, IL, 1973.

TABLE 1

Chemical Compositions of Base and Filler Metals

Material	C	Mn	P	S	Si	Ni	Cr	Mo	Cu	Fe
ASTM A36*	0.21	1.1	0.12	0.021	<0.10	<0.10	<0.08	<0.10	0.10	Bal.
E60S-3	0.09	1.0	0.017	0.024	0.50	---	---	---	---	Bal.
ASTM A514*	0.20	0.82	0.010	0.016	0.24	0.08	0.51	0.20	<0.01	Bal.
E110	0.08	1.70	0.005	0.009	0.46	2.40	0.05	0.50	---	Bal.

	Si	Fe	Cu	Mn	Mg	Cr	Zn	Ti	Zr	Al
ASTM 5083-0	0.14	0.22	0.05	0.64	4.50	0.08	0.04	0.03	<0.001	Bal.
5183	0.12	0.17	0.02	0.57	4.96	0.07	0.03	0.09	---	Bal.

All compositions are in wt. percent and are typical unless otherwise noted (*).

TABLE 2

Welding Parameters

Weld (Base/Filler Metal)	Plate Thickness (mm)	Electrode Diameter (mm)	Voltage (V)	Current (amps)	Travel Speed (mm/sec)	Preheat Temperature (°C)	Heat Input (kJ/mm)	Shielding Gas Composition (vol. percent)
A36/E60S-3	16.8	1.59	30	290	432	22	1.20	Ar - 2% O_2
A514F/E110	12.7	1.59	35	500	370	96	2.80	Ar - 2% O_2
5083-O/5183	9.6	1.59	22	230	686	22	0.44	He - 25% Ar
	25.4	1.59	24	280	420	22	0.95	He - 25% Ar
TIG Dressing	12.7	--	20	200	50	22	4.8	Ar

TABLE 3

Mechanical Properties of Base and Weld Metal
Materials for ASTM 5083-O/5183 Aluminum Welds

Property	5083-BM	5183-WM
Hardness, DPH/BHN	106/93	105/92
Modulus of Elasticity, E x 10^3 ksi (MPa)	10.3 (71)	10.3 (71)
0.2% Offset Yield Strength, ksi (MPa)	19 (131)	20 (138)
Ultimate Tensile Strength, Su, ksi (MPa)	42.6 (294)	43.3 (299)
Percent Reduction in Area, %RA	30	33
True Fracture Strength, σ_f, ksi (MPa)	60 (414)	61 (421)
True Fracture Ductility, ε_f	0.36	0.40
Strain Hardening Exponent, n	0.129	0.133
Strength Coefficient, K, ksi (MPa)	43.4 (300)	44.5 (307)

TABLE 4

Cyclic and Fatigue Properties of Base and Weld Materials for ASTM 5083-O/5183 Aluminum Welds

Material	5083-BM	5183-WM
Cyclic Yield Strength, 0.2% Offset, ksi (MPa)	42 (290)	39 (269)
Cyclic Strain Hardening Exponent, n'	0.114	0.072
Cyclic Strength Coefficient, K', ksi (MPa)	84 (580)	73.5 (507)
Fatigue Strength Coefficient, σ_f', ksi (MPa)	103 (711)	92.5 (638)
Fatigue Ductility Coefficient, ε_f'	0.405	0.581
Fatigue Strength Exponent, b	-0.122	-0.107
Fatigue Ductility Exponent, c	-0.692	-0.890
Transition Fatigue Life, $2N_{tr}$, Reversals	640	205

TABLE 5

Mechanical Properties of Base, Weld, and Heat-Affected Materials for ASTM A514F/E110 Welds

Material	A514-BM	A514-HAZ	E110-WM(1P)	E110-WM(2P)
Hardness, DPH/BHN	320/303	496/461	382/362	327/310
Modulus of Elasticity, E, x 10^3 ksi (MPa)	30.3 (210)	30.3 (210)	30.3 (210)	30.3 (210)
0.2% Offset Yield Strength, ksi (MPa)	129 (890)	171 (1180)	121 (835)	110 (760)
Ultimate Tensile Strength, Su, ksi (MPa)	136 (938)	204 (1408)	150 (1035)	132 (910)
Percent Reduction in Area, %RA	63.0	52.7	57.6	59.3
True Fracture Strength, σ_f, ksi (MPa)	216 (1490)	326 (2250)	320 (2208)	241 (1663)
True Fracture Ductility, ε_f	0.994	0.750	0.857	0.899
Strain Hardening Exponent, n	0.060	0.092	0.092	0.085
Strength Coefficient, K, ksi (MPa)	127 (1187)	306 (2110)	226 (1560)	187 (1290)

TABLE 6

Cyclic and Fatigue Properties of Base, Weld, and Heat-Affected Materials for ASTM A514F/E110 Welds

Material	A514-BM	A514-HAZ	E110-WM(1P)	E110-WM(2P)
Cyclic Yield Strength, 0.2% Offset, ksi (MPa)	87.6 (604)	136 (938)	94.2 (650)	87.4 (603)
Cyclic Strain Hardening Exponent, n'	0.091	0.103	0.177	0.166
Cyclic Strength Coefficient, K', ksi (MPa)	158 (1090)	256 (1765)	293 (2021)	242 (1670)
Fatigue Strength Coefficient, σ_f', ksi (MPa)	189 (1305)	290 (2000)	274 (1890)	204 (1408)
Fatigue Ductility Coefficient, ε_f'	0.975	0.783	0.848	0.595
Fatigue Strength Exponent, b	-0.079	-0.087	-0.115	-0.079
Fatigue Ductility Exponent, c	-0.699	-0.713	-0.734	-0.590
Transition Fatigue Life, $2N_{tr}$, Reversals	3,461	1,138	1,536	6,448

TABLE 7

Mechanical Properties of Base, Weld, and Heat-Affected Materials for ASTM A36/E60S-3 Butt Welds

Material	A36-BM	A36-HAZ	E60S-3-WM(1P)	E60S-3-WM(2P)
Hardness, DPH/BHN	168/160	255/243	245/233	211/201
Modulus of Elasticity, E, x 10^3 ksi (MPa)	27.5 (190)	27.4 (189)	27.4 (189)	27.4 (189)
0.2% Offset Yield Strength, ksi (MPa)	32.5 (224)	77.5 (534)	84.1 (580)	59.2 (408)
Ultimate Tensile Strength, Su, ksi (MPa)	60.0 (414)	96.7 (667)	103 (710)	84.0 (580)
Percent Reduction in Area, %RA	69.7 (481)	52.5 (362)	44.6 (308)	60.7 (419)
True Fracture Strength, σ_f, ksi (MPa)	138 (952)	133 (918)	143 (987)	147 (1014)
True Fracture Ductility, ϵ_f	1.19	0.745	0.590	0.933
Strain Hardening Exponent, n	0.0146/0.258	0.102	0.098	0.130
Strength Coefficient, K, ksi (MPa)	113 (780)	142 (980)	143 (987)	123 (849)

TABLE 8

Cyclic and Fatigue Properties of Base, Weld, and Heat-Affected Materials for ASTM A36/E60S-3 Welds

Material	A36-BM	A36-HAZ	E60S-3-WM(1P)	E60S-3-WM(2P)
Cyclic Yield Strength, 0.2% Offset, ksi (MPa)	33.6 (232)	58.2 (402)	55.8 (385)	52.6 (363)
Cyclic Strain Hardening Exponent, n'	0.249	0.215	0.155	0.197
Cyclic Strength Coefficient, K', ksi (MPa)	159 (1097)	216 (1490)	146 (1007)	179 (1235)
Fatigue Strength Coefficient, σ_f', ksi (MPa)	147 (1014)	105 (724)	131 (904)	149 (1028)
Fatigue Ductility Coefficient, ε_f'	0.271	0.218	0.607	0.602
Fatigue Strength Exponent, b	-0.132	-0.066	-0.075	-0.090
Fatigue Ductility Exponent, c	-0.451	-0.492	-0.548	-0.567
Transition Fatigue Life, $2N_{tr}$, Reversals	200,000	13,234	28,022	19,259

TABLE 9

Test Results for Low Cycle Fatigue Strain Control Tests
of Aluminum ASTM 5083-0 Base Metal and 5183 Weld Metal

Material	Total Strain Amplitude ϵ_a	Total Stress Amplitude σ_a, ksi (MPa)	Elastic Strain $\Delta\epsilon_E/2$	Plastic Strain $\Delta\epsilon_p/2$	Reversals to Failure $2N_f$
ASTM 5083-0 Aluminum	0.0102	46.5 (320)	0.0045	0.0057	564
	0.0071	44.0 (304)	0.0043	0.0028	1,150
	0.0052	42.0 (290)	0.0040	0.0012	4,070
	0.0041	37.0 (255)	0.0036	0.0005	12,400
	0.0031	34.0 (235)	0.0027	0.0004	26,200
	0.0025	27.0 (186)	0.0025	--	150,000
	0.0021	22.0 (152)	0.0021	--	319,680
	0.0018	19.0 (130)	0.0018	--	2,068,000
ASTM 5183 Aluminum	0.0102	52.5 (362)	0.0050	0.0052	178
	0.0073	28.7 (336)	0.0046	0.0027	468
	0.0052	45.8 (316)	0.0045	0.0007	2,078
	0.0042	40.8 (282)	0.0041	0.0001	9,956
	0.0031	31.5 (218)	0.0031	--	67,004
	0.0027	27.5 (190)	0.0027	--	146,356
	0.0022	22.1 (152)	0.0022	--	238,000
	0.0018	18.2 (126)	0.0018	--	3,140,000

TABLE 10

Mean Stress Relaxation Results under Neuber Control Conditions
for Uncycled (Virgin) and Cyclically Stabilized A36 HAZ and 5183 WM

Specimen	Material Condition	Neuber Parameter 2N=1	Neuber Parameter 2N>1	$\sigma_{0,i}$ ksi (MPa)	ε_a	k_ε Strain Control	k_N Neuber Control
A36 HAZ 103-1	Virgin	0.91	0.61	21.7 (150)	0.0026	-0.16	----
A36 HAZ 104-1	Virgin	1.24	0.83	20.0 (138)	0.0032	-0.21	----
A36 HAZ 105-1	Virgin	0.87	0.54	24.0 (165)	0.0022	-0.13	----
A36 HAZ 105-2	Stabilized	0.56	0.31	40.4 (279)	0.0017	-0.08	-0.05
A36 HAZ 105-3	Stabilized	0.55	0.31	33.0 (228)	0.0016	-0.07	-0.05
A36 HAZ 105-4	Stabilized	0.42	0.23	38.7 (267)	0.0013	-0.03	-0.01
A36 HAZ 106-1	Virgin	1.09	0.71	20.0 (138)	0.0030	-0.20	----
A36 HAZ 106-2	Stabilized	0.68	0.41	26.5 (183)	0.0021	-0.12	-0.11
A36 HAZ 106-3	Stabilized	1.35	0.68	20.8 (143)	0.0030	-0.20	-0.23
A36 HAZ 107-1	Virgin	0.69	0.41	26.4 (182)	0.0020	-0.12	-0.10
A36 HAZ 207-1	Virgin	1.18	1.84	8.8 (61)	0.0055	-0.30	-0.28
5183-12	Virgin	0.55	0.31	3.2 (25)	0.0028	-0.16	-0.14

TABLE 11

Peterson's "a" Value and Assumed Crack Growth Rate Constants for Materials at the Crack Initiation Site

Initiation Site Material	S_u ksi (MPa)	"a" in. (mm)	C in./cycle (mm/cycle)	m
A514 HAZ	204 (1408)	0.002 (0.051)	2×10^{-8} (5.1×10^{-7})	2.7
A36 HAZ	98 (676)	0.005 (0.127)	10×10^{-10} (2.5×10^{-9})	3.3
5183 WM	44 (305)	0.002 (0.051)	3.7×10^{-10} (9.4×10^{-9})	2.2

TABLE 12

Weld Geometry and Parameters Required to Estimate Crack Initiation Life for Welds

Butt Weld	ϕ	θ	a in. (mm)	t in. (mm)	t/r	K_t	$K_{f\ max}$
A514F/E110	90°	60°	0.002 (0.051)	0.5 (12.7)	250	5.30	3.15
A514F/E110 (TIG)	90°	60°	0.002 (0.051)	0.5 (12.7)	2.5	1.42	1.42**
A36/E60S	90°	60°	0.005 (0.127)	0.675 (15.9)	125	4.02	2.51
Waterloo G40.S	120°	45°	0.005 (0.127)	0.25 (6.4)	50	3.20*	2.10
A36/E60S	90°	45°-60°	0.005 (0.127)	0.375 (9.6)	75	3.34	2.17

* Approximated from known K_T values for ϕ and θ.
** Not $K_{f\ max}$, but K_f.

TABLE 13

Test Results for ASTM A514F/E110 Weldments with Tensile and Compressive Residual Stresses

Specimen	ΔS (R=0) ksi	N_f	Assumed σ_r ksi (MPa)	Condition
T1	55 (380)	118,080	120 (830)	As-welded.
T2	55 (380)	69,420	120 (830)	As-welded.
T9	55 (380)	116,460	120 (830)	As-welded.
T3	55 (380)	285,640	-120 (-830)	Overload 115 ksi (794).
T4	55 (380)	137,440	-120 (-830)	Overload 95 ksi (655).
T5	55 (380)	463,130	-120 (-830)	Overload 115 ksi (794).
T7	55 (380)	263,260	-120 (-830)	Overload 100 ksi (690).
T13	55 (380)	517,190	-120 (-830)	Overload 115 ksi (794).
T10	35 (242)	633,320	120 (830)	As-welded.
T11	35 (242)	478,560	120 (830)	As-welded.
T12	35 (242)	207,110	120 (830)	As-welded.
T15	80 (552)	77,450	-120 (-830)	As-welded Tig dressed, Overload 115 ksi (794).
T16	80 (552)	126,650	-120 (-830)	As-welded Tig dressed, Overload 115 ksi (794).
T2	80 (552)	47,210	-120 (-830)	As-welded, Tig dressed.
T8	80 (552)	48,890	-120 (-830)	As-welded, Tig dressed.

TABLE 14

Test Results for ASTM A36/E60S-3 Weldments with Tensile and Compressive Residual Stresses

Specimen	S (R=0) ksi (MPa)	N_f	Assumed σ_r ksi (MPa)	Comments
A8	32 (220)	585,960	35 (242)	As-welded
B7	36 (250)	378,330	35 (242)	As-welded
B8	32 (220)	504,780	35 (242)	As-welded
C2	32 (220)	788,920	35 (242)	As-welded
C3	32 (220)	985,000	35 (242)	As-welded
C1	26 (180)	4,000,000+	-20 (-138)	Overload 36 ksi (248)
C5	28 (194)	1,757,080	-20 (-138)	Overload 36 ksi (248)
B1	36 (250)	973,210	-20 (-138)	Overload 36 ksi (248)
B5	32 (220)	4,000,000+	-35 (-242)	Hammer peened
C6	32 (220)	1,052,010	-35 (-242)	Hammer peened

+ Did not fail.

TABLE 15

Test Results for ASTM 5083-O/5183 3/8 in. (10 mm) Aluminum Butt Welds

Specimen	ϕ (degrees)	θ (degrees)	ΔS (R=0) ksi (MPa)	N_f (cycles)
W9-2	120	45	12 (82)	1,889,000
W9-7	120	45	15 (104)	499,000
W9-8	120	45	19 (130)	130,000
M532-1	112	32	19 (130)	84,000
W10C-2	122	30	19 (130)	155,000
R15-3	100	32	15 (104)	392,000
W10C-4	122	30	15 (104)	274,000
M532-5	112	30	12 (82)	733,000
R15-6	100	32	12 (82)	3,517,000
W11B-1	130	35	19 (130)	118,000
R14-2	95	45	19 (130)	148,000
M533-3	110	25	15 (104)	124,000
R14-4	95	45	15 (104)	348,000
W11B-5	130	35	12 (82)	783,000
M533-6	110	25	12 (82)	339,000
R13-1	96	58	19 (130)	87,000
M534-2	110	30	19 (130	70,000
R13-4	96	58	12 (82)	2,519,000
M534-6	110	30	15 (104)	394,000

TABLE 16

Test Results for ASTM 5083-O/5183 1-in. (25 mm) Aluminum Butt Welds

Specimen	ϕ (degrees)	θ (degrees)	ΔS ksi (MPa)	N_f (cycles)
W21-1	80	25	12 (82)	946,000
R4-6	82	25	19 (130)	71,000
W21-8	80	25	12 (82)	368,000
W21-9	80	25	15 (104)	228,000
M536-1	82	20	19 (130)	60,000
M536-3	82	20	15 (104)	360,000
R3-4	90	26	15 (104)	129,000
W23-1	75	28	15 (104)	211,000
W23-2	75	28	19 (130)	58,000
W23-3	75	28	19 (130)	71,000
R2-5	84	32	15 (104)	118,000
W24A-1	70	50	12 (82)	201,000
R1-5	50	60	15 (104)	71,000

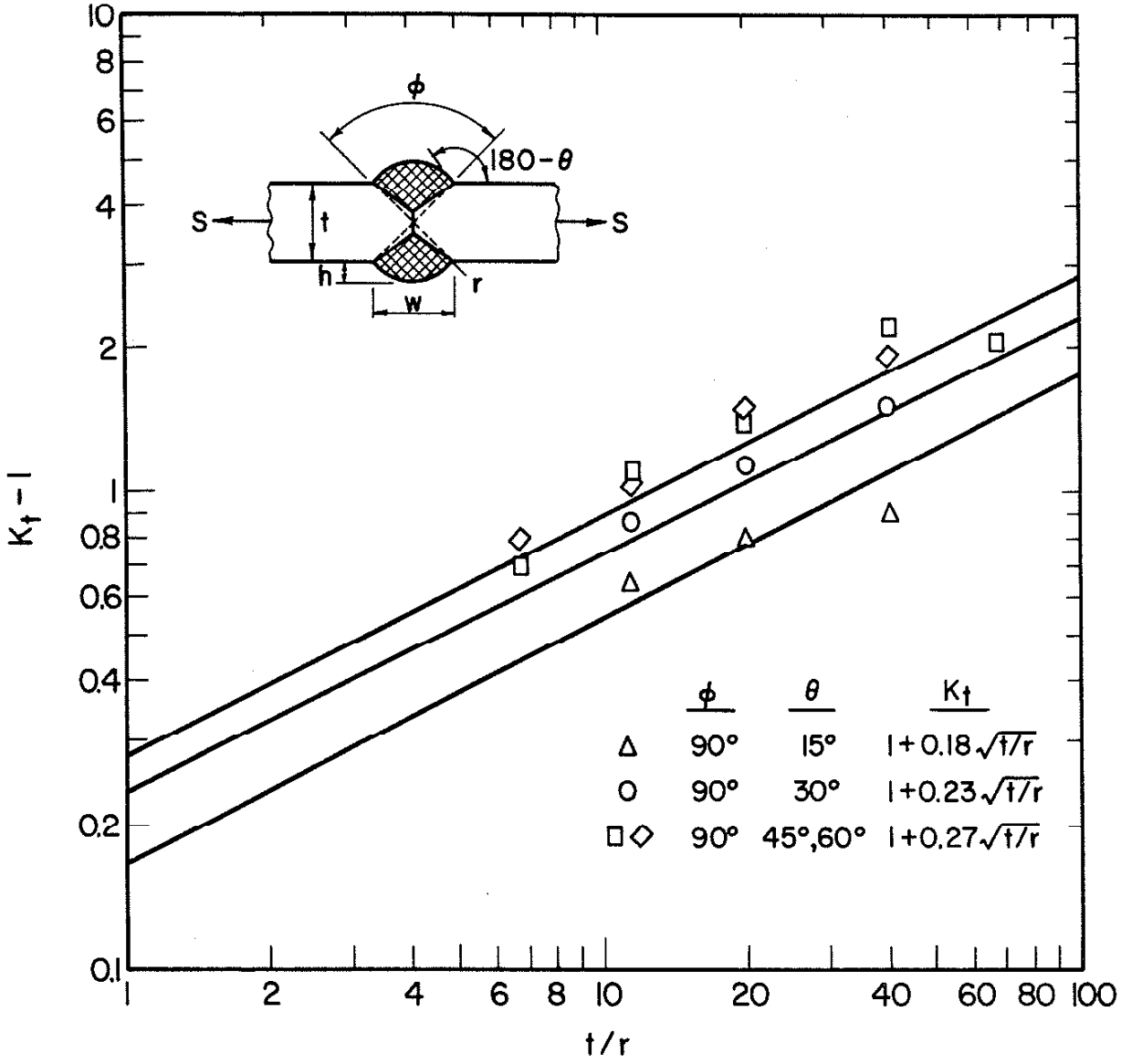

FIGURE 1. THEORETICAL STRESS CONCENTRATION FACTOR (K_t) AS A FUNCTION OF WELD TOE ROOT RADIUS AND BUTT WELD GEOMETRY (ϕ = 90°, θ = 15°, 30°, 45°, 60°).

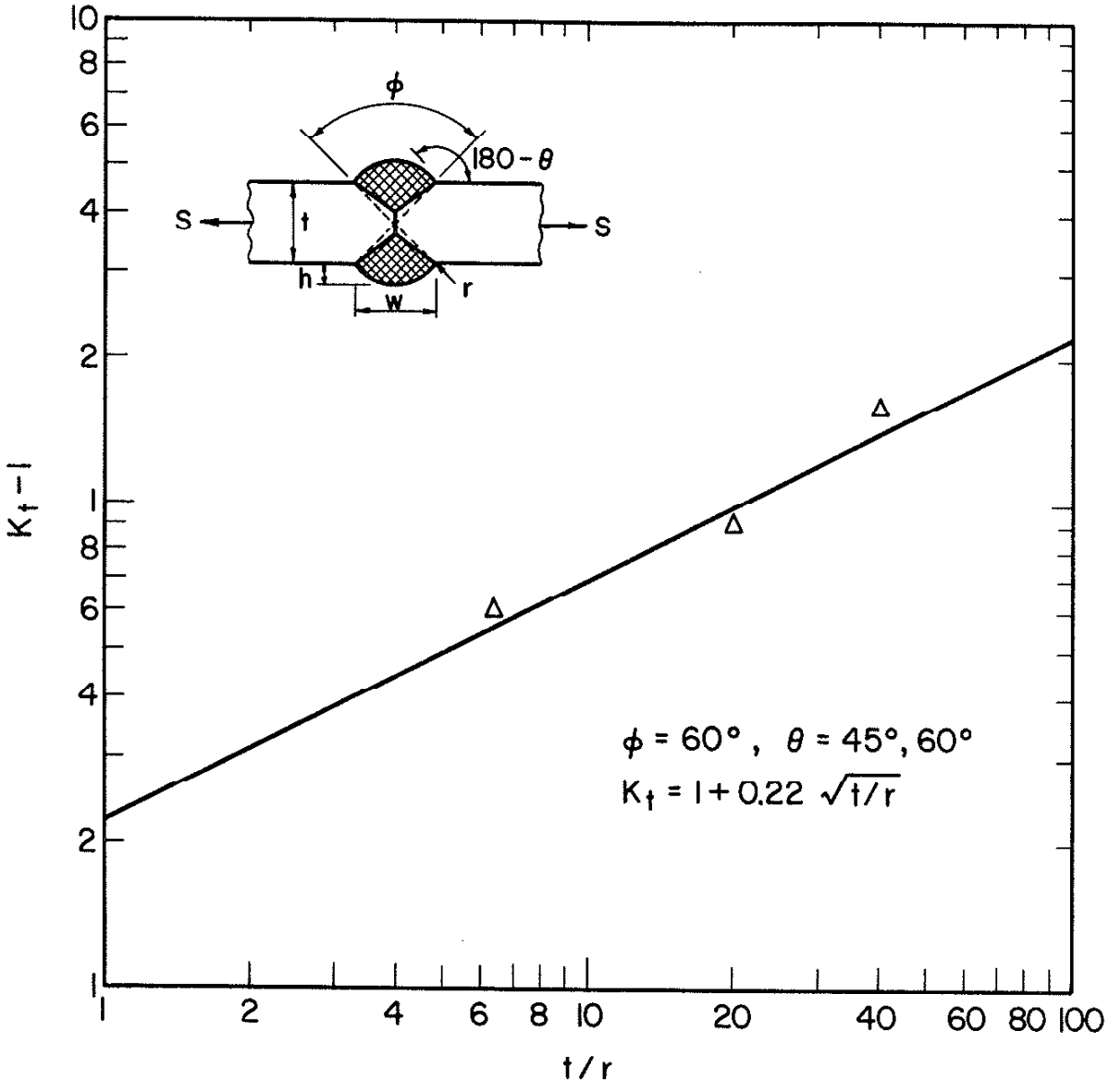

FIGURE 2. THEORETICAL STRESS CONCENTRATION FACTOR (K_t) AS A FUNCTION OF WELD TOE ROOT RADIUS AND BUTT WELD GEOMETRY (ϕ = 60°, θ = 45°, 60°).

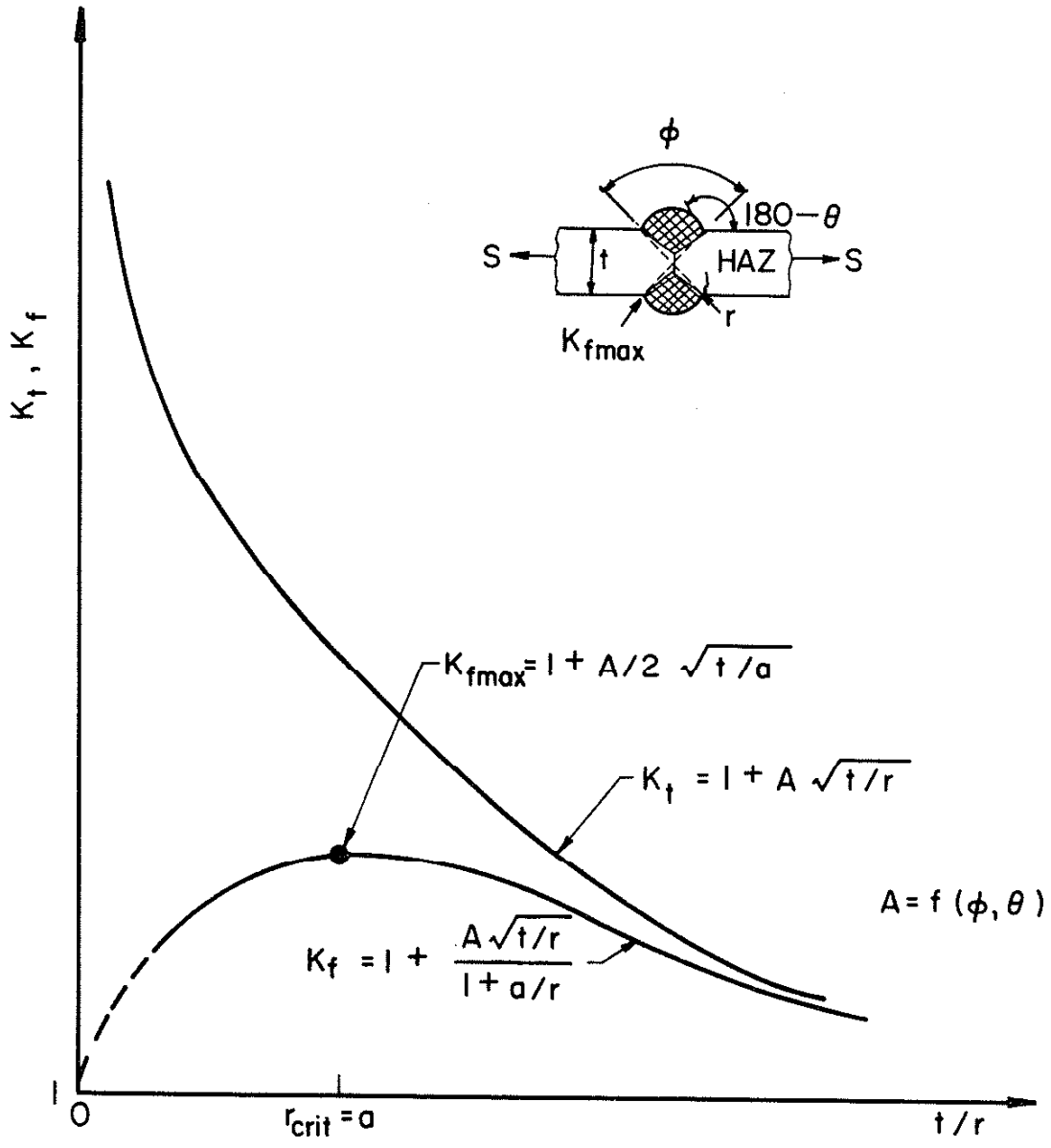

FIGURE 3. MAXIMUM FATIGUE NOTCH FACTOR ($K_{f\ max}$) FOR A BUTT WELD.

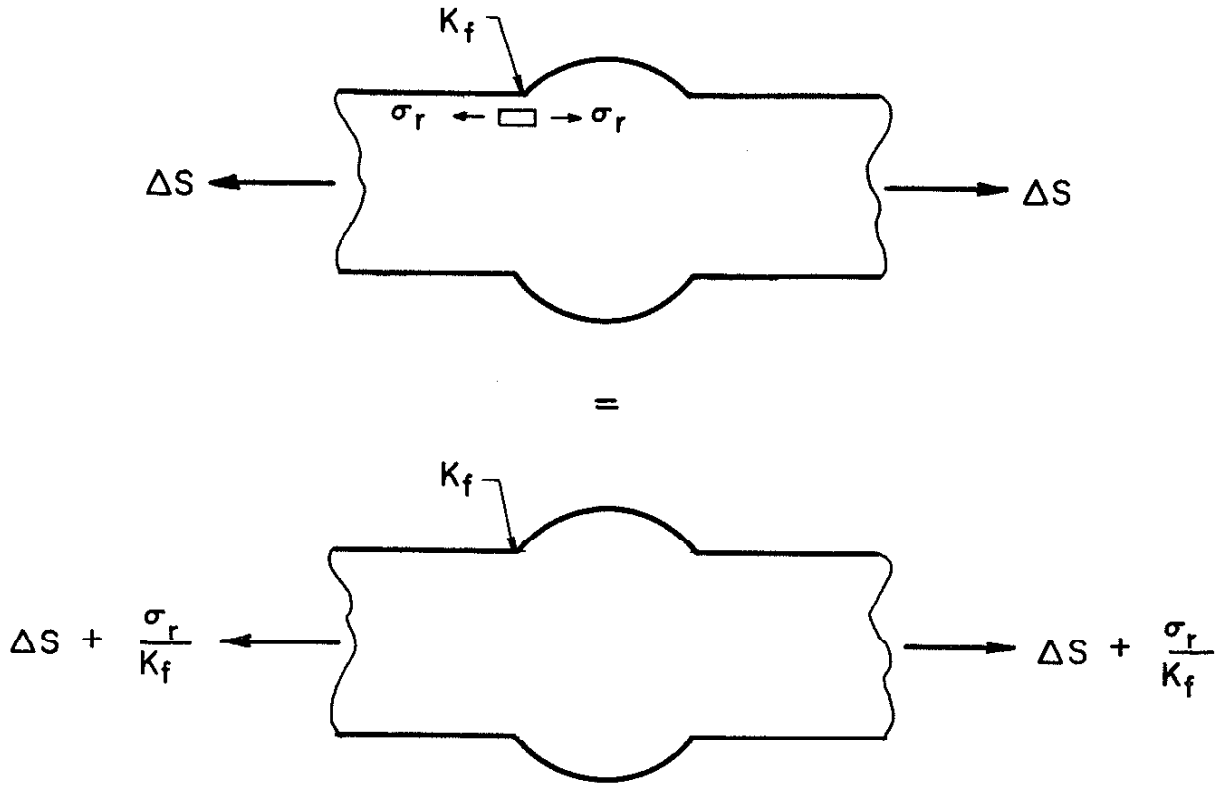

$$(K_f \Delta S + \sigma_r)^2 / E = \Delta\sigma \, \Delta\epsilon$$

FIGURE 4. MECHANICAL SIMULATION OF RESIDUAL STRESS (σ_r) AT THE WELD TOE BY ELASTIC SUPERPOSITION AND NEUBER'S RULE.

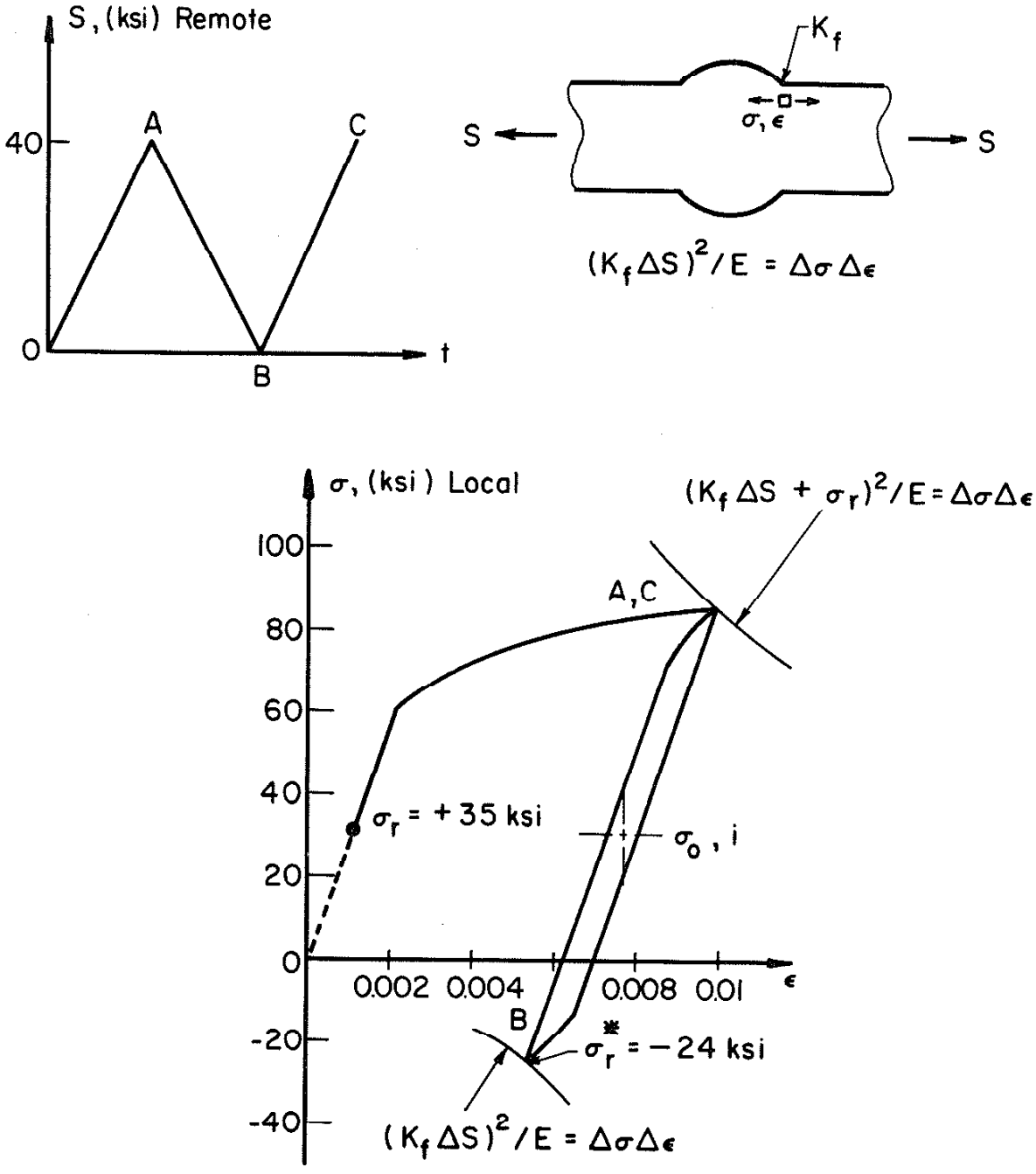

FIGURE 5. COMPUTER SIMULATED LOCAL STRESS-STRAIN RESPONSE AT THE WELD TOE FOR A BUTT WELD WITH TENSILE RESIDUAL STRESSES (A36 HAZ MATERIAL, σ_r = +35 ksi (242 MPa)).

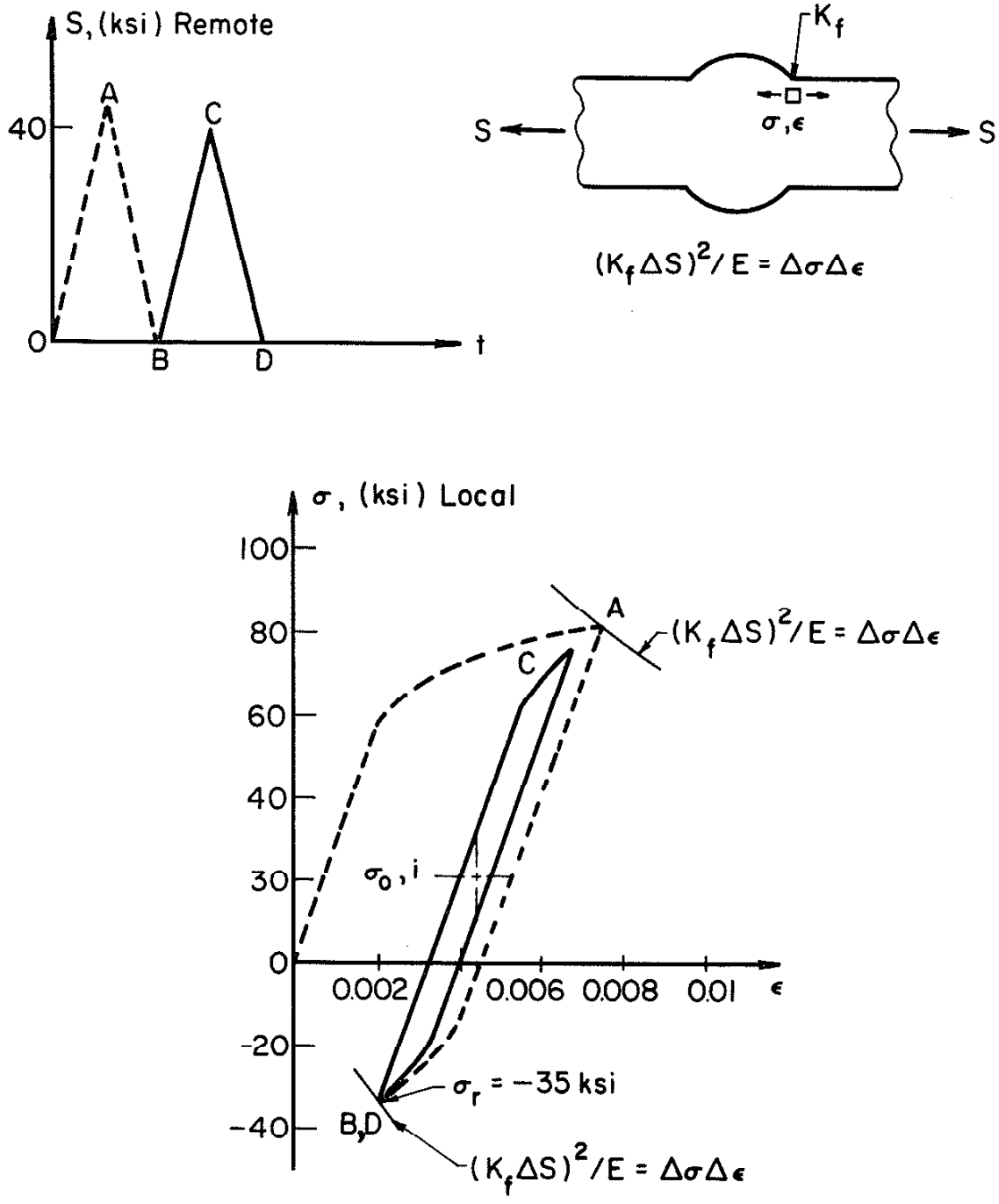

FIGURE 6. COMPUTER SIMULATED LOCAL STRESS-STRAIN RESPONSE AT THE WELD TOE FOR A BUTT WELD WITH COMPRESSIVE RESIDUAL STRESSES (A36 HAZ MATERIAL, σ_r = -35 ksi (-242 MPa)).

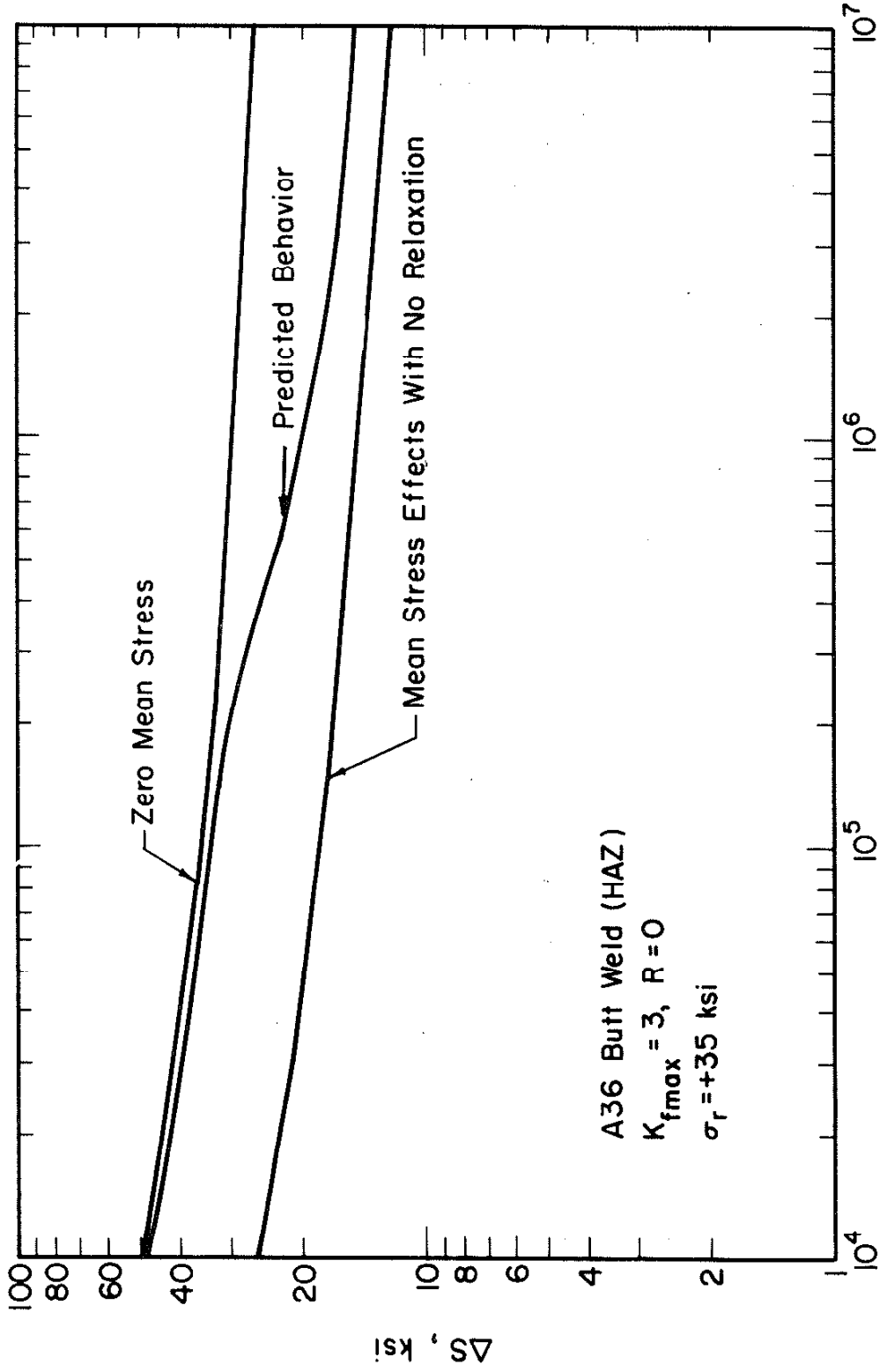

FIGURE 7. MEAN STRESS RELAXATION BEHAVIOR INFLUENCE ON FATIGUE CRACK INITIATION LIFE (A36 HAZ MATERIAL, K_f = 3, R = 0, σ_r = +35 ksi (242 MPa)).

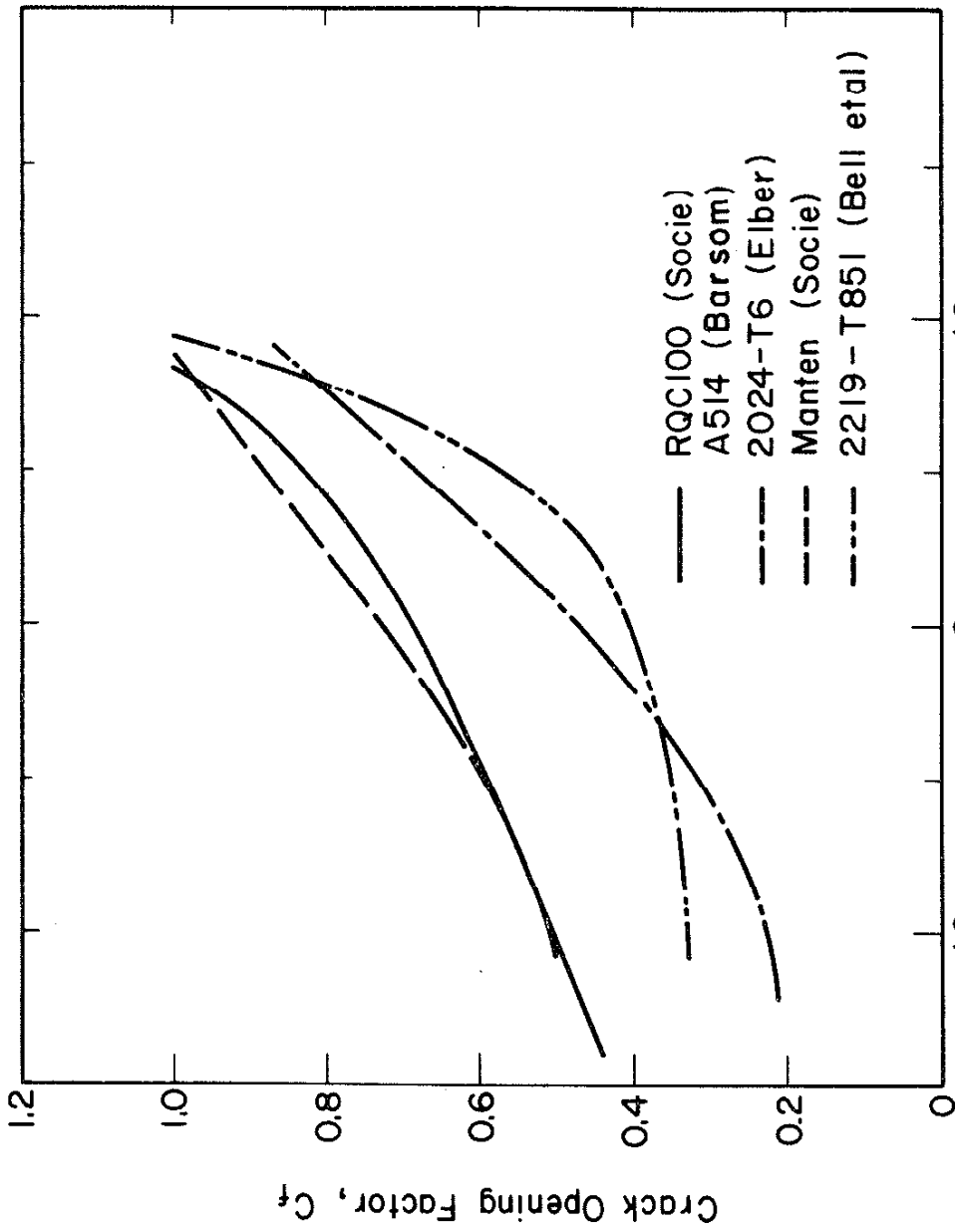

FIGURE 8. AVERAGED CRACK OPENING FACTOR (c_f) AS A FUNCTION OF THE STRESS RATIO FOR RQC100, A514, AND MANTEN STEELS AND 2024-T6 AND 2219-T851 ALUMINUMS (REF. 38, 43-45).

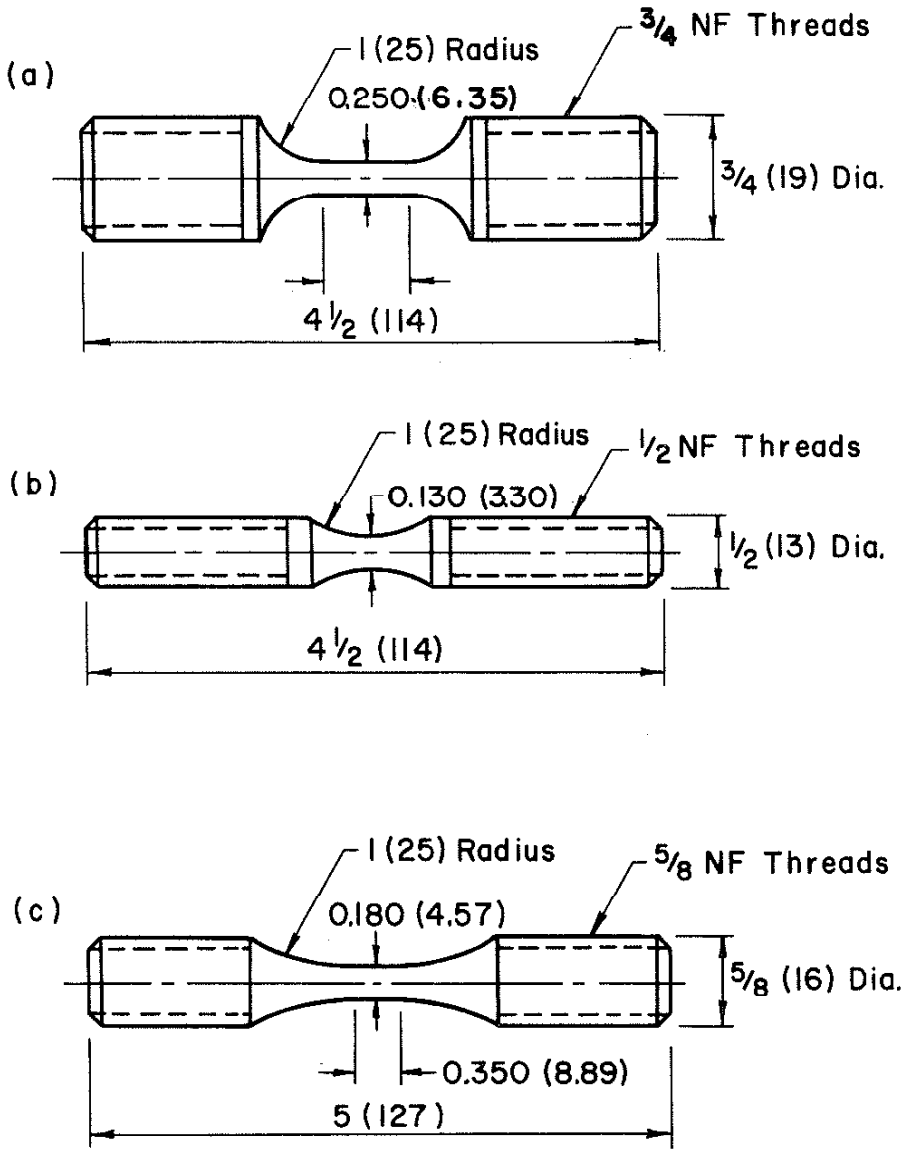

FIGURE 9. SMOOTH SPECIMENS OF (a) 5083-0 ALUMINUM BASE METAL, (b) 5183 ALUMINUM WELD METAL AND (c) A36 SIMULATED WELD HAZ. (ALL DIMENSIONS ARE IN INCHES (mm)).

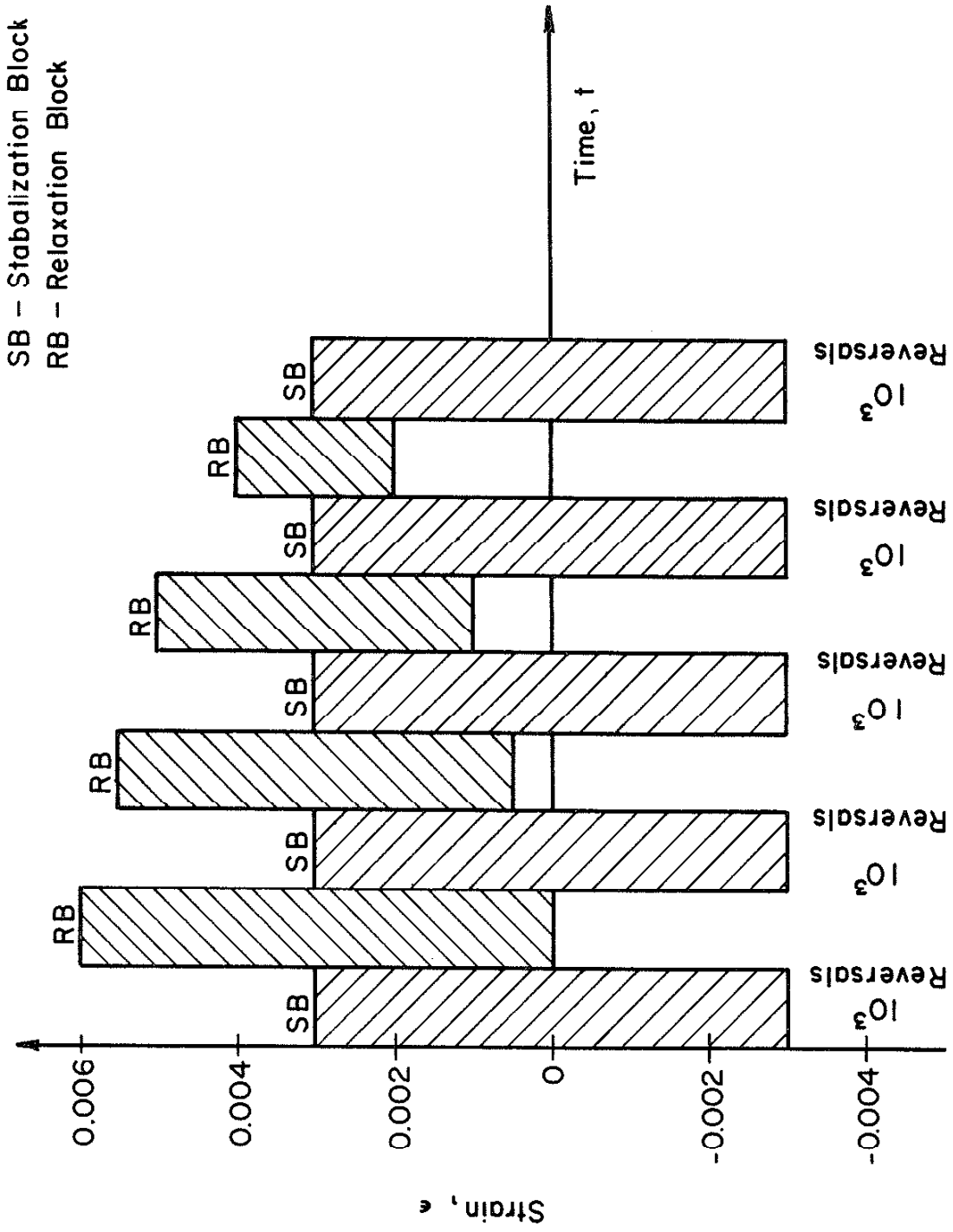

FIGURE 10. MEAN STRESS RELAXATION TEST STRAIN CONTROL HISTORY FOR 5183 ALUMINUM WELD METAL.

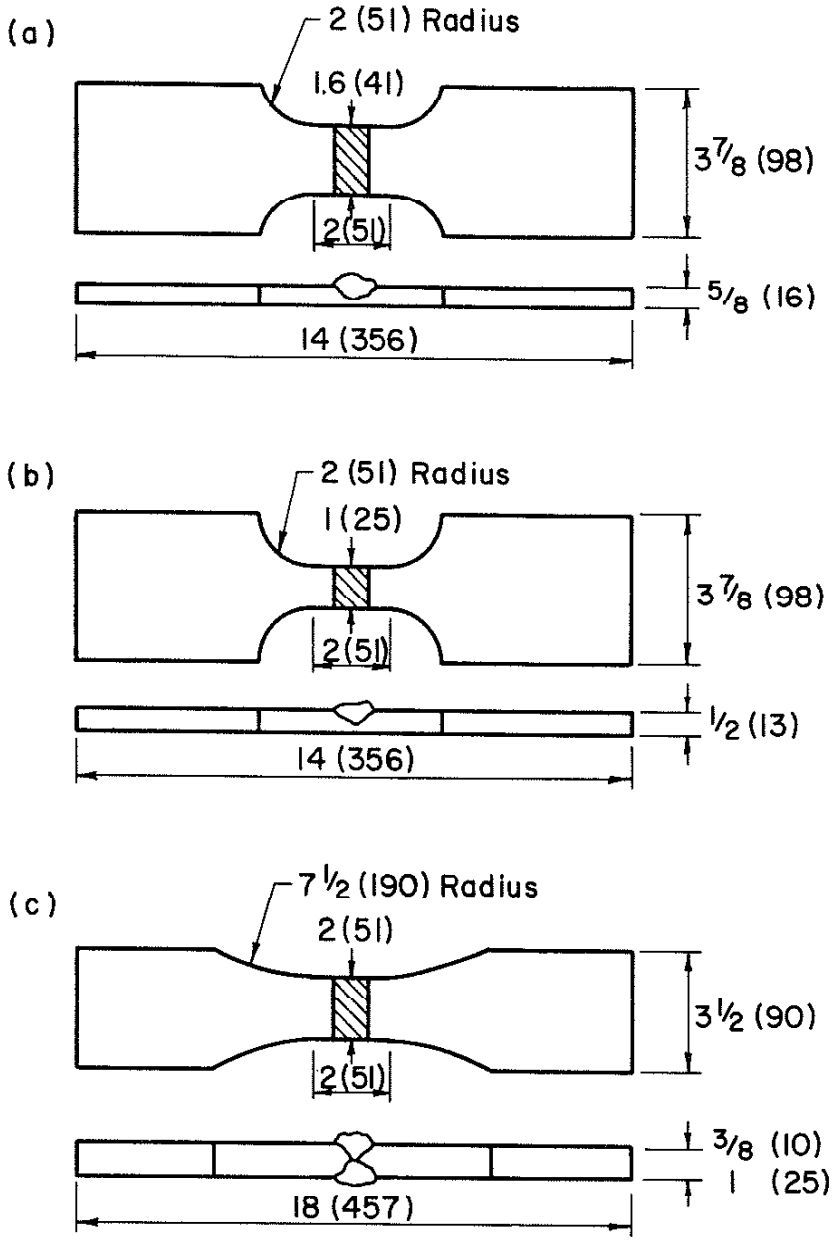

FIGURE 11. SHAPE OF (a) A36/E60S-3 STEEL, (b) A514F/E110 STEEL, AND (c) 5083-0/5183 ALUMINUM BUTT WELD TEST SPECIMENS. (ALL DIMENSIONS ARE IN INCHES (mm)).

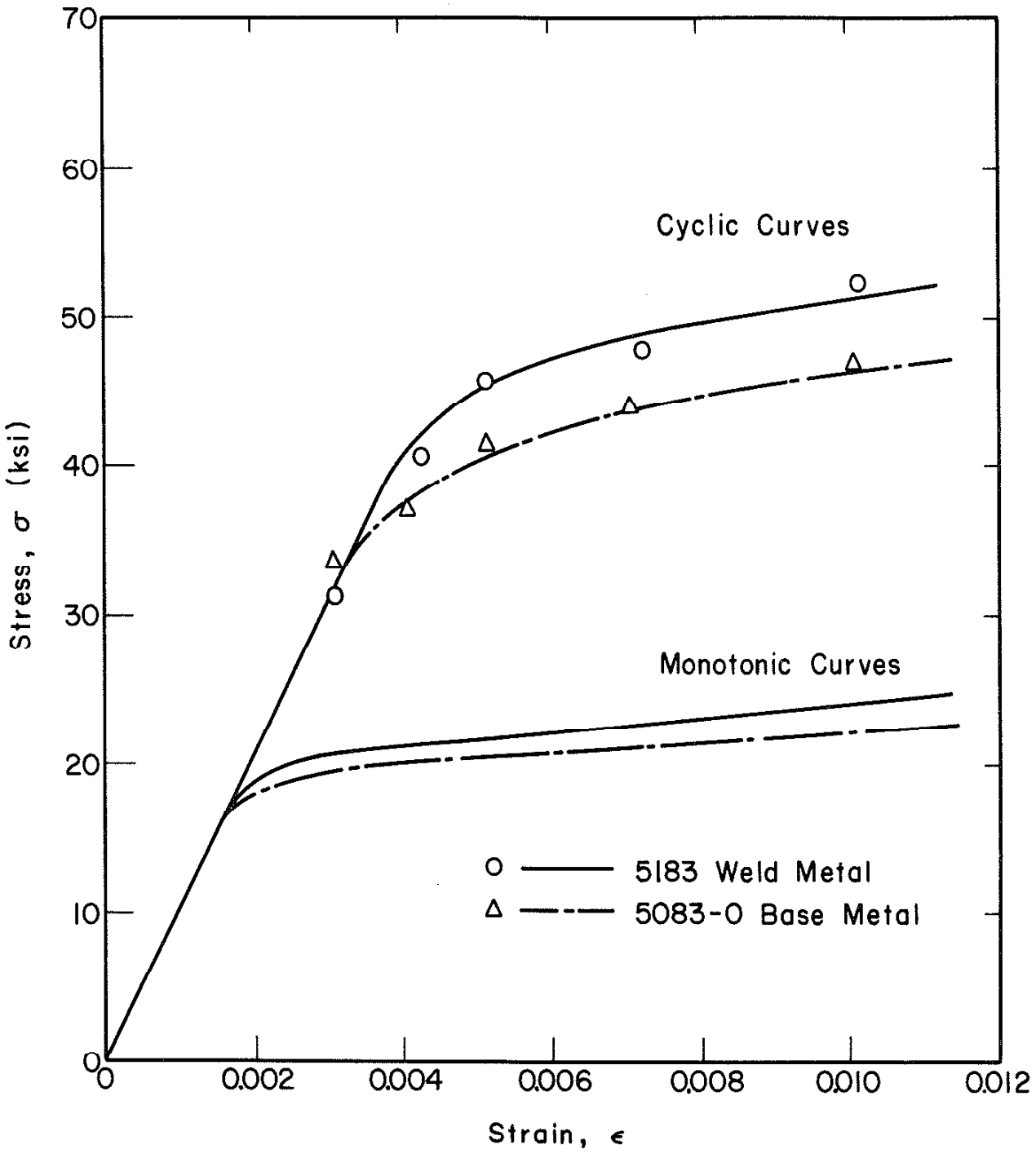

FIGURE 12. MONOTONIC AND CYCLIC TRUE STRESS-STRAIN BEHAVIOR OF ALUMINUM 5083-O BASE AND 5183 WELD METAL.

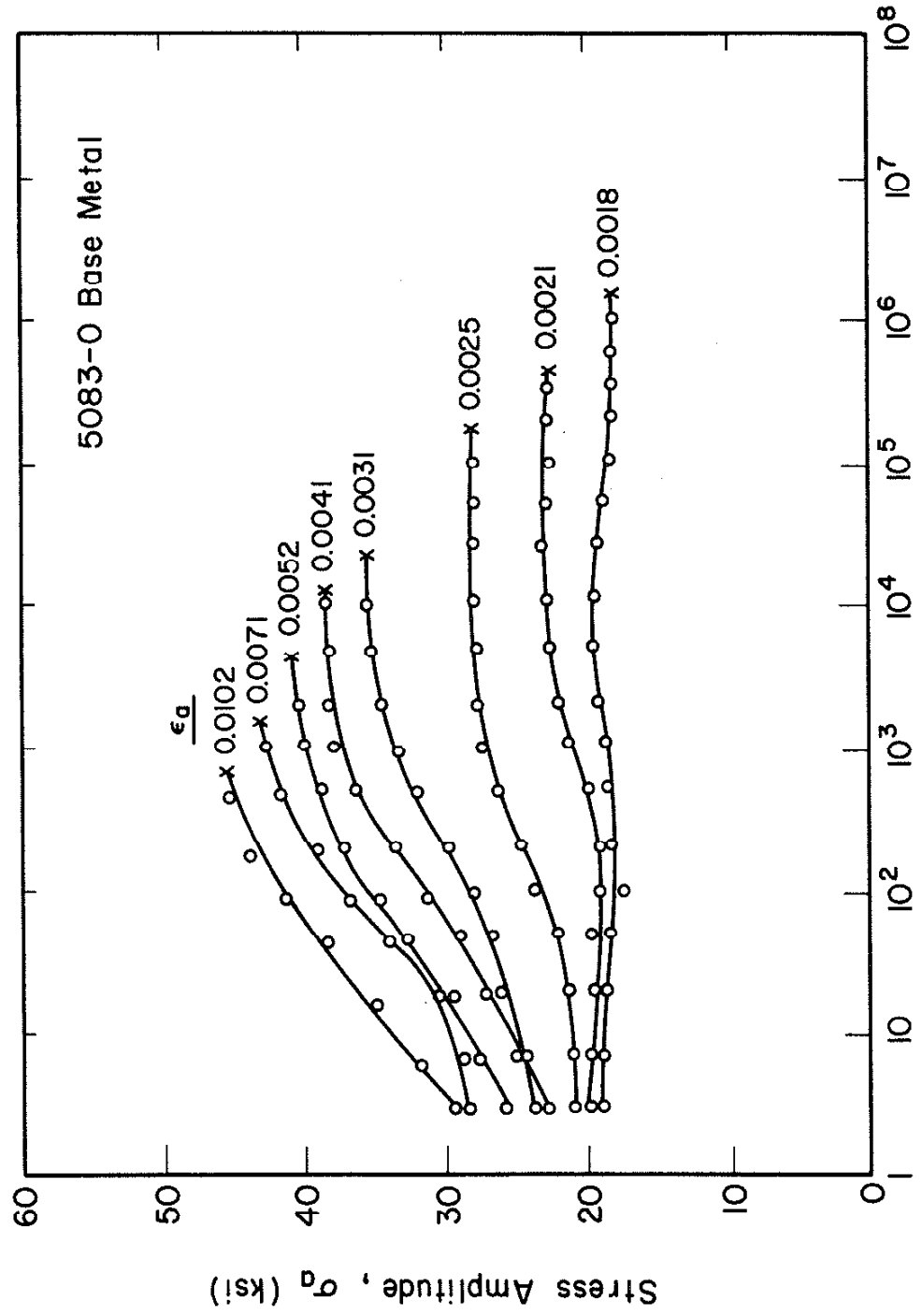

FIGURE 13. CYCLIC HARDENING BEHAVIOR OF 5083-O ALUMINUM BASE METAL.

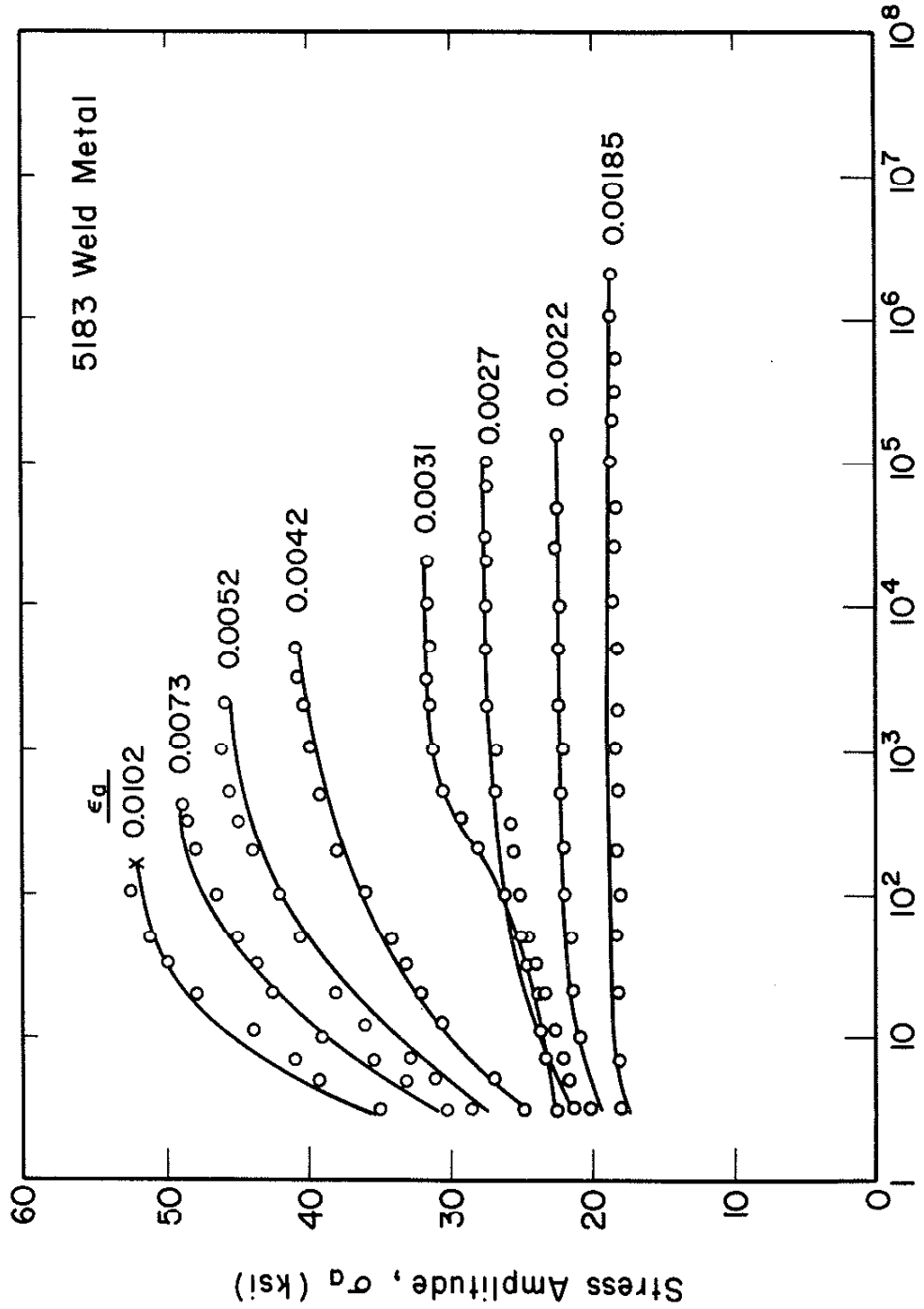

FIGURE 14. CYCLIC HARDENING BEHAVIOR OF 5183 ALUMINUM WELD METAL.

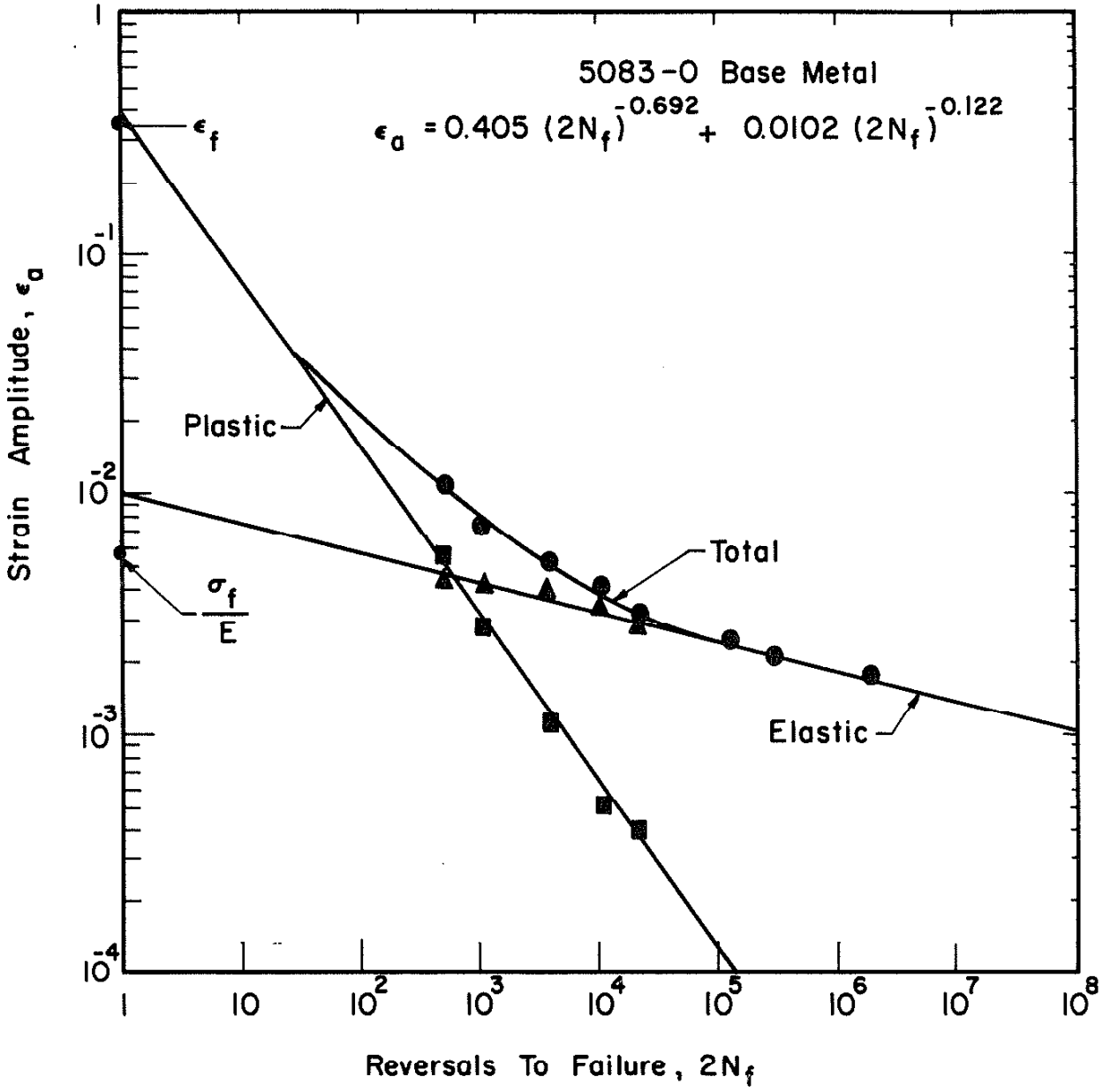

FIGURE 15. STRAIN-LIFE PLOT FOR 5083-0 ALUMINUM BASE METAL.

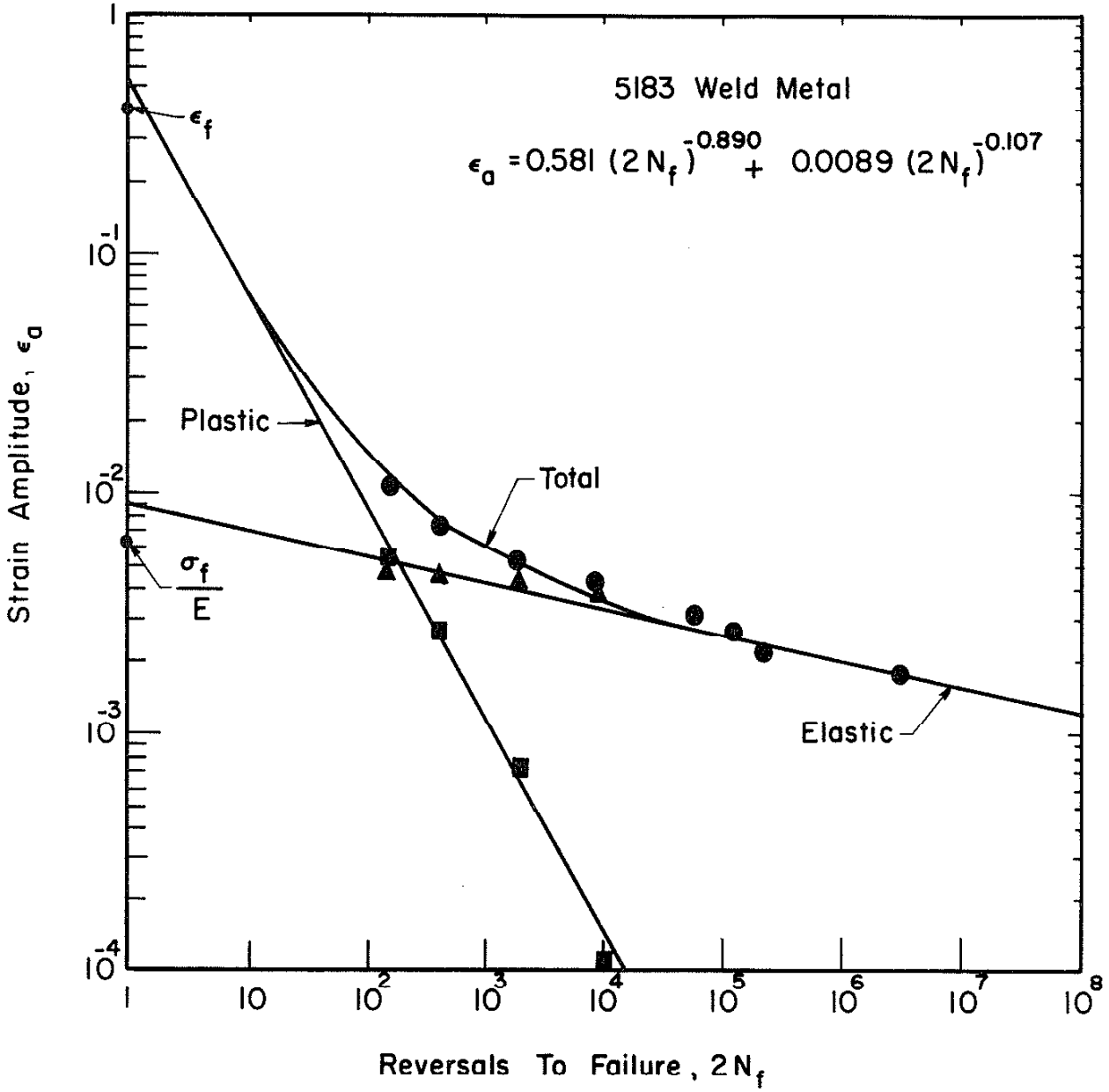

FIGURE 16. STRAIN-LIFE PLOT FOR 5183 ALUMINUM WELD METAL.

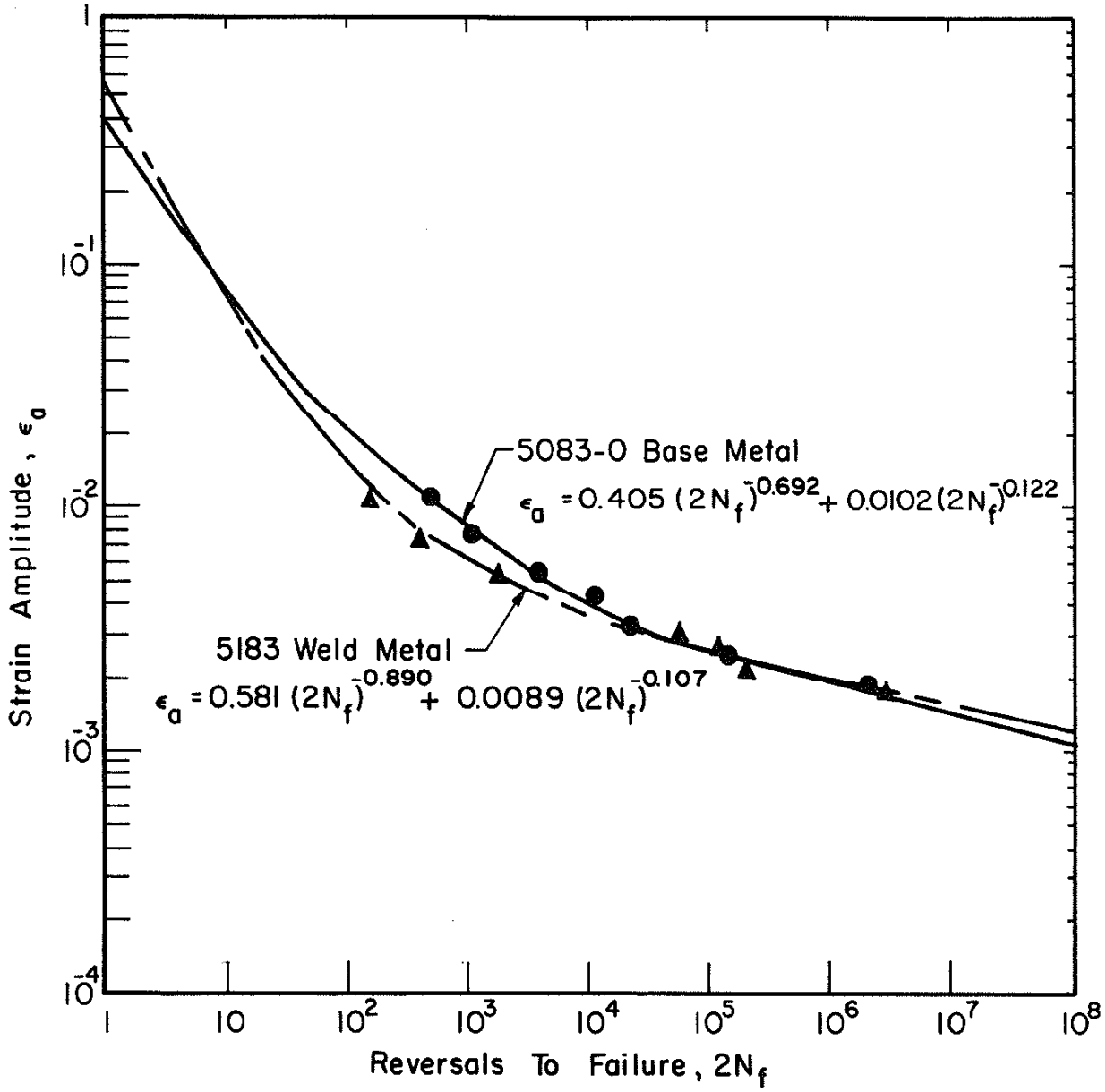

FIGURE 17. COMPARATIVE STRAIN-LIFE PLOT OF ALUMINUM 5083-O BASE AND 5183 WELD METAL FATIGUE BEHAVIOR.

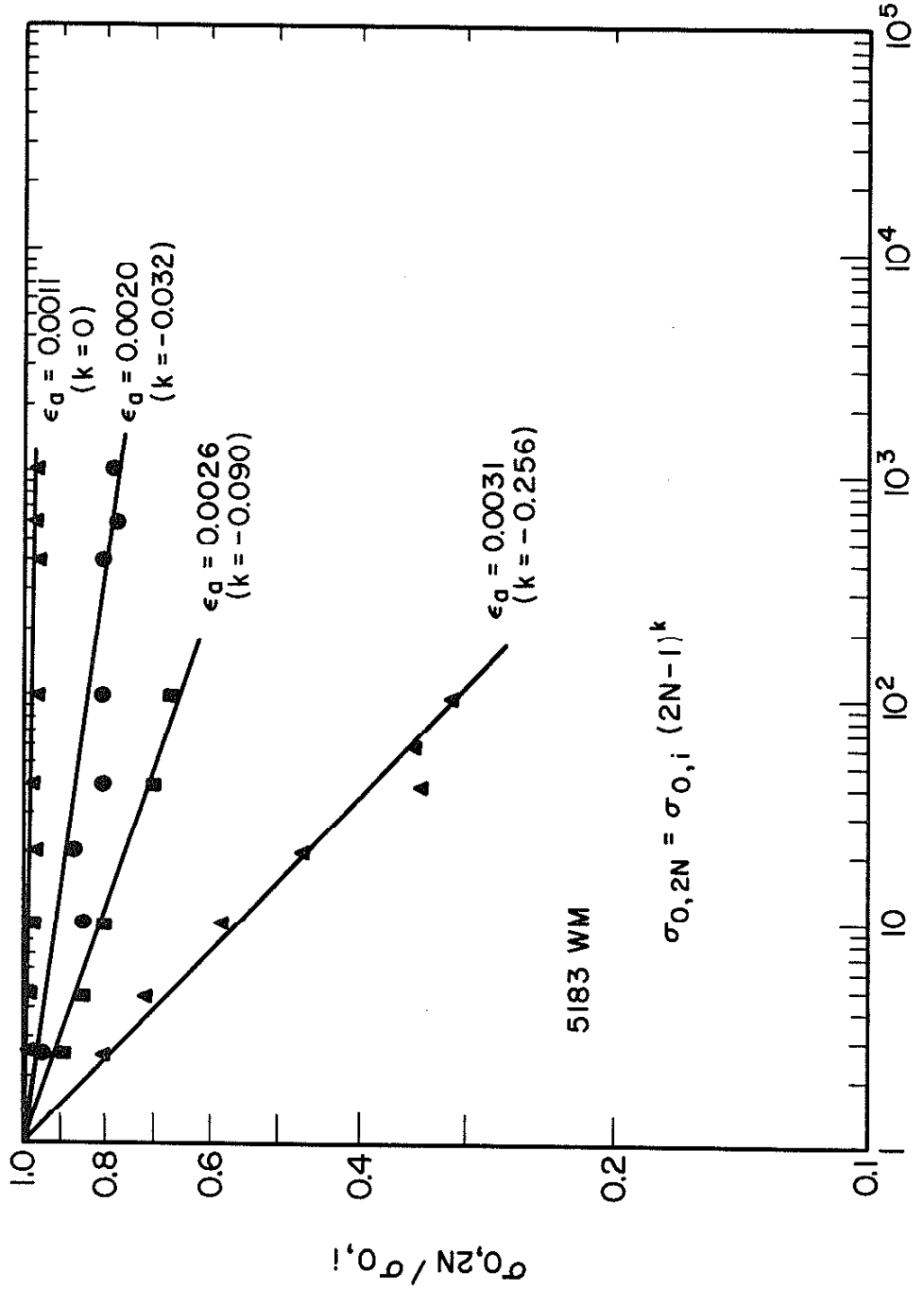

FIGURE 18. NORMALIZED MEAN STRESS RELAXATION BEHAVIOR OF 5183 ALUMINUM WELD METAL.

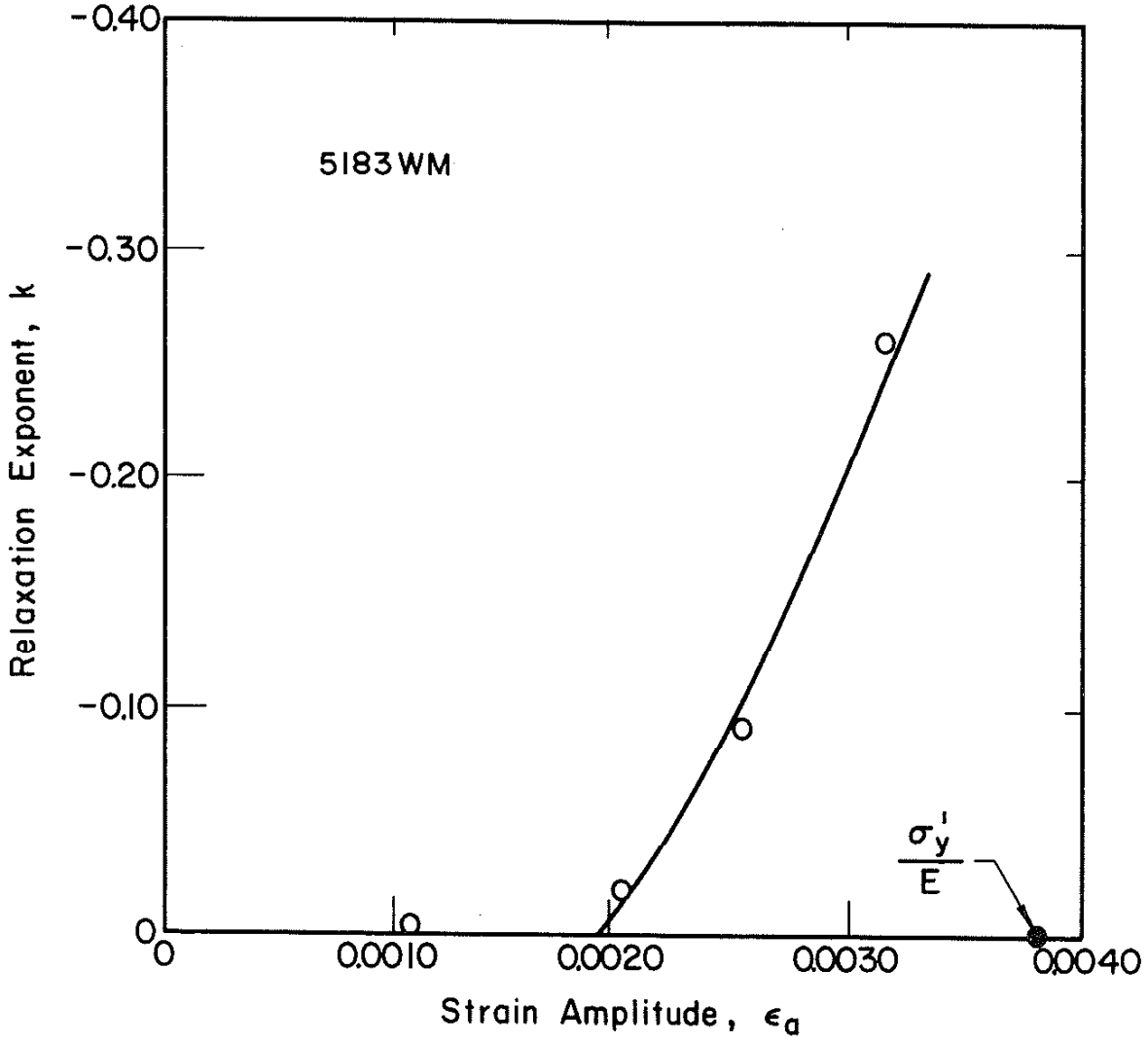

FIGURE 19. MEAN STRESS RELAXATION EXPONENT (k) AS A FUNCTION OF THE STRAIN AMPLITUDE FOR 5183 ALUMINUM WELD METAL.

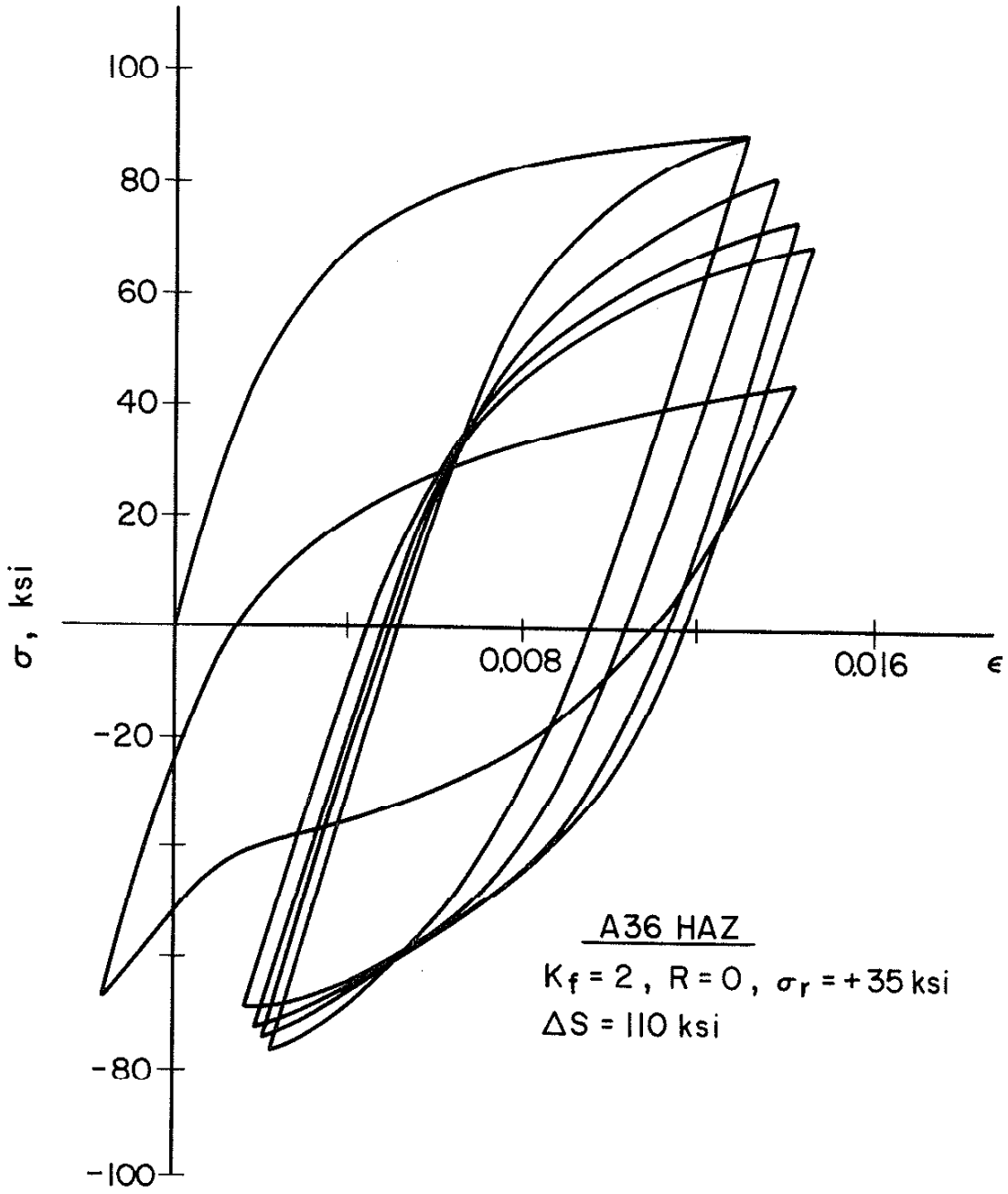

FIGURE 20. STRESS-STRAIN RESPONSE OF A A36 SIMULATED HAZ SMOOTH SPECIMEN TESTED UNDER NEUBER CONDITIONS.

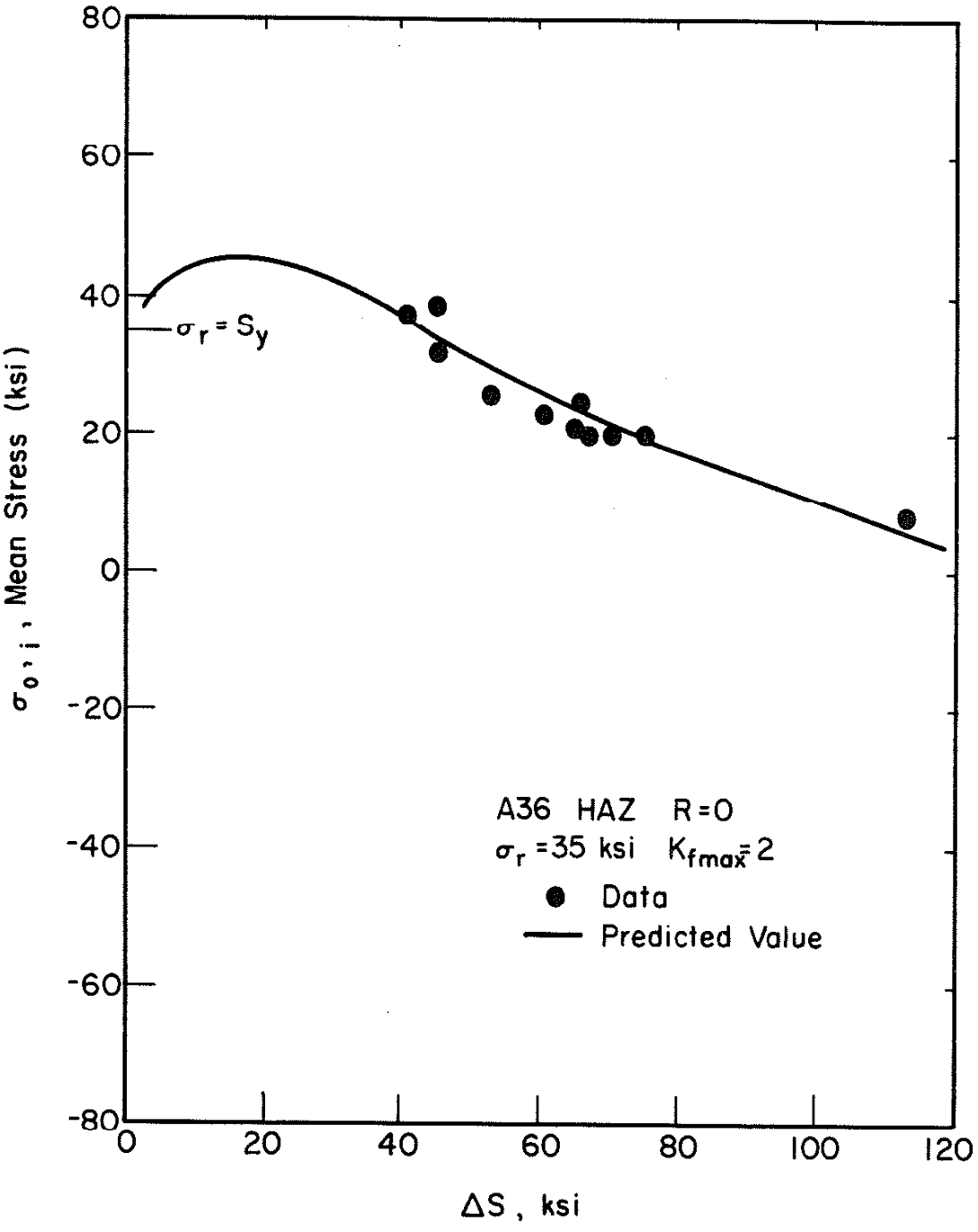

FIGURE 21. COMPARISON OF COMPUTER SIMULATION PREDICTION AND EXPERIMENTALLY DETERMINED SET-UP CYCLE INITIAL MEAN STRESS FOR A36 HAZ MATERIAL.

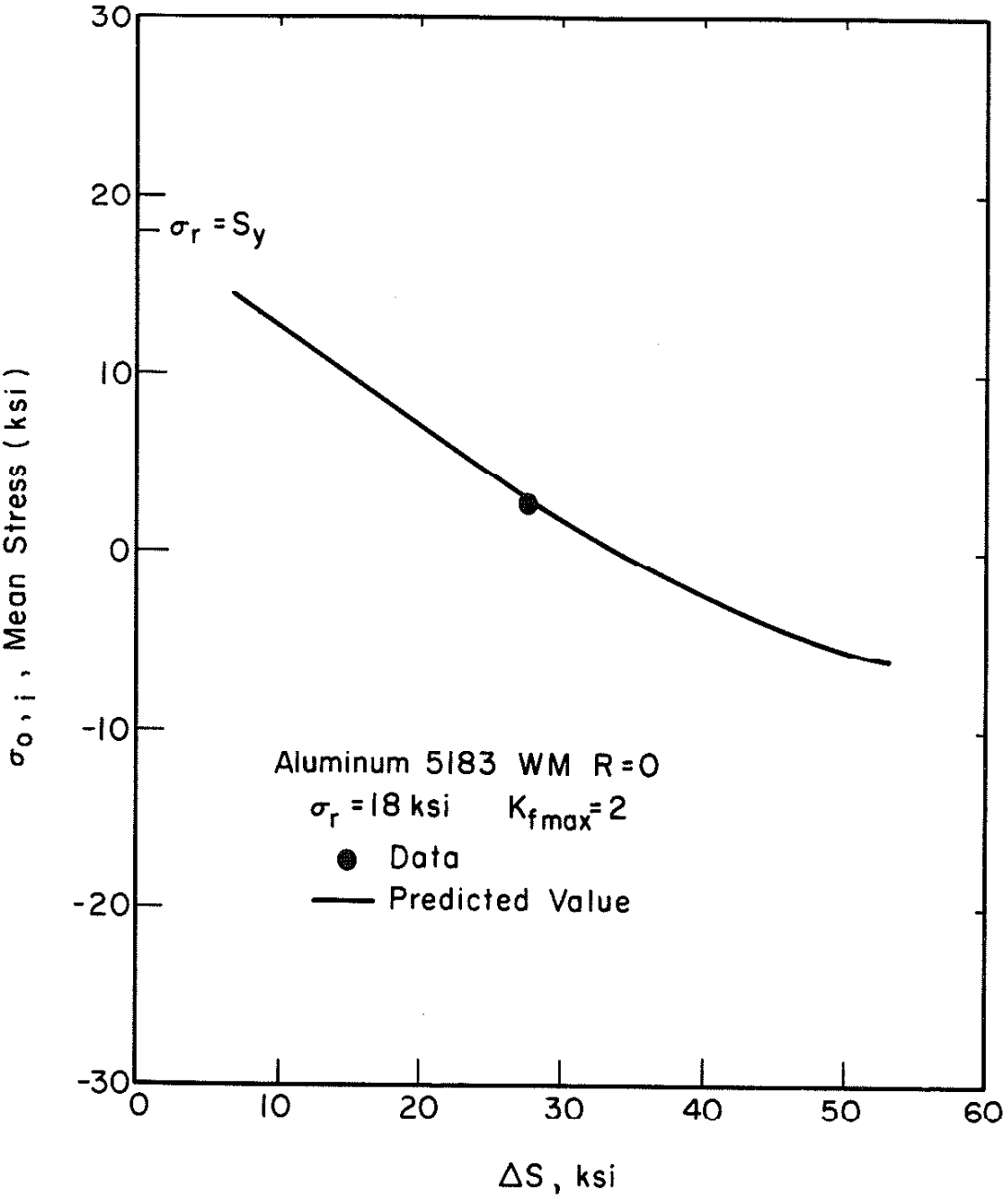

FIGURE 22. COMPARISON OF COMPUTER SIMULATION PREDICTION AND EXPERIMENTALLY DETERMINED SET-UP CYCLE INITIAL MEAN STRESS FOR 5183 ALUMINUM WELD METAL.

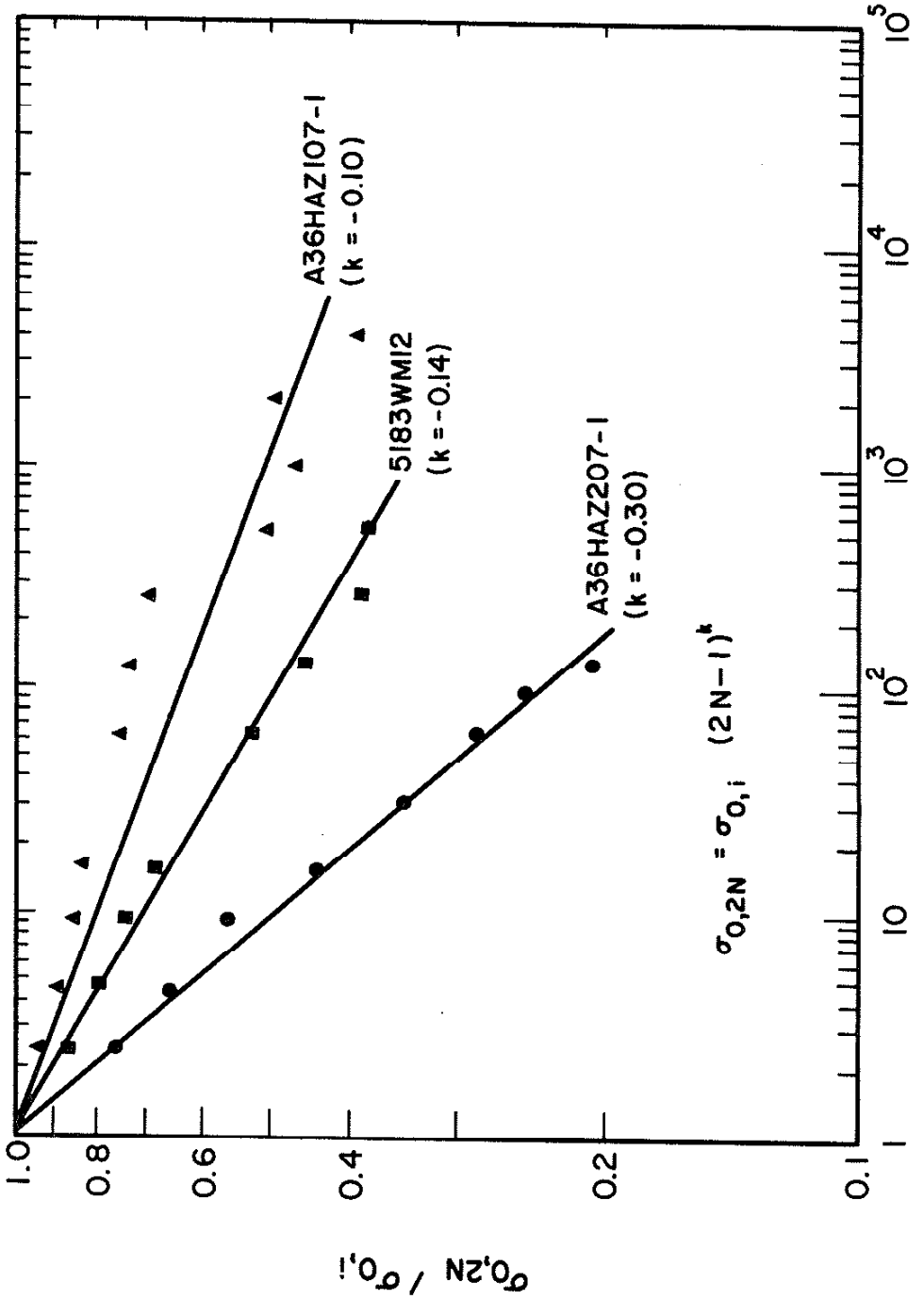

FIGURE 23. NORMALIZED MEAN STRESS RELAXATION BEHAVIOR OF UNCYCLED (VIRGIN) A36 HAZ MATERIAL AND 5183 ALUMINUM WELD METAL UNDER NEUBER CONTROL CONDITIONS.

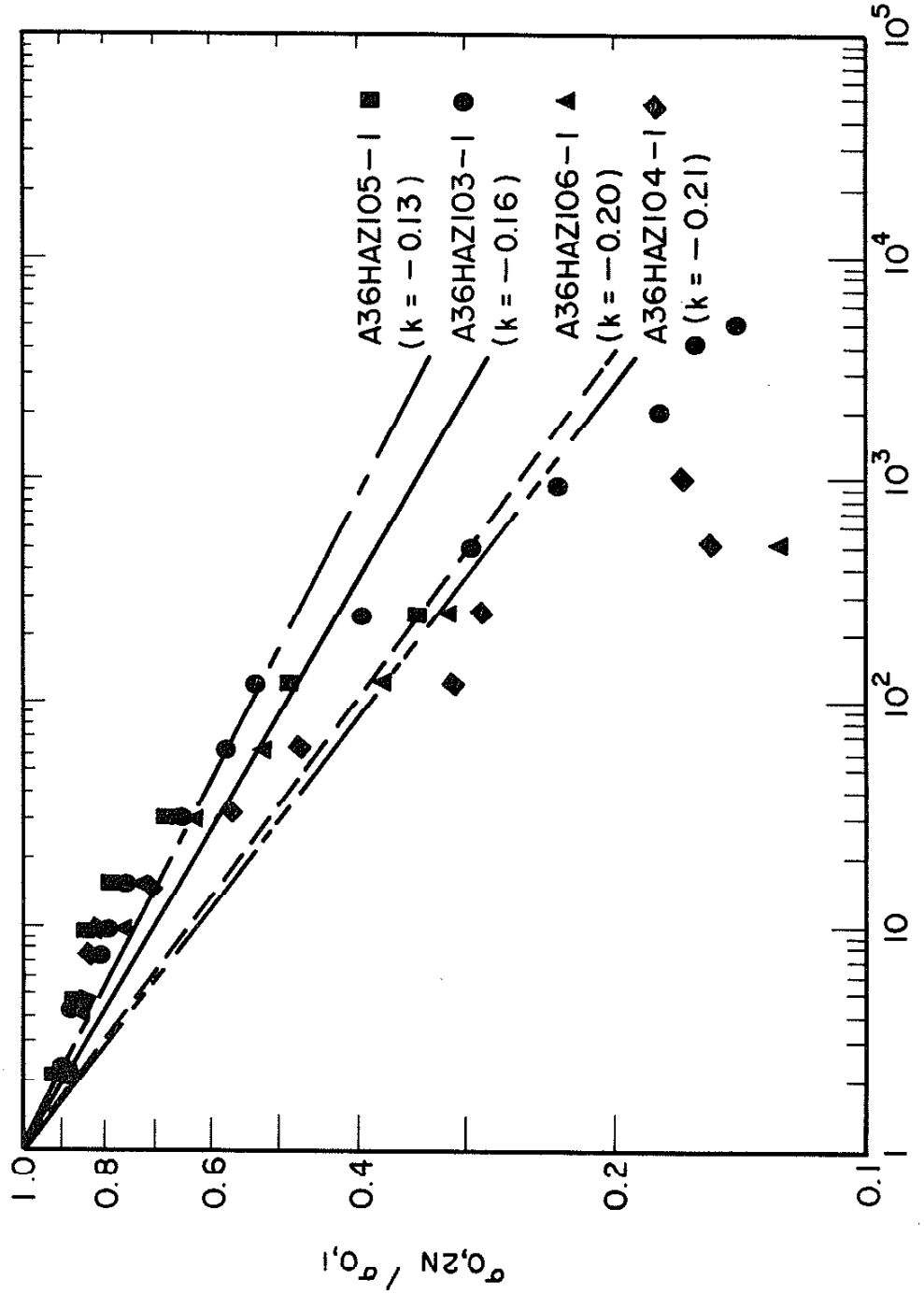

FIGURE 24. NORMALIZED MEAN STRESS RELAXATION BEHAVIOR OF UNCYCLED (VIRGIN) A36 HAZ MATERIAL UNDER NEUBER CONTROL CONDITIONS.

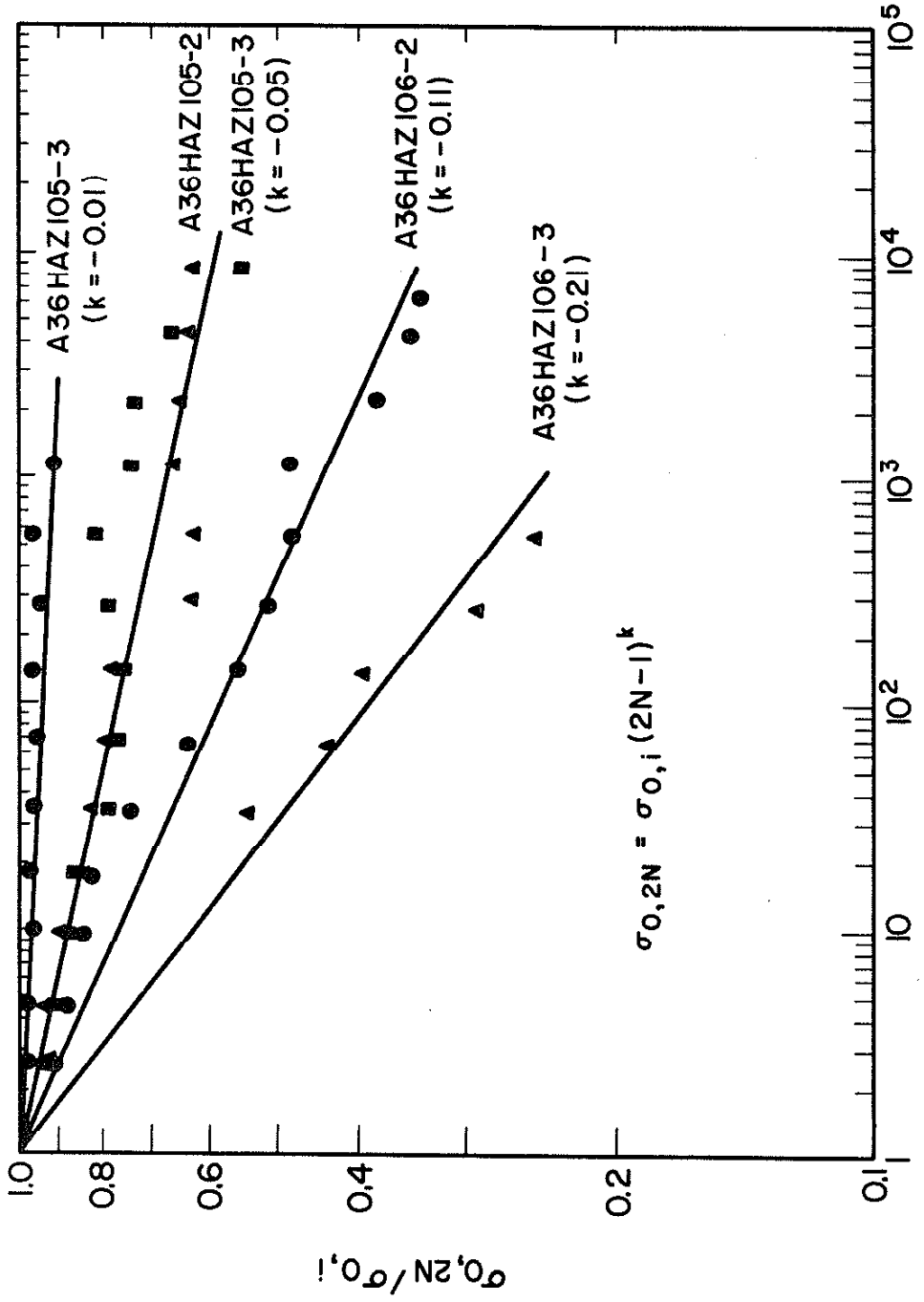

FIGURE 25. NORMALIZED MEAN STRESS RELAXATION BEHAVIOR OF PRECYCLED (STABILIZED) A36 HAZ MATERIAL UNDER NEUBER CONTROL CONDITIONS.

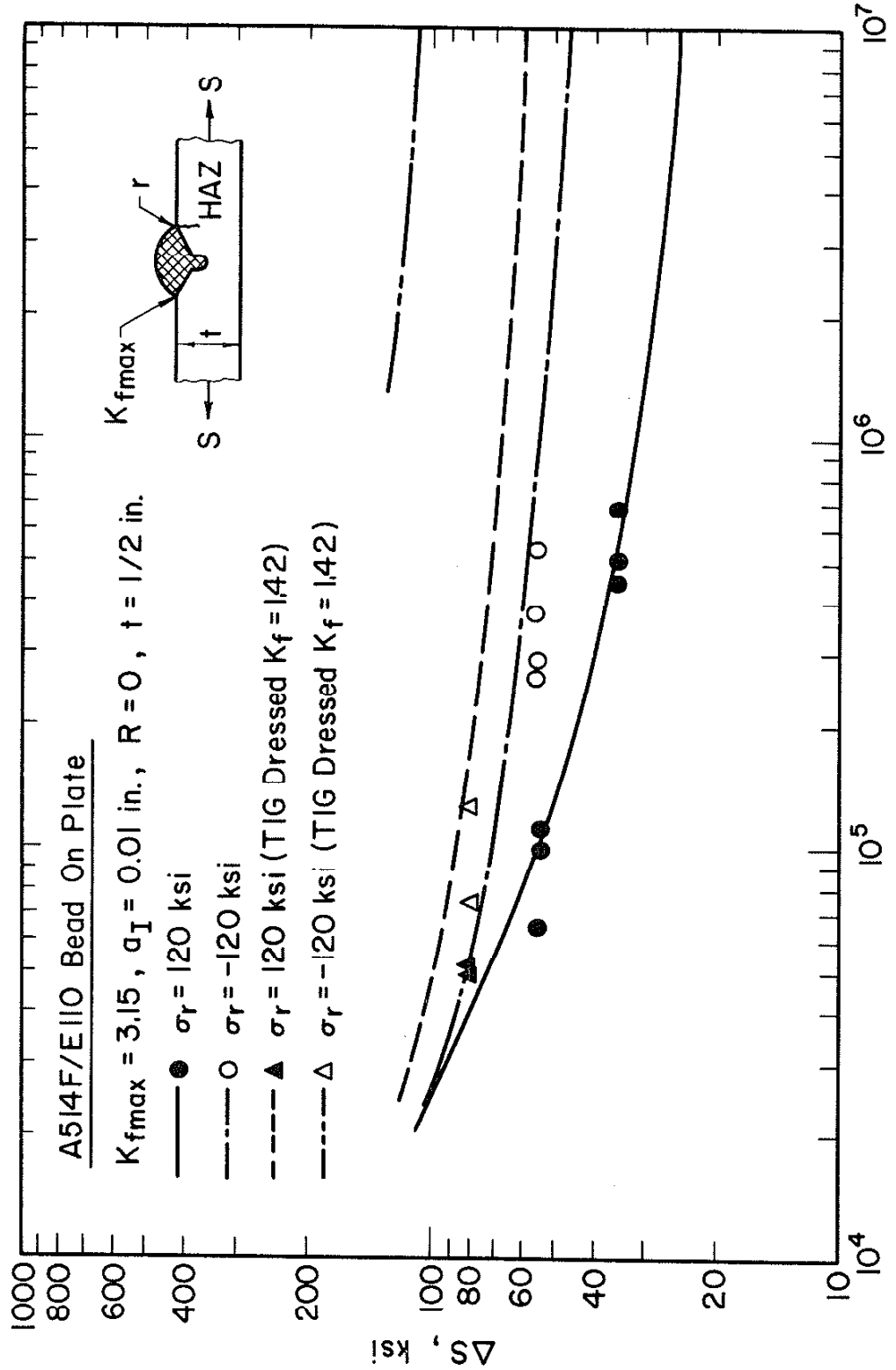

FIGURE 26. TOTAL FATIGUE LIFE PREDICTIONS AND EXPERIMENTAL RESULTS FOR A514F/E110 BEAD ON PLATE WELDMENTS WITH TENSILE AND COMPRESSIVE RESIDUAL STRESSES.

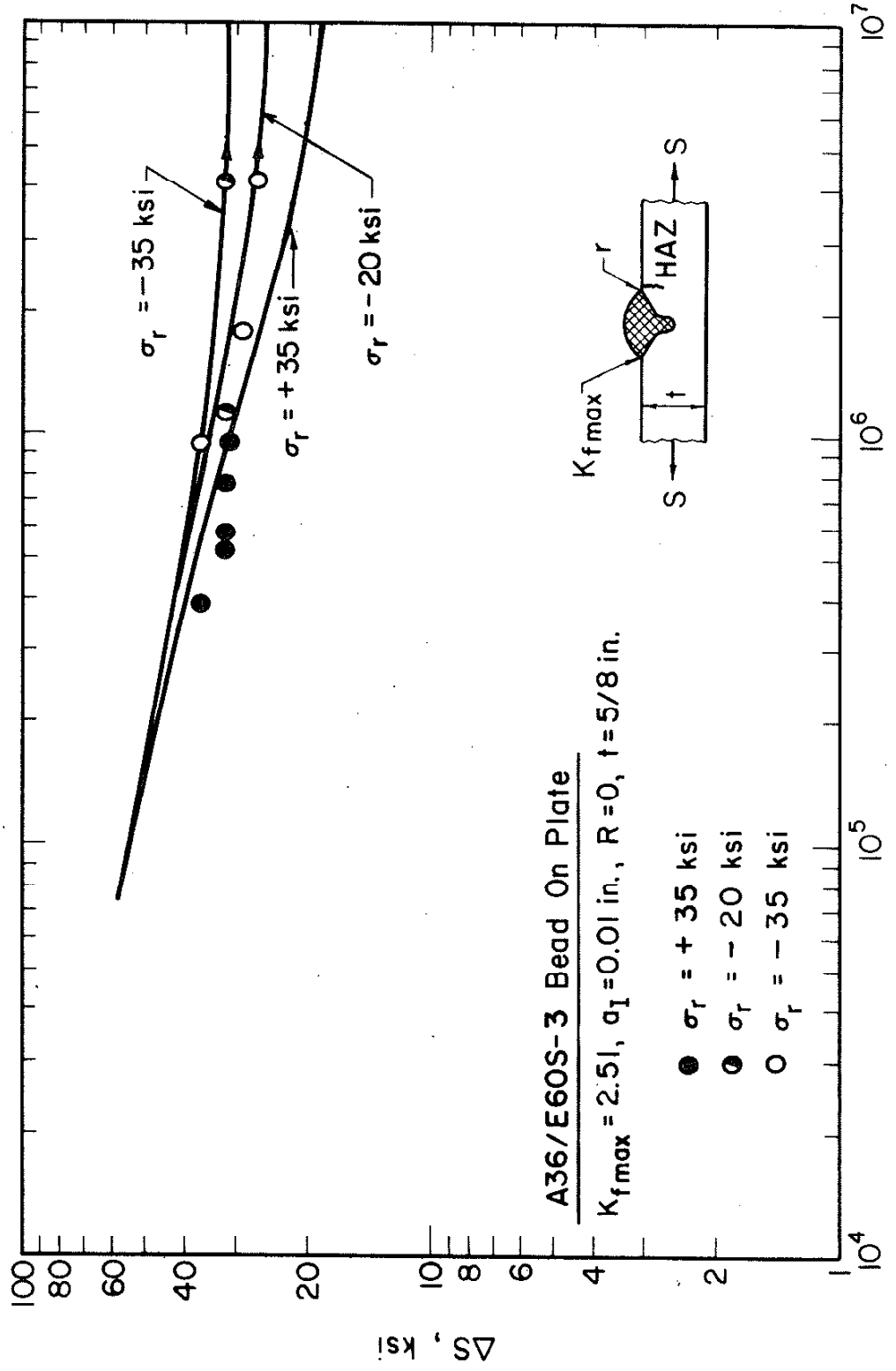

FIGURE 27. TOTAL FATIGUE LIFE PREDICTIONS AND EXPERIMENTAL RESULTS FOR A36/E60S-3 BEAD ON PLATE WELDMENTS WITH TENSILE AND COMPRESSIVE RESIDUAL STRESSES.

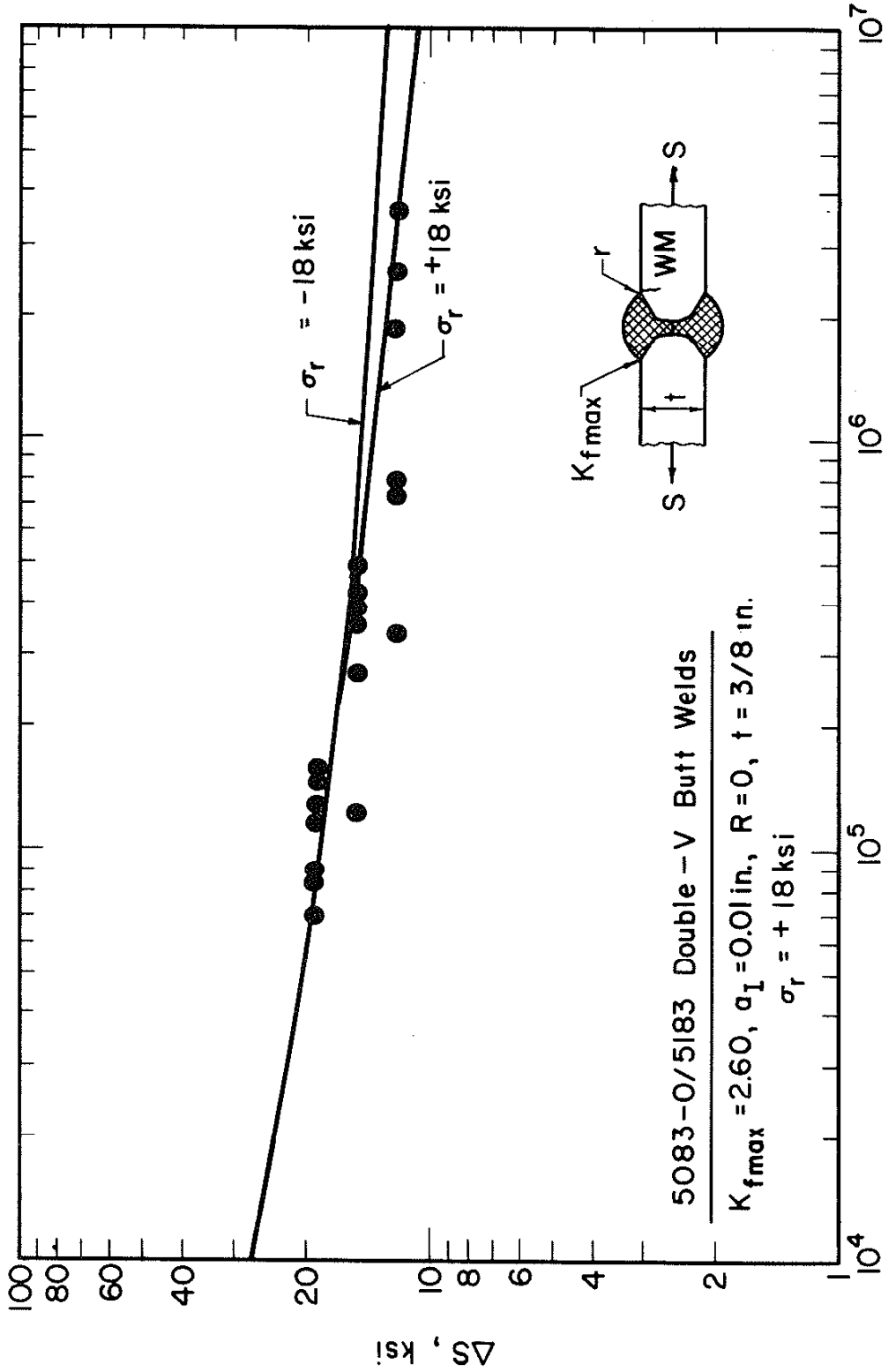

FIGURE 28. TOTAL FATIGUE LIFE PREDICTIONS AND EXPERIMENTAL RESULTS FOR 5083-O/5183 3/8 IN. (10 mm) BUTT WELDS.

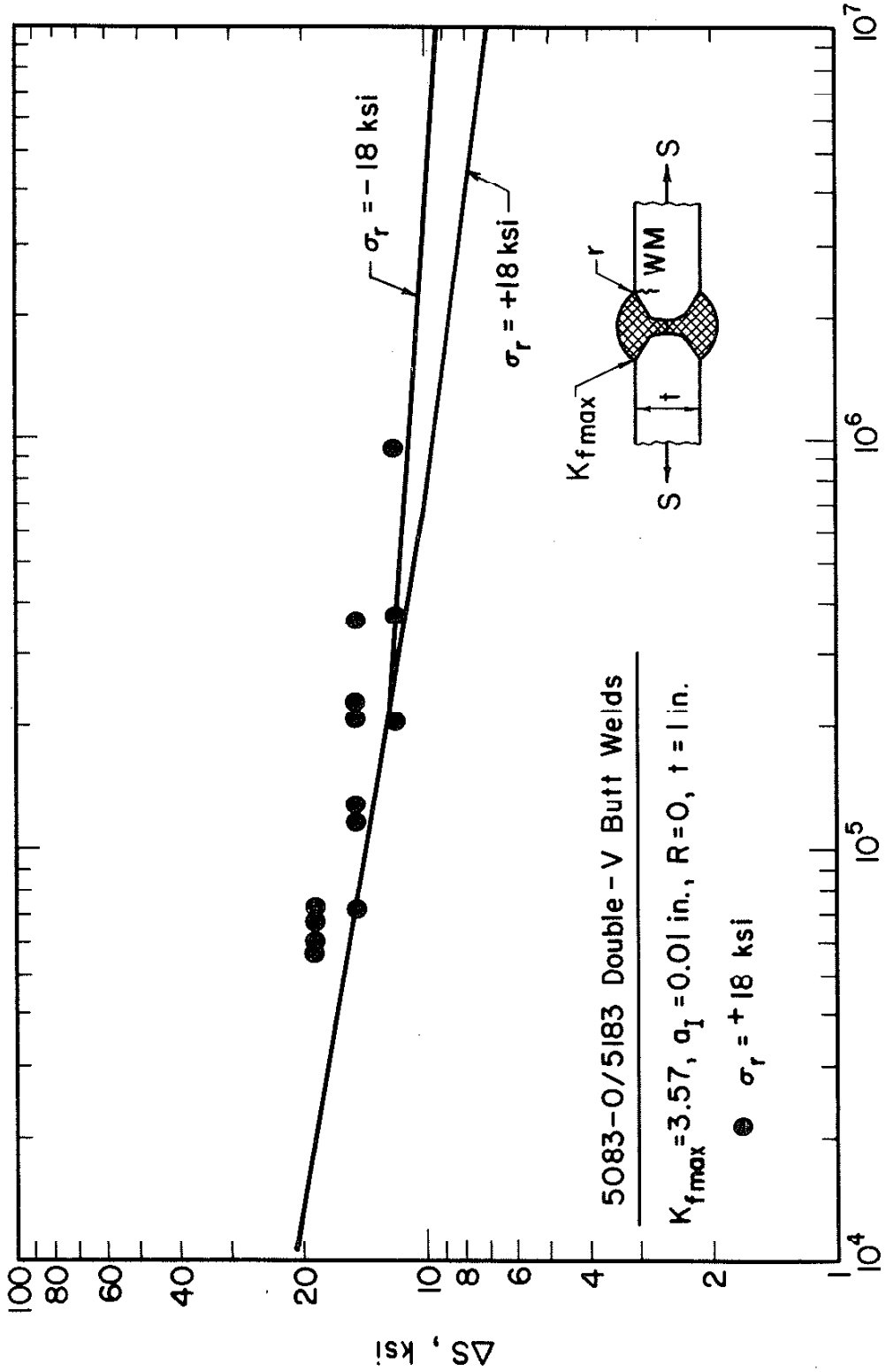

FIGURE 29. TOTAL FATIGUE LIFE PREDICTIONS AND EXPERIMENTAL RESULTS FOR 5083-O/5183 1 IN. (25 mm) BUTT WELDS.

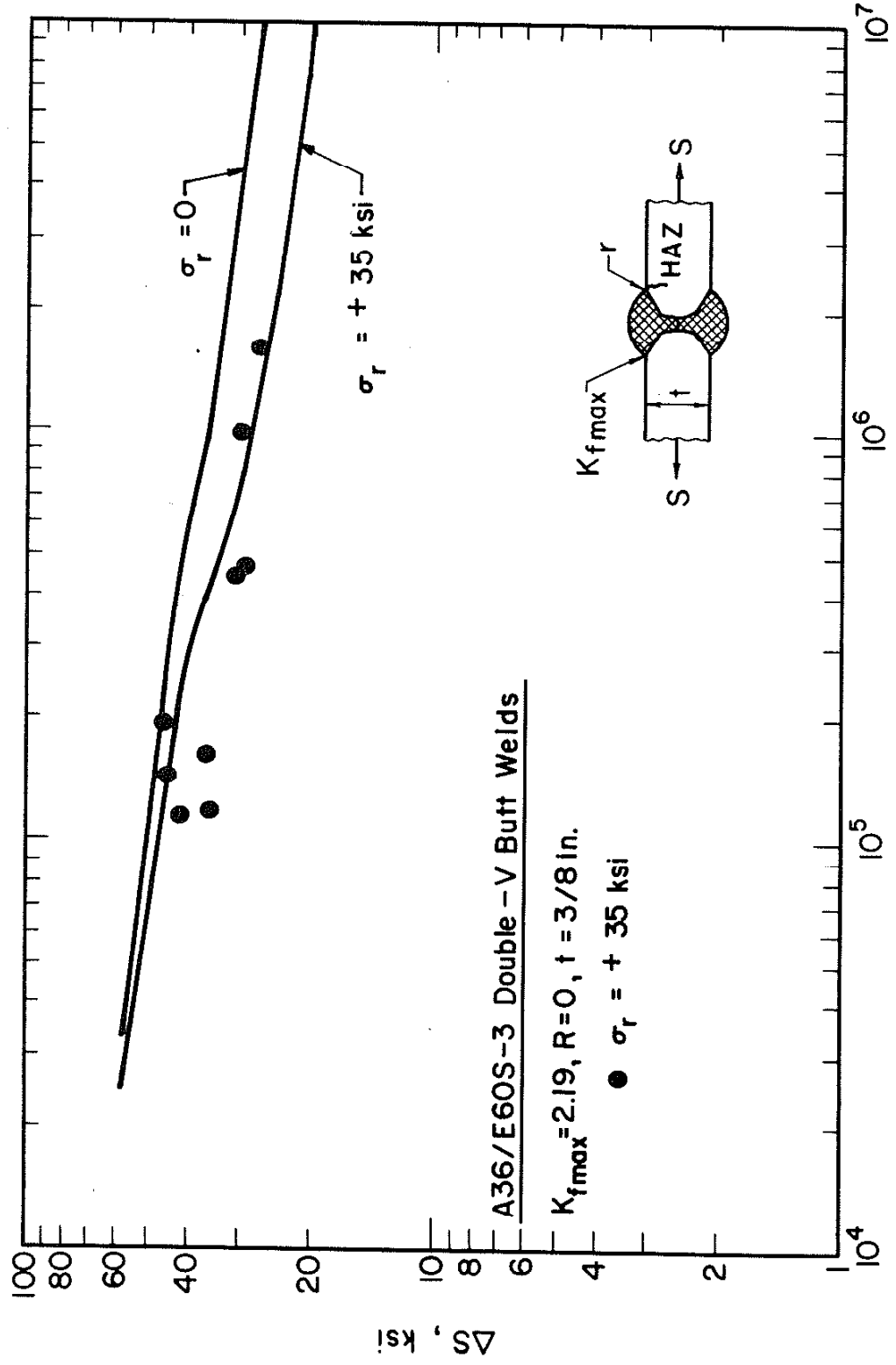

FIGURE 30. FATIGUE CRACK INITIATION LIFE PREDICTIONS AND EXPERIMENTAL RESULTS FOR 3/8 IN. (10 mm) A36/E60S-3 BUTT WELDS (REF. 20).

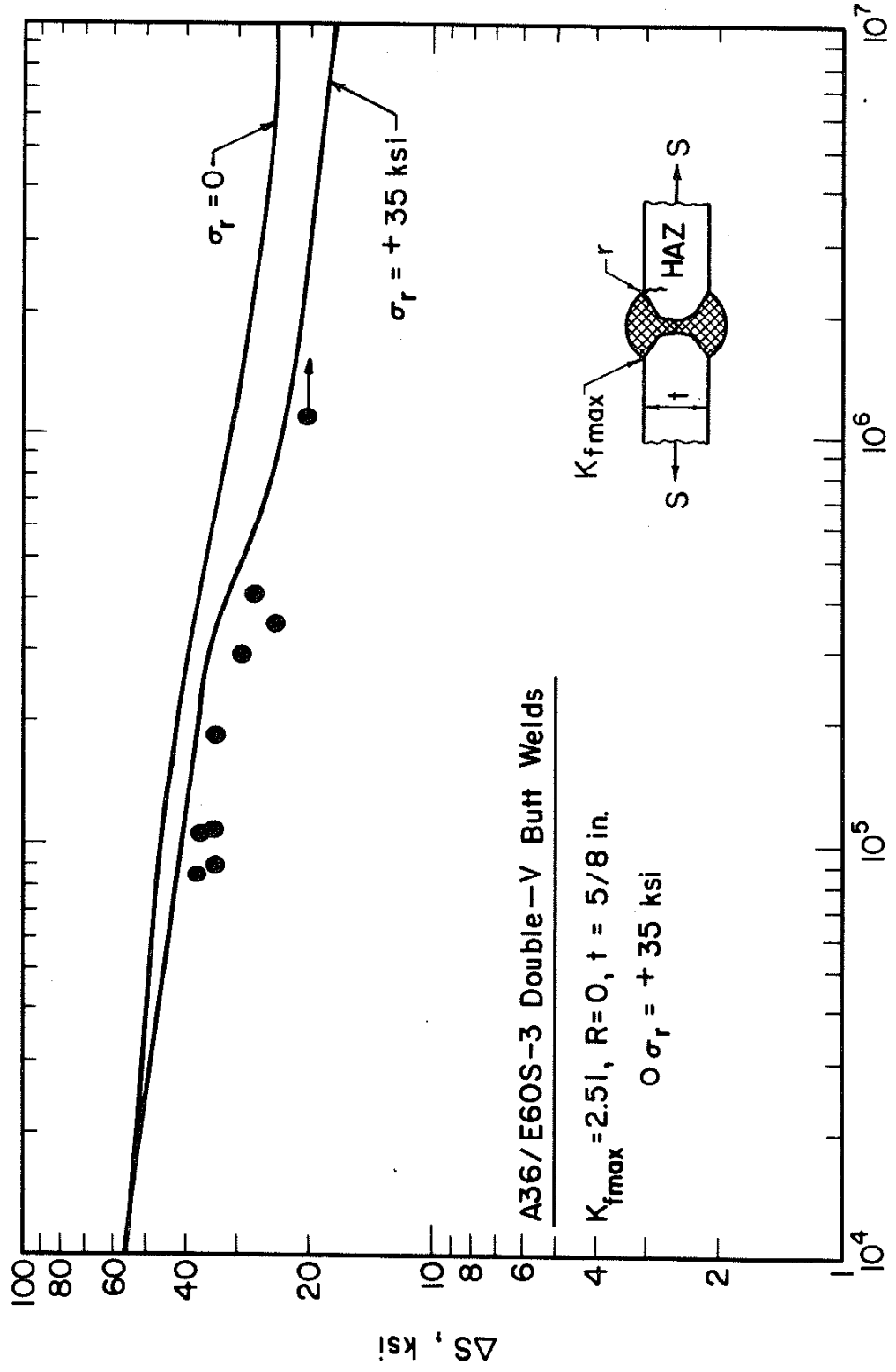

FIGURE 31. FATIGUE CRACK INITIATION LIFE PREDICTIONS AND EXPERIMENTAL RESULTS FOR 5/8 IN. (16 mm) A36/E60S-3 BUTT WELDS (REF. 20).

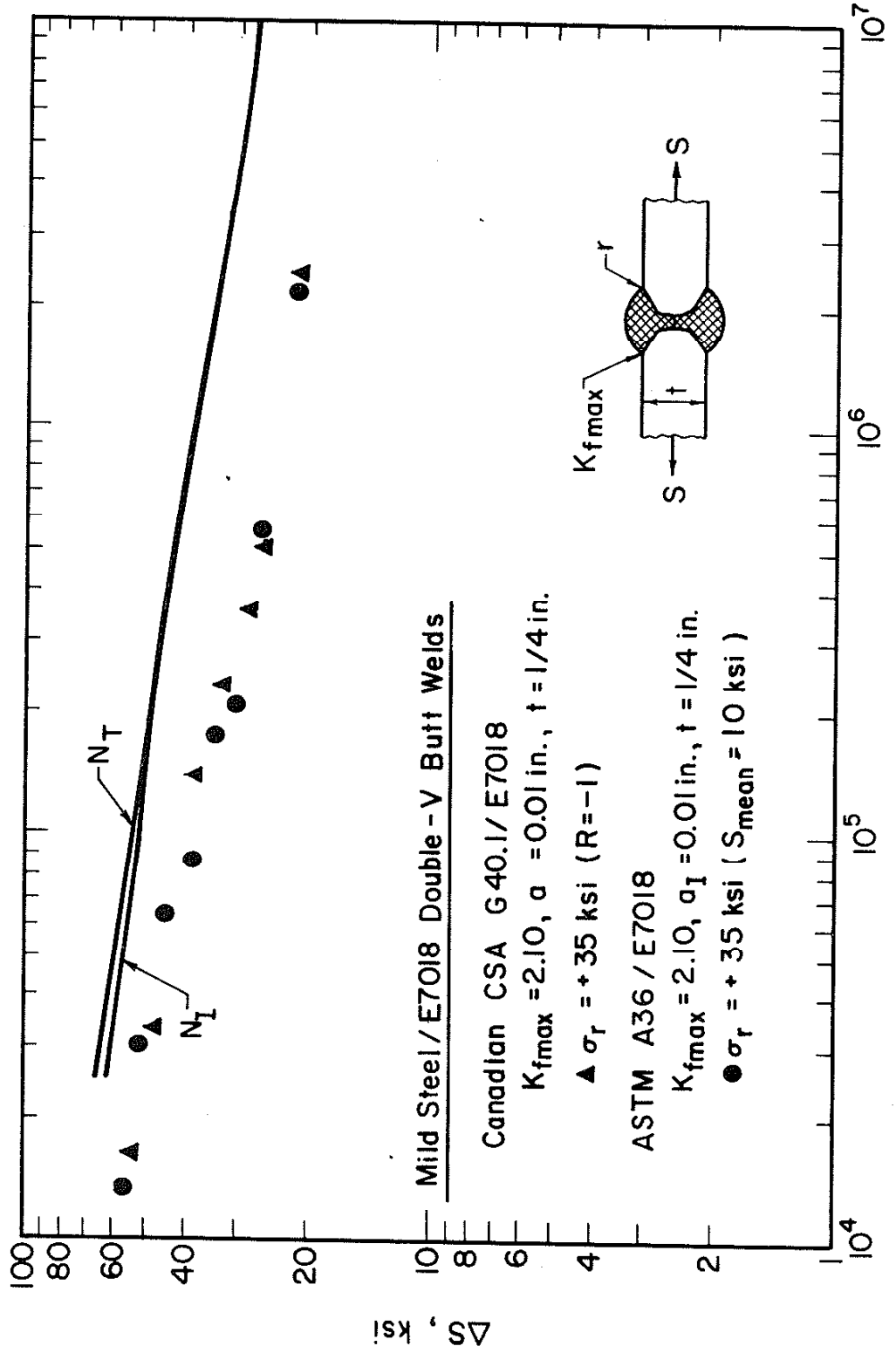

FIGURE 32. PREDICTIONS OF TOTAL FATIGUE LIFE AND FATIGUE CRACK INITIATION LIFE AND EXPERIMENTAL TOTAL LIFE DATA FOR MILD STEEL/E1018 BUTT WELDS (REF. 23).

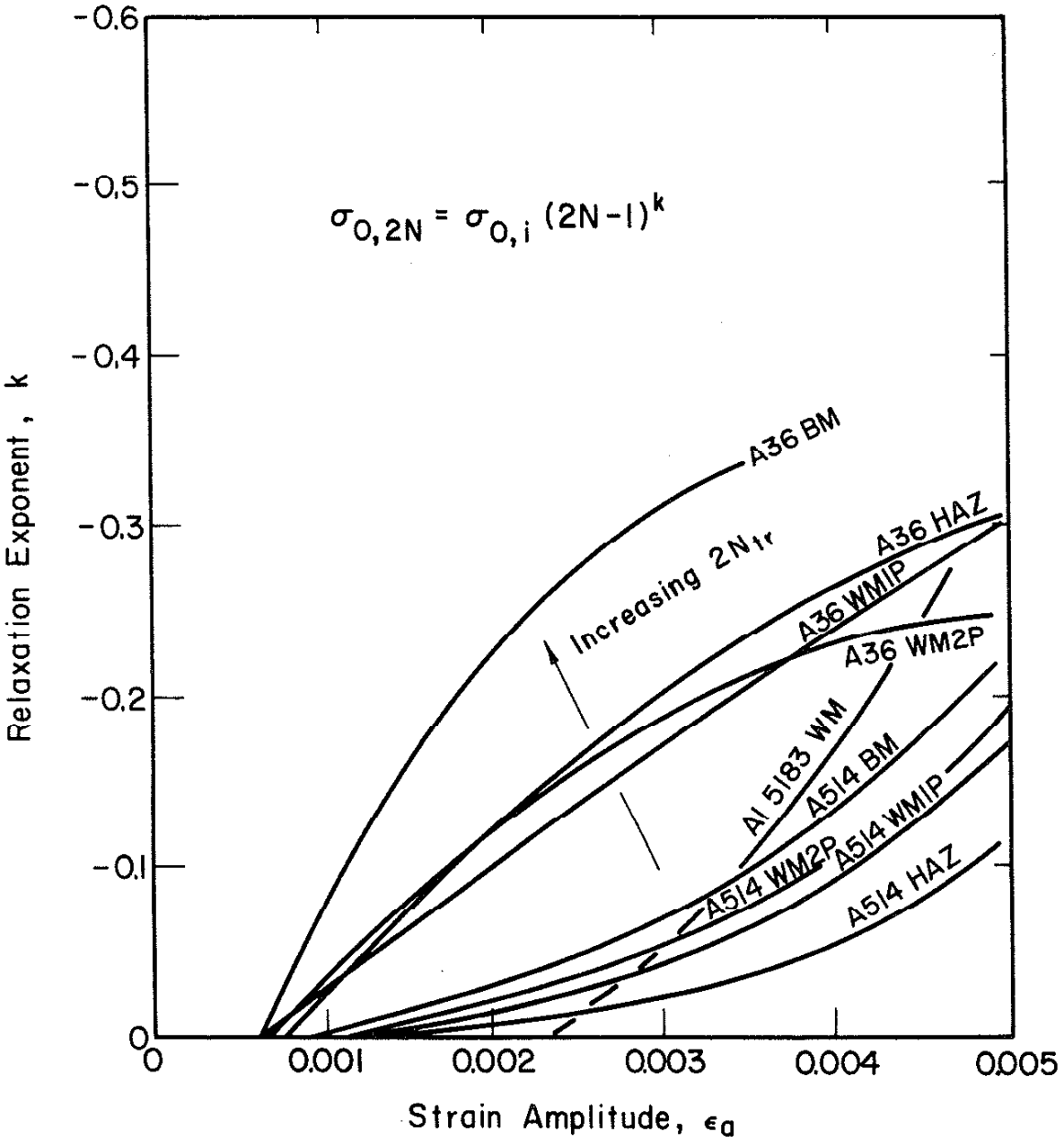

FIGURE 33. RELAXATION EXPONENT (k) AS A FUNCTION OF THE STRAIN AMPLITUDE FOR SEVERAL MATERIALS.

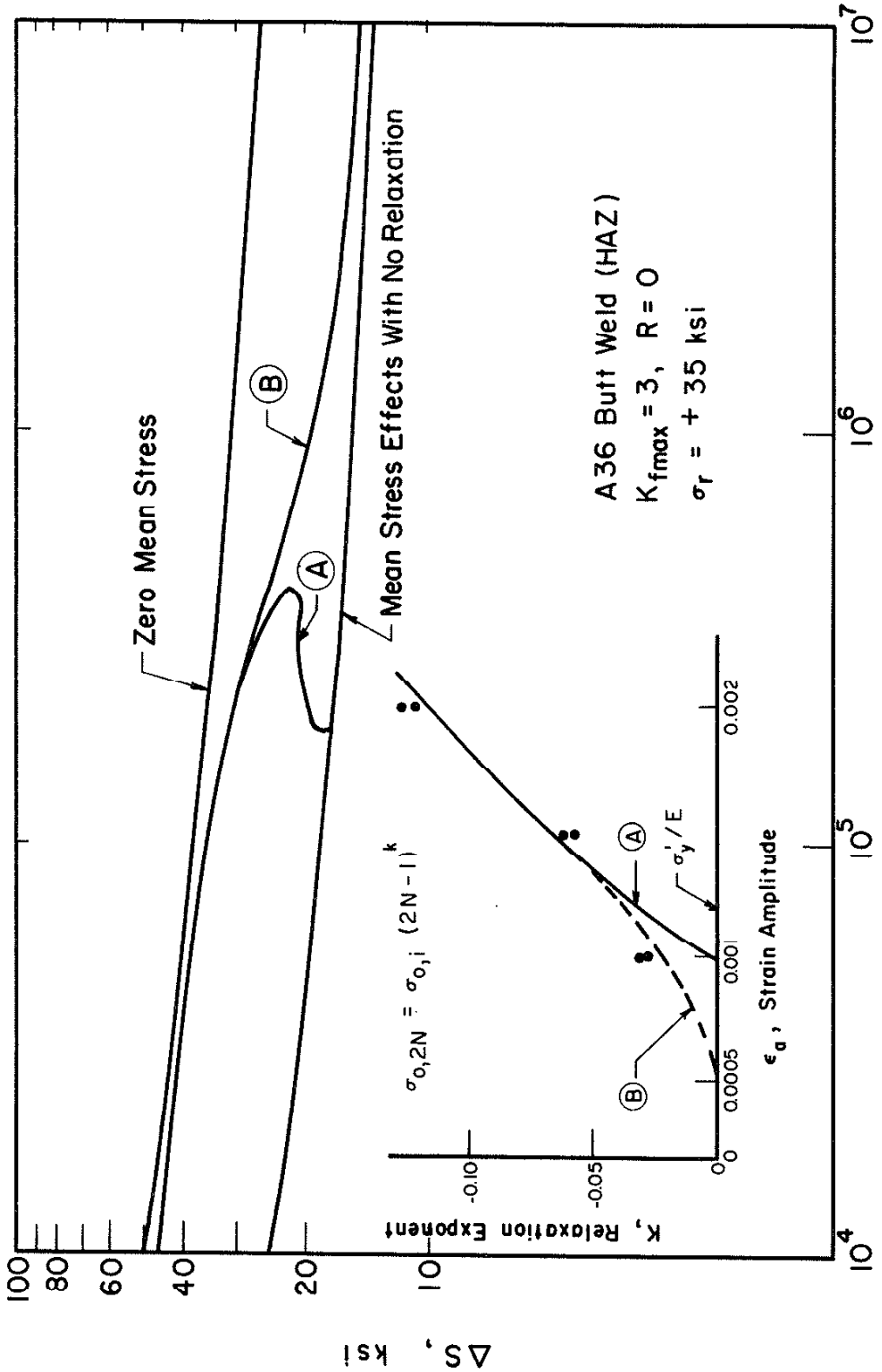

FIGURE 34. MEAN STRESS RELAXATION BEHAVIOR IN THE LOW k REGION AND ITS INFLUENCE ON PREDICTED CRACK INITIATION LIFE.

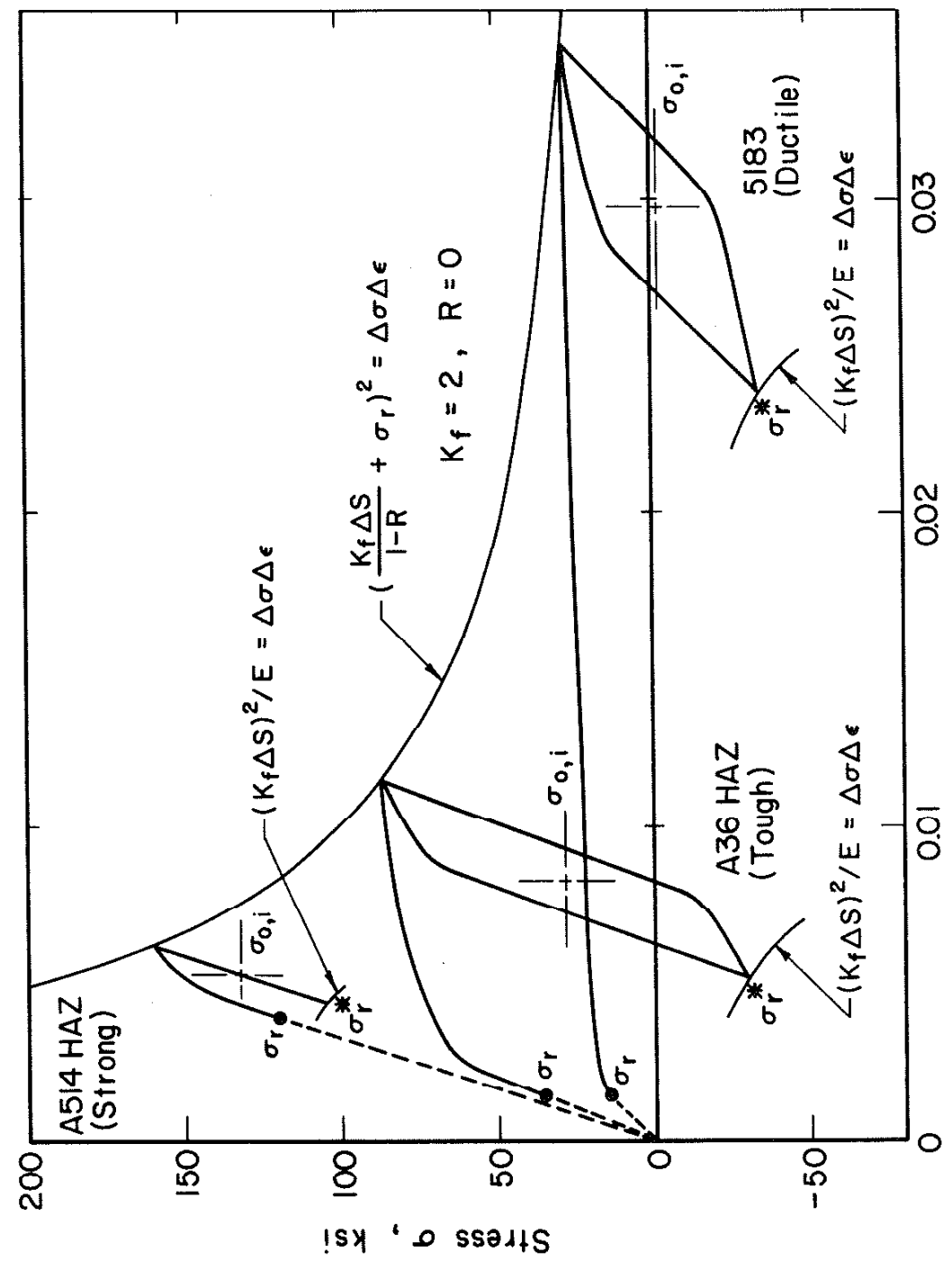

FIGURE 35. SET-UP CYCLE STRESS-STRAIN RESPONSE FOR A514 HAZ (STRONG), A36 HAZ (TOUGH), AND 5183 WM (DUCTILE) MATERIALS.

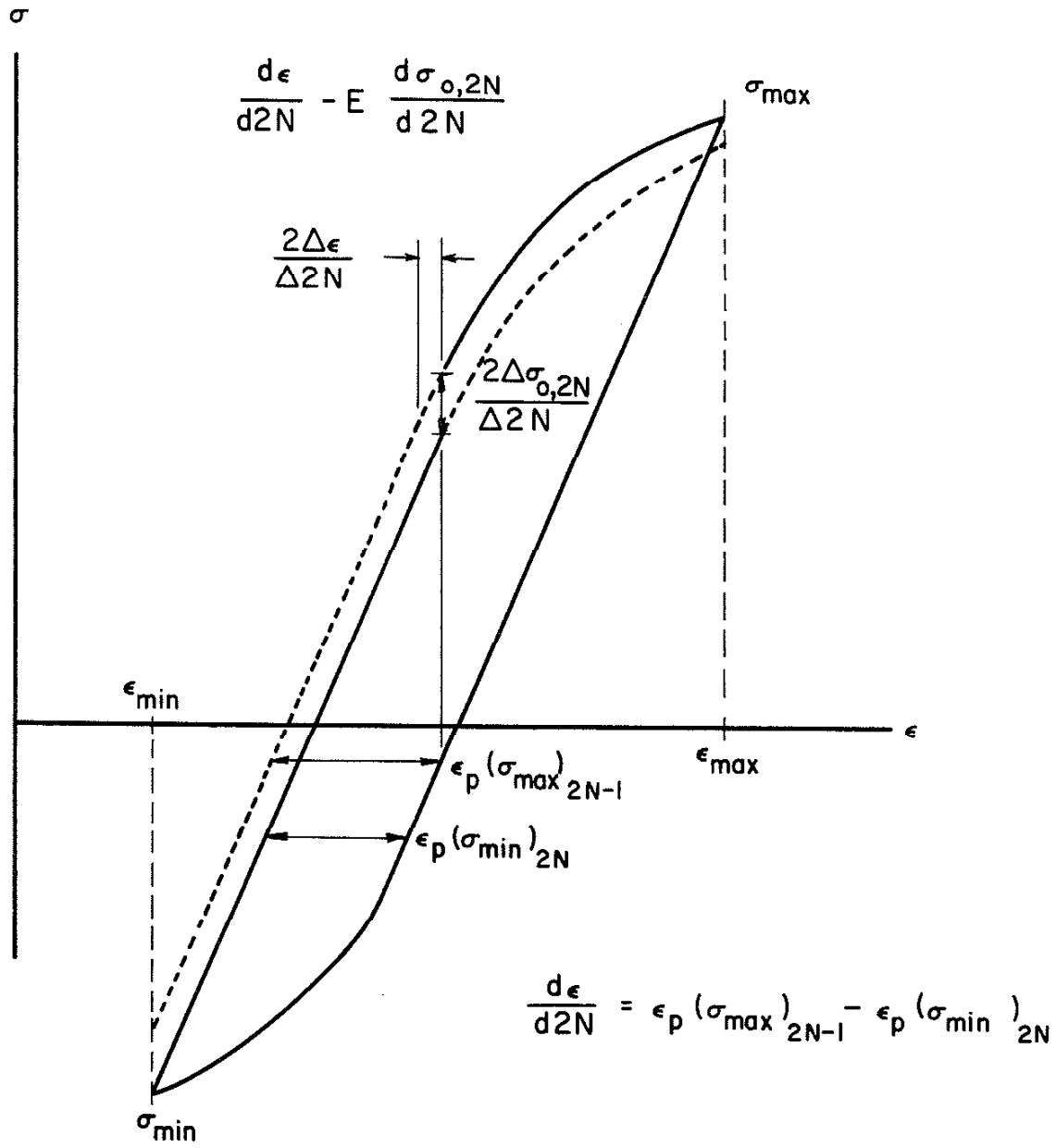

FIGURE 36. MEAN STRESS RELAXATION BEHAVIOR BASED ON LOOP NONCLOSURE AND UNEQUAL PLASTIC STRAINS (REF. 39).

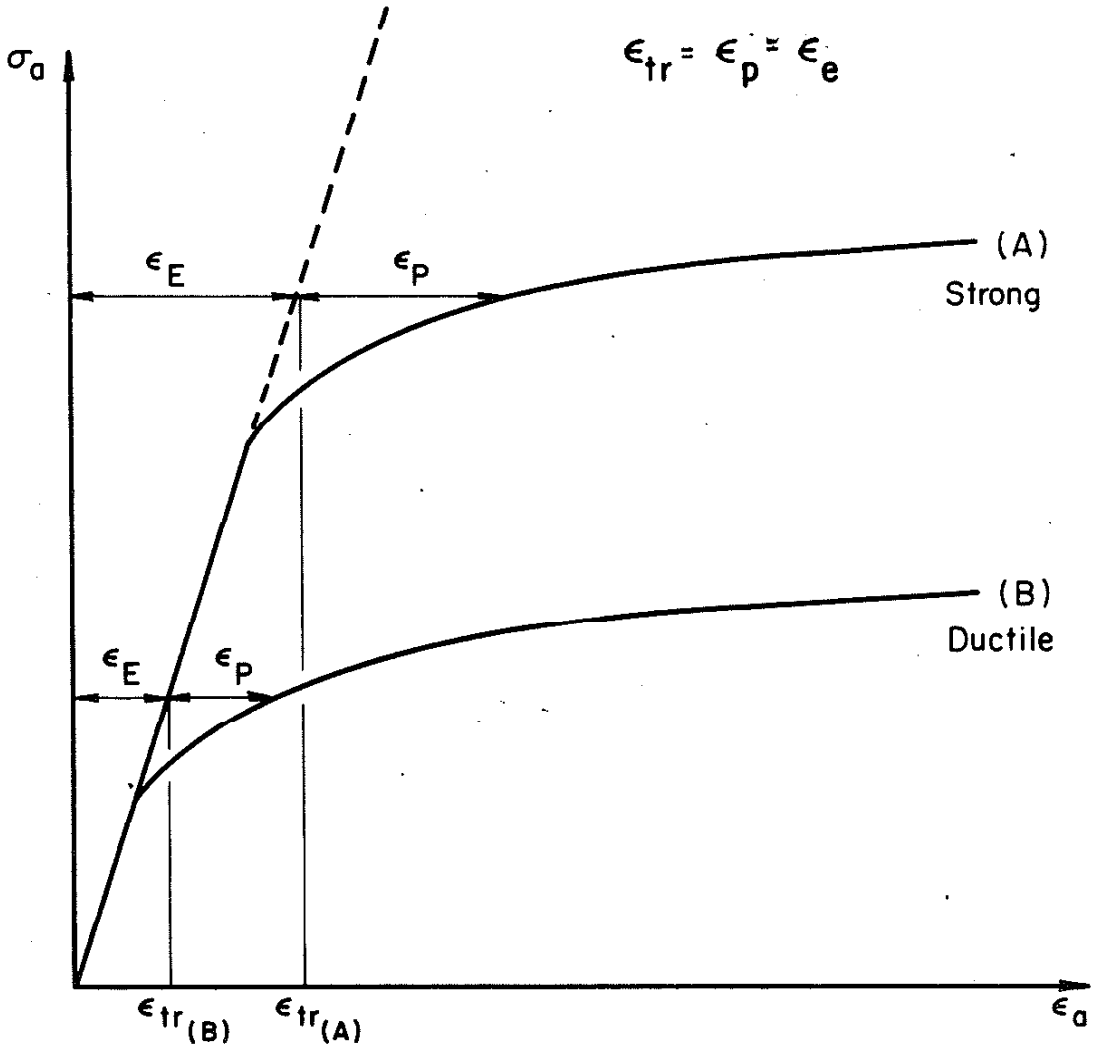

FIGURE 37. TRANSITION STRAIN (ϵ_{tr}) FOR STRONG (A) AND DUCTILE (B) MATERIALS.

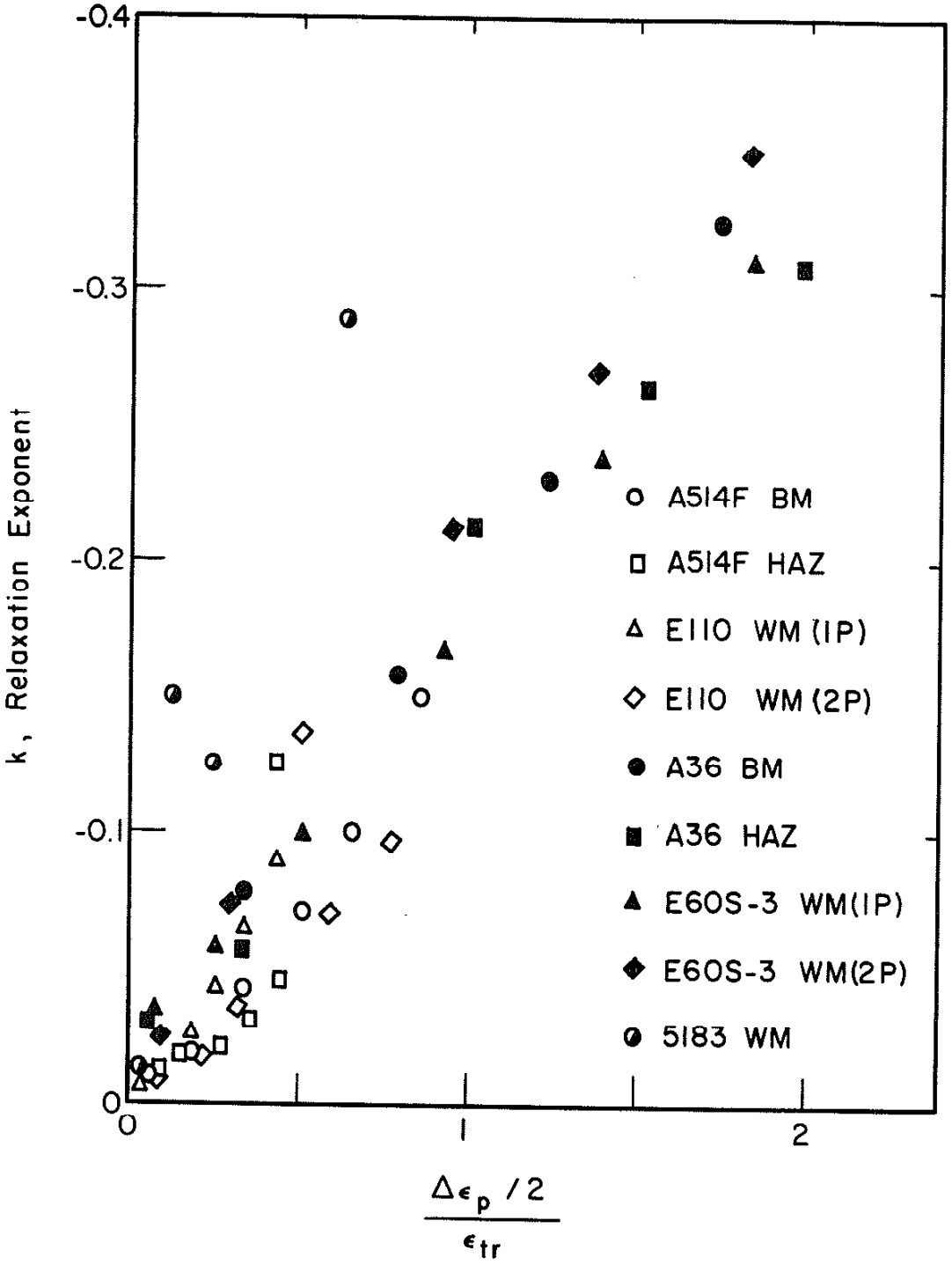

FIGURE 38. RELAXATION EXPONENT (k) AS A FUNCTION OF THE PLASTIC STRAIN AMPLITUDE NORMALIZED BY THE TRANSITION STRAIN (ϵ_{tr}).

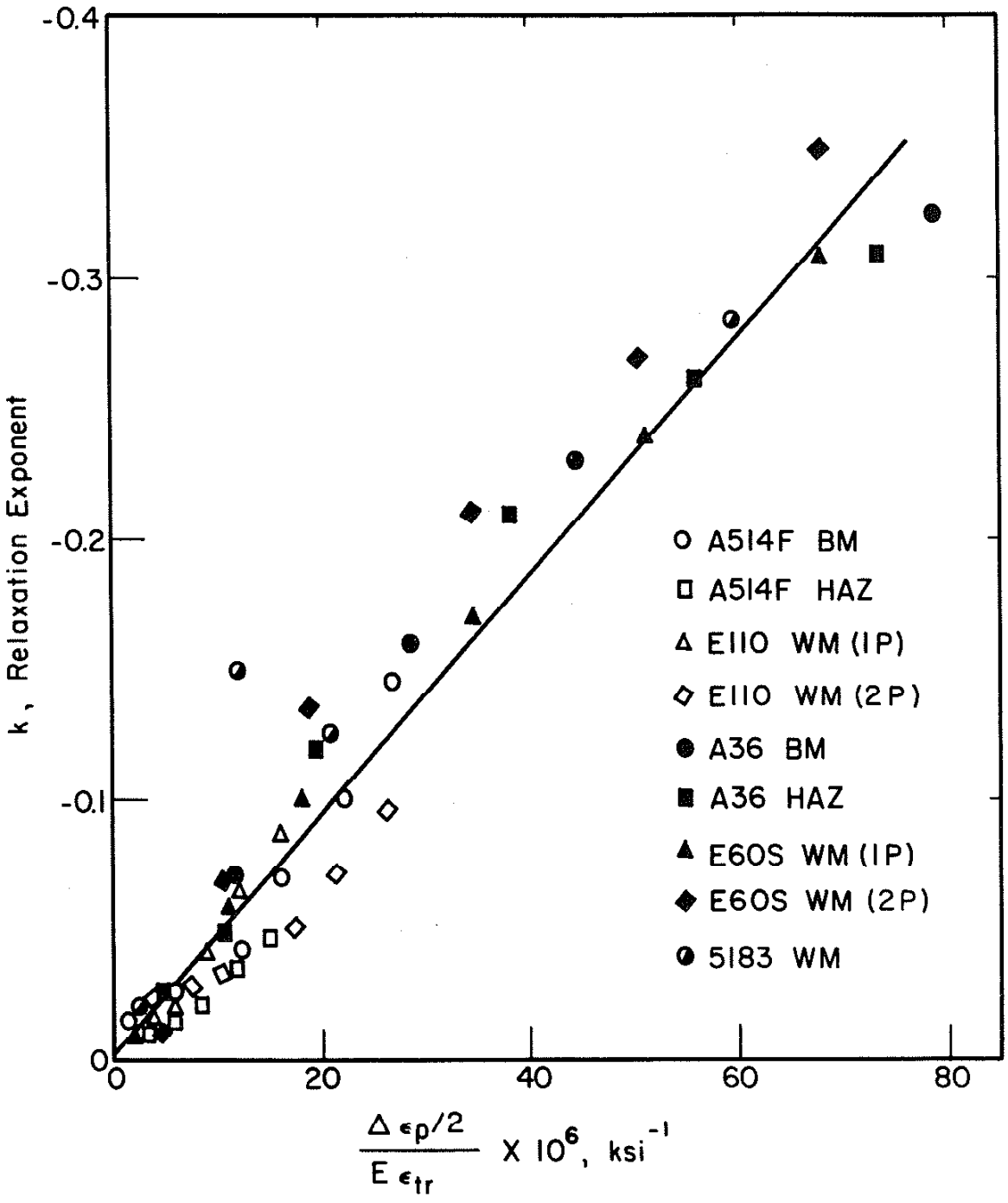

FIGURE 39. RELAXATION EXPONENT (k) AS A FUNCTION OF THE NORMALIZED PLASTIC STRAIN AMPLITUDE DIVIDED BY THE MODULUS FOR SEVERAL MATERIALS.

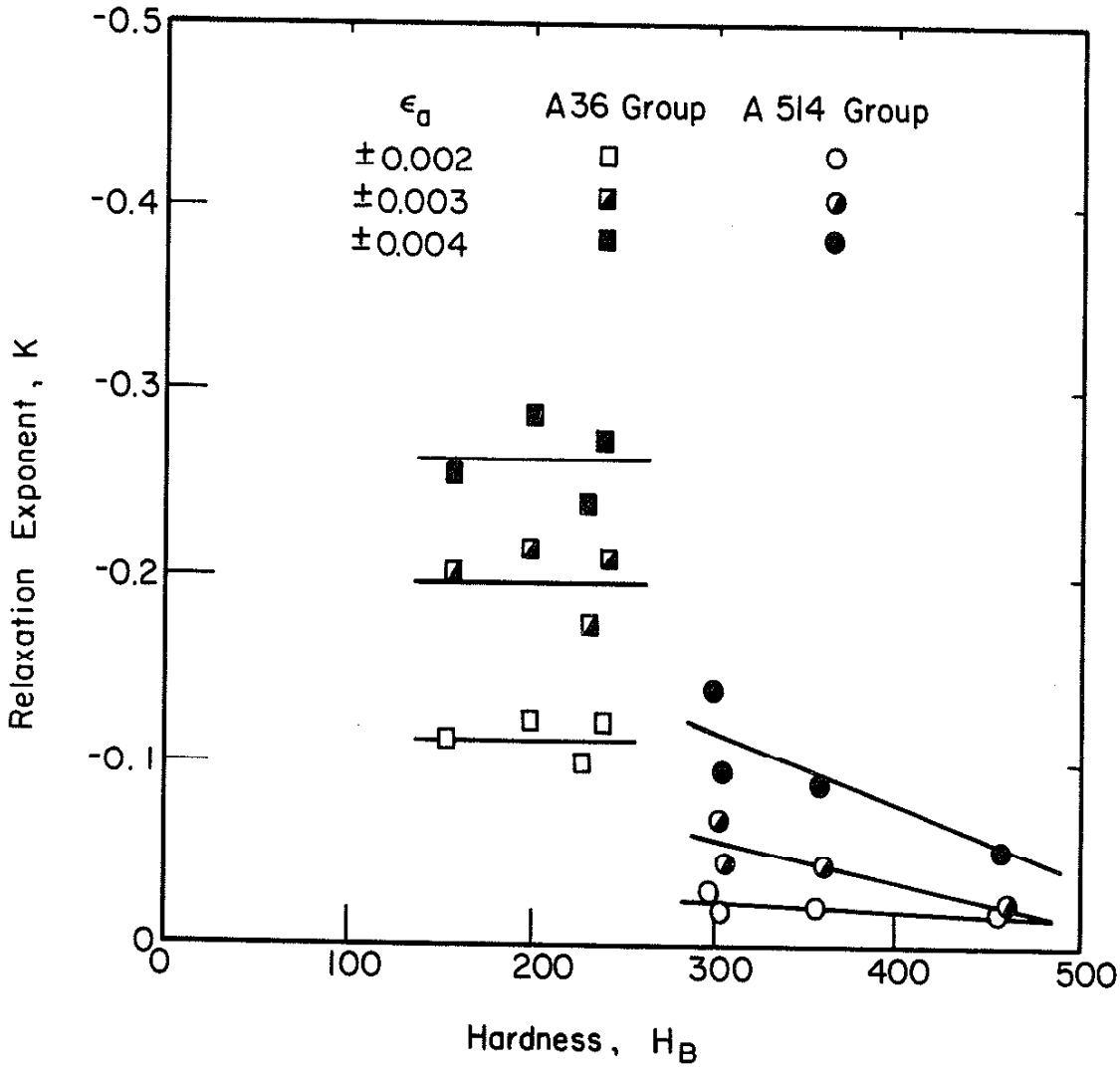

FIGURE 40. RELAXATION EXPONENT AS A FUNCTION OF HARDNESS FOR A36 AND A514 WELD MATERIALS.

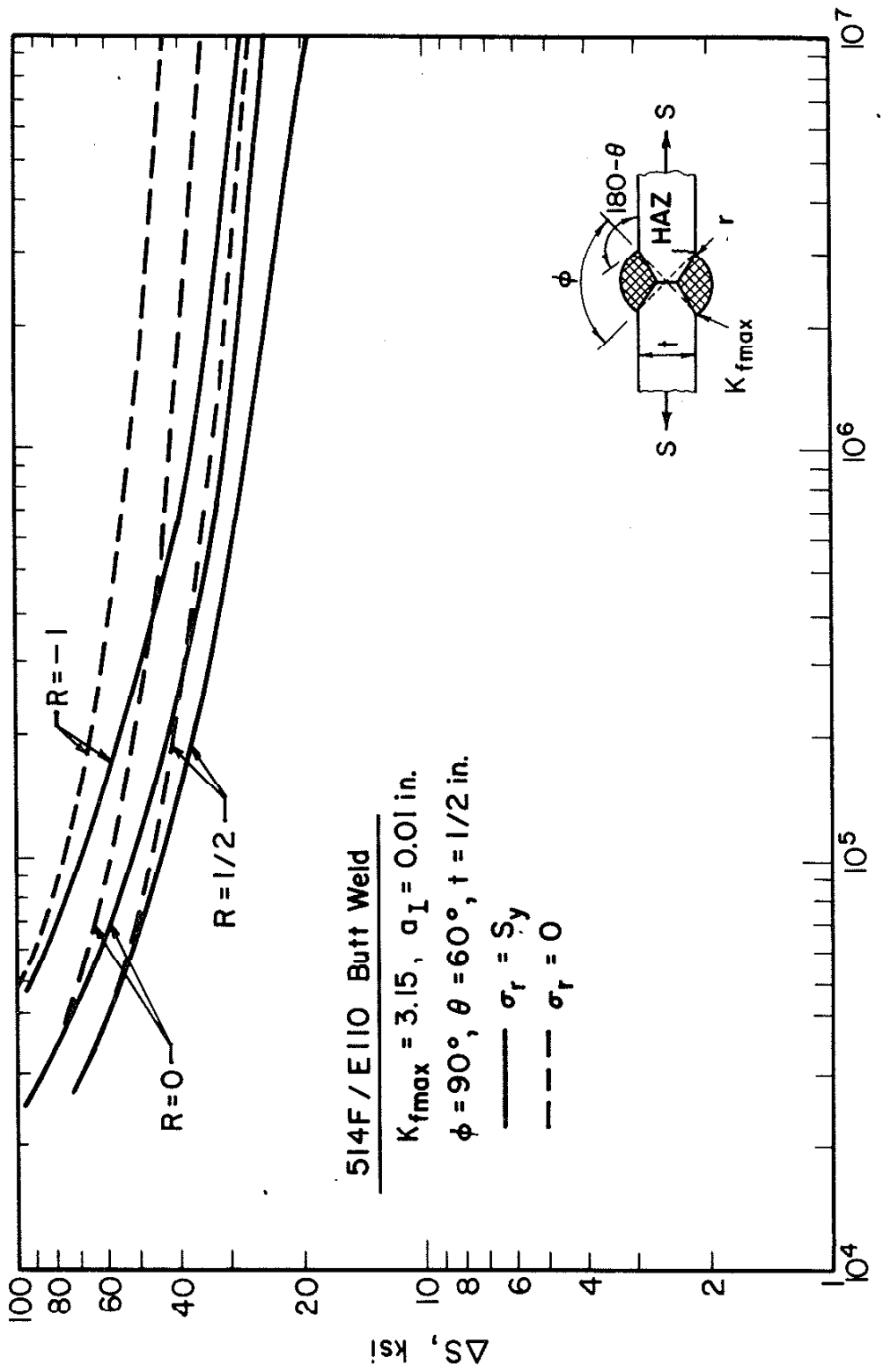

FIGURE 41. PREDICTED EFFECT OF STRESS RELIEF AND STRESS RATIO ON A514/E110 BUTT WELD FATIGUE LIFE.

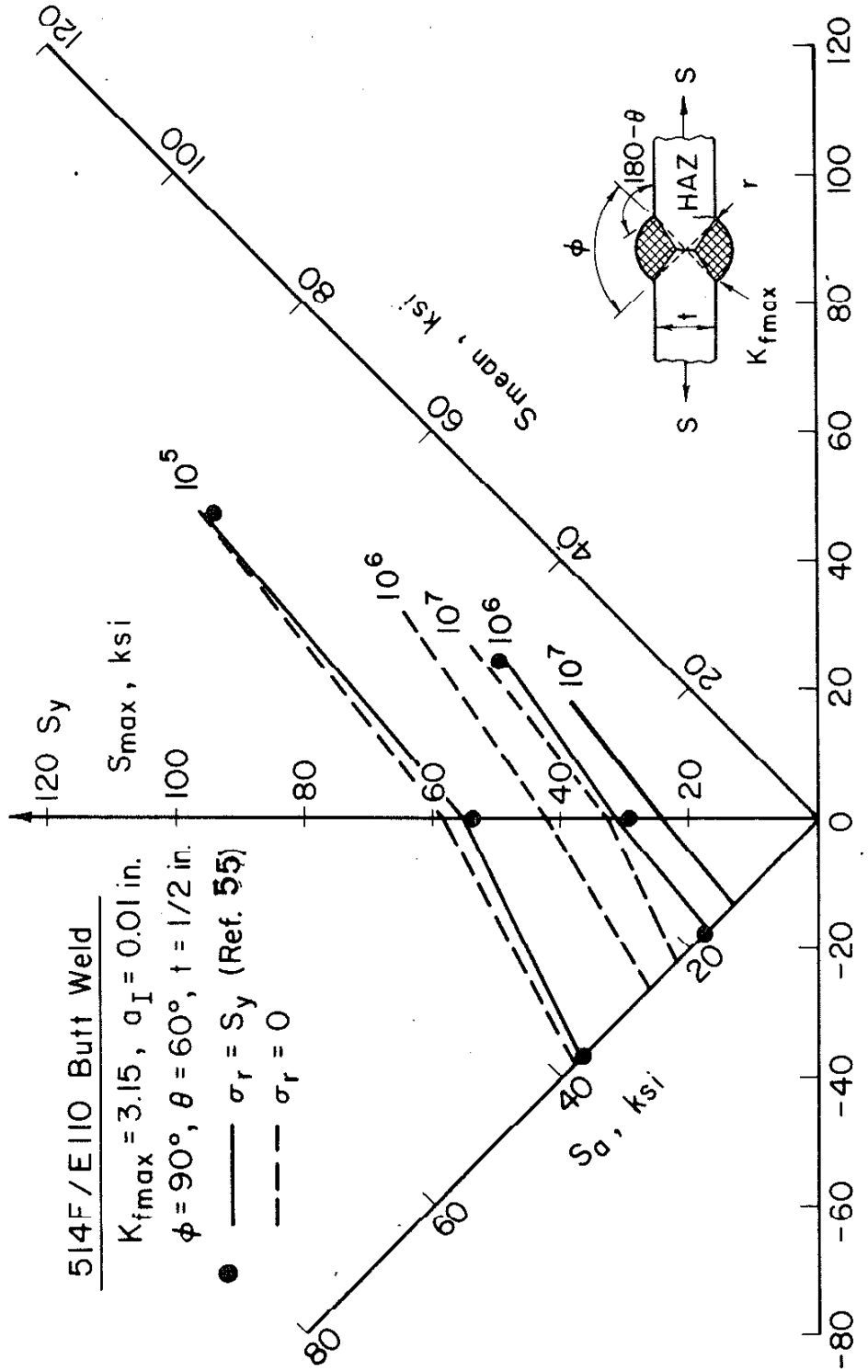

FIGURE 42. MODIFIED GOODMAN DIAGRAM FOR A514F/E110 BUTT WELDS IN THE AS-WELDED (TENSILE RESIDUAL STRESSES) AND STRESS RELIEVED CONDITIONS.

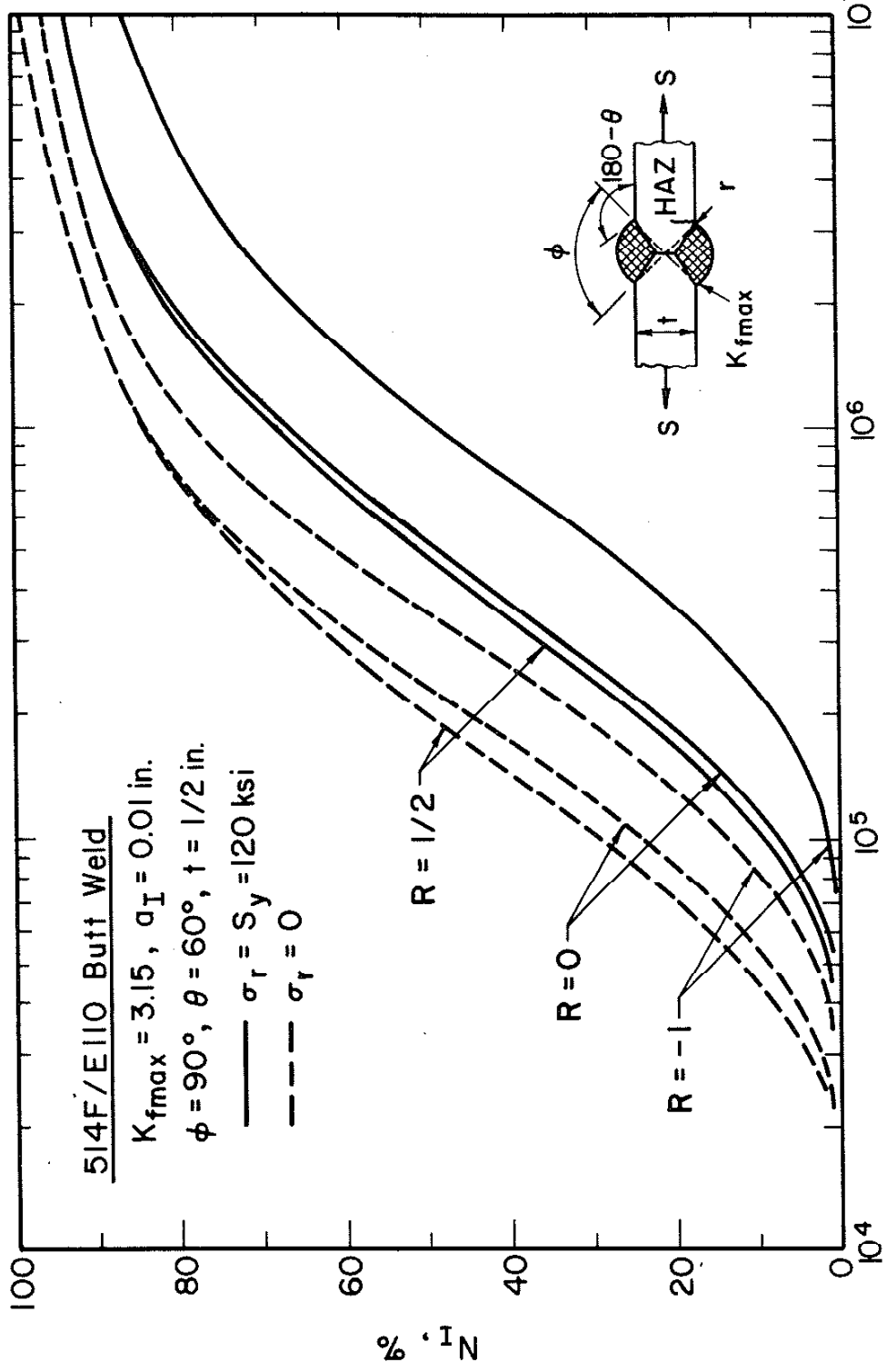

FIGURE 43. PREDICTED PARTITIONING OF THE CRACK INITIATION AND CRACK PROPAGATION LIFE OF A514F/E110 BUTT WELDS AS A FUNCTION OF THE TOTAL FATIGUE LIFE FOR TENSILE AND COMPRESSIVE RESIDUAL STRESSES AND VARIOUS STRESS RATIOS (R = -1, 0, 1/2).

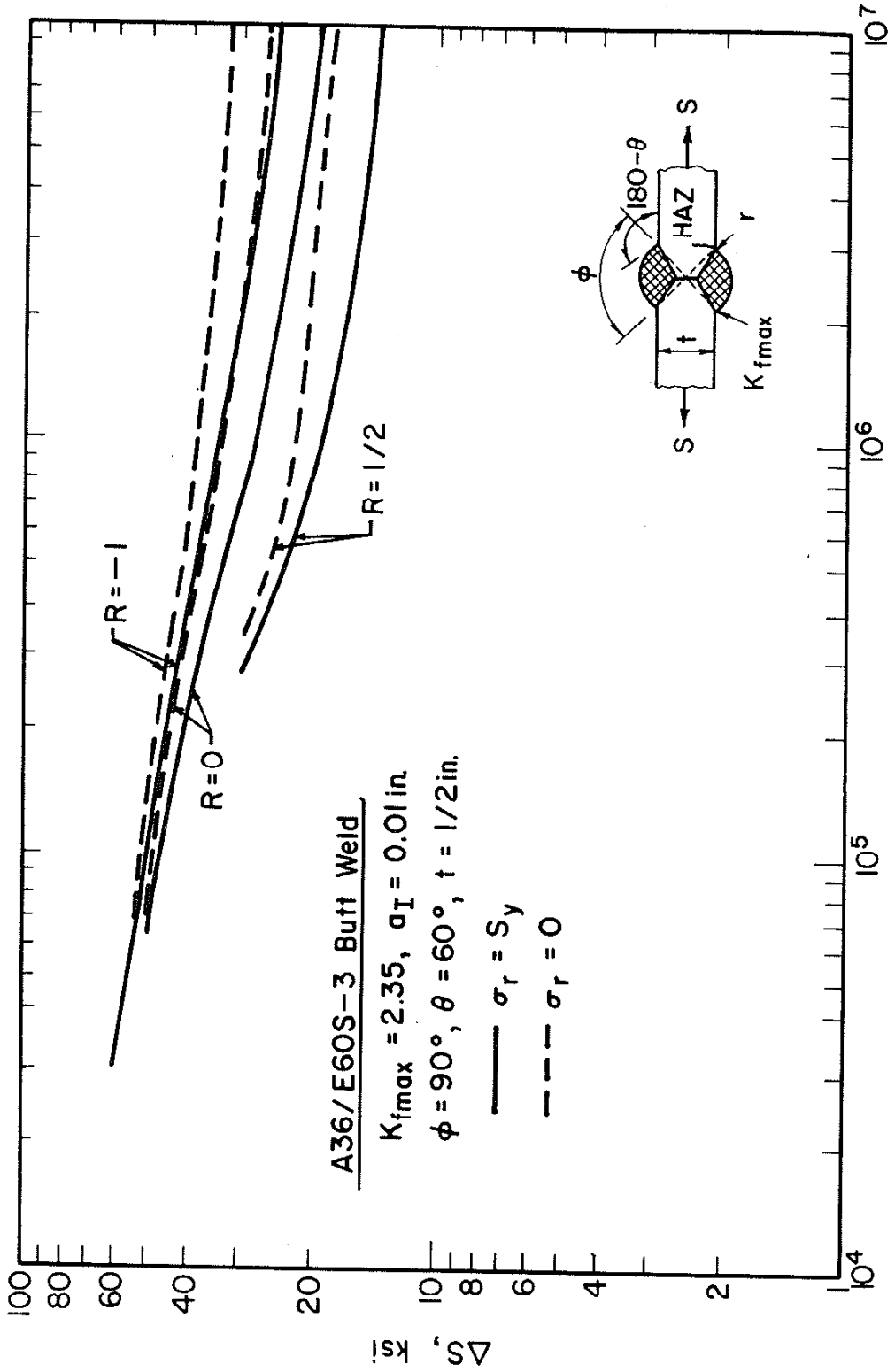

FIGURE 44. PREDICTED EFFECT OF STRESS RELIEF AND STRESS RATIO ON A36/E60S-3 BUTT WELD FATIGUE LIFE.

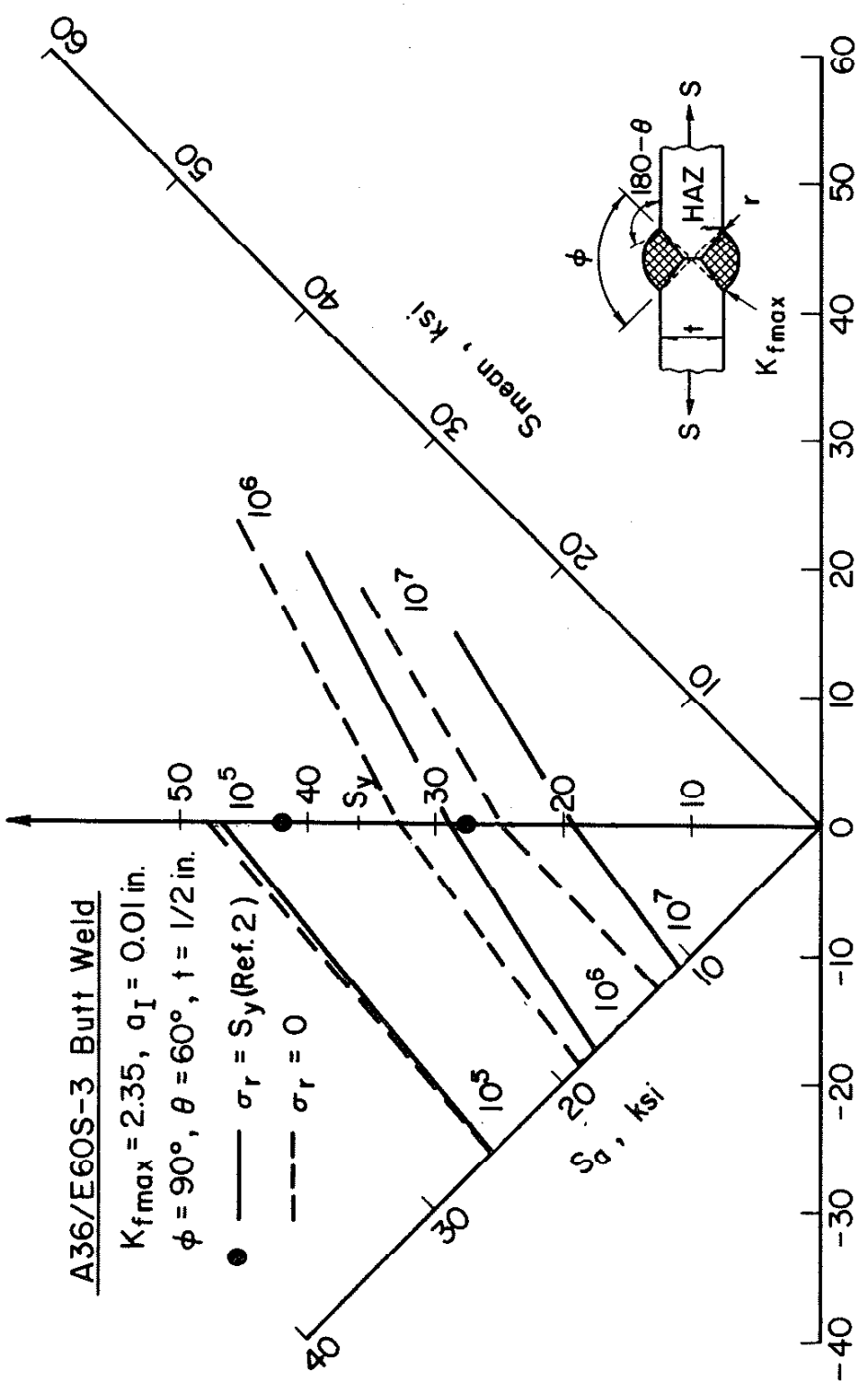

FIGURE 45. MODIFIED GOODMAN DIAGRAM FOR A36/E60S-3 BUTT WELDS IN THE AS-WELDED (TENSILE RESIDUAL STRESSES) AND STRESS RELIEVED CONDITIONS.

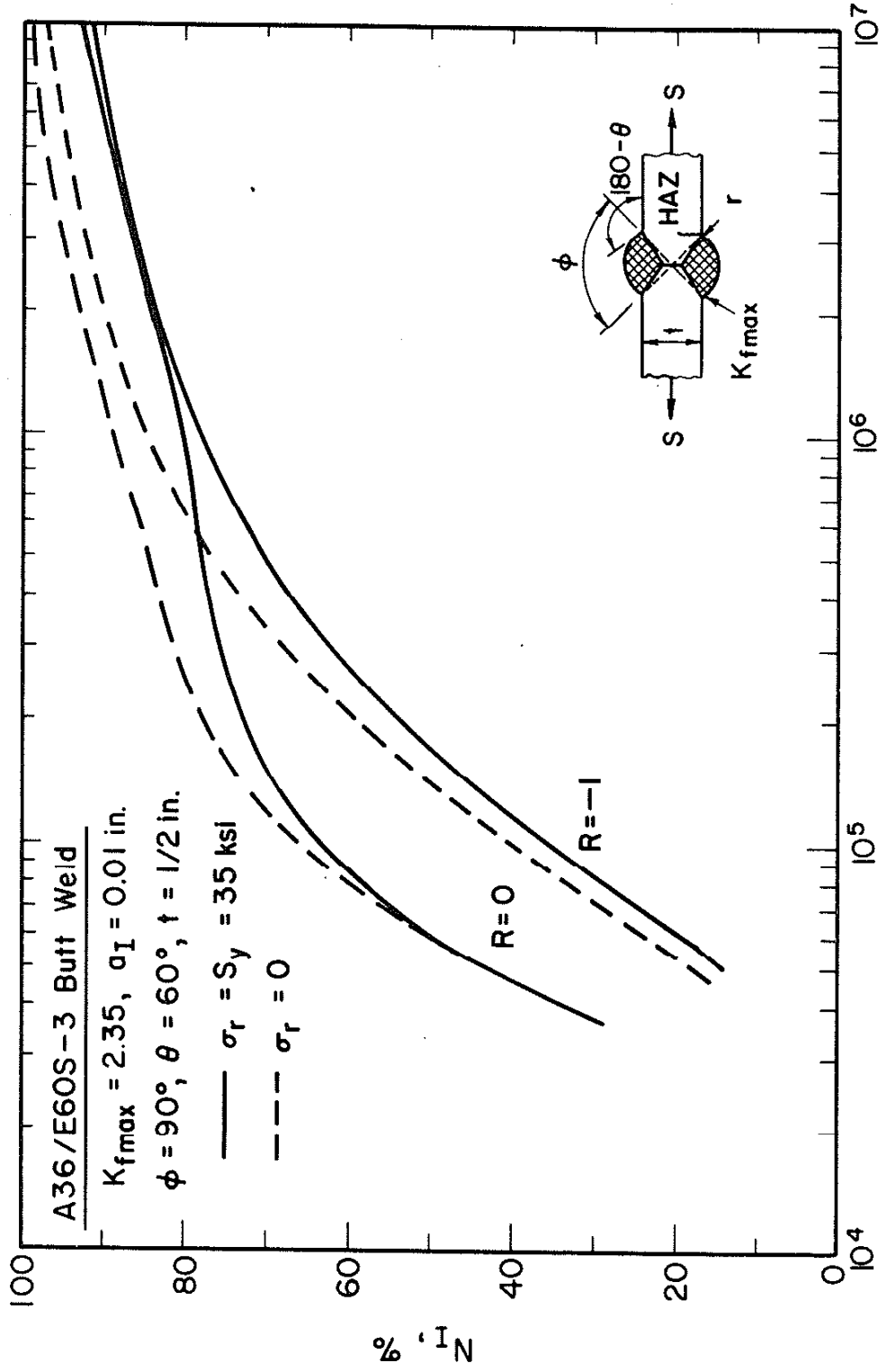

FIGURE 46. PREDICTED PARTITIONING OF THE CRACK INITIATION AND CRACK PROPAGATION LIFE OF A36/E60S-3 BUTT WELDS AS A FUNCTION OF THE TOTAL FATIGUE LIFE FOR TENSILE AND COMPRESSIVE RESIDUAL STRESSES AND VARIOUS STRESS RATIOS (R = -1, 0).

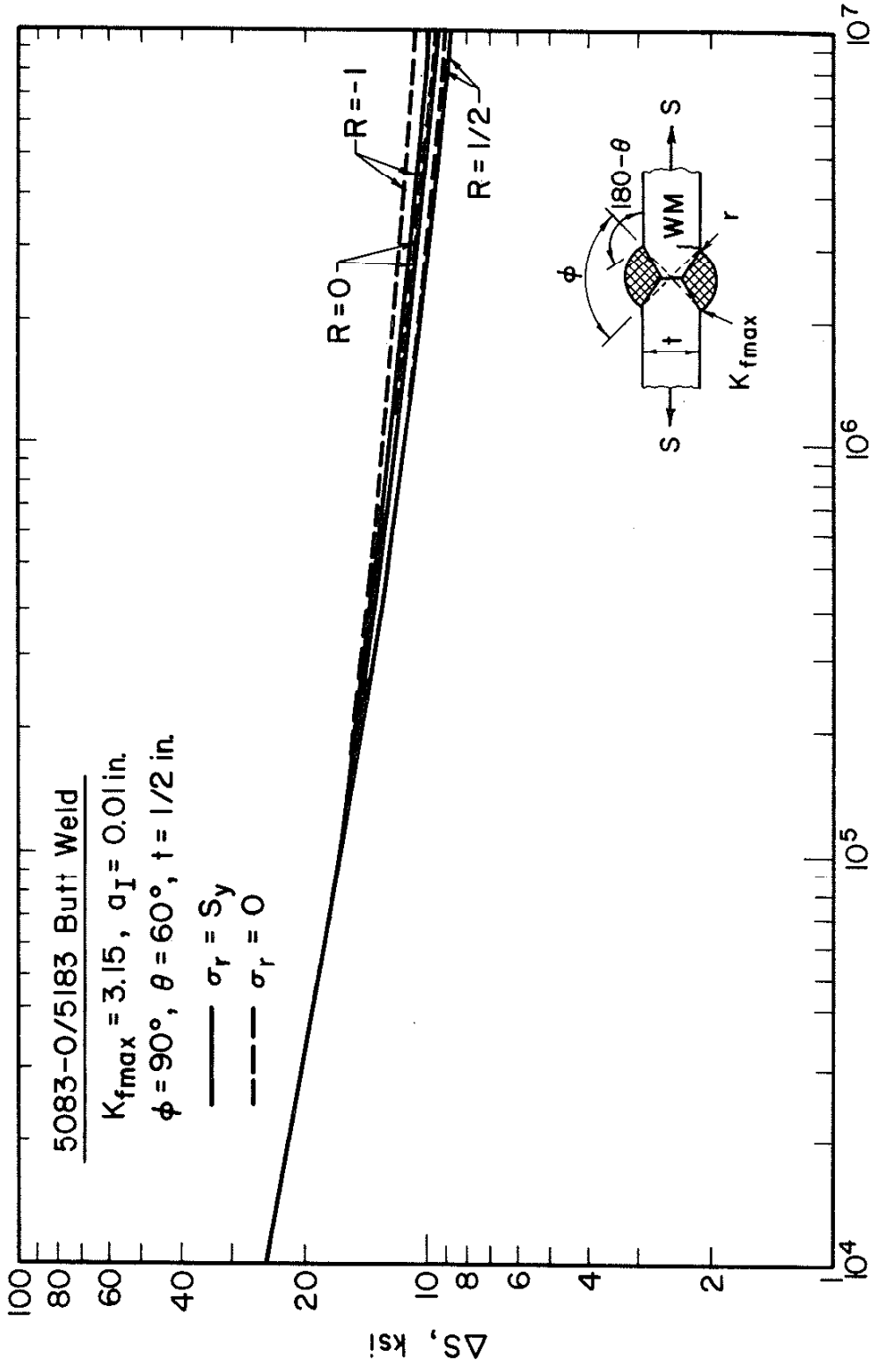

FIGURE 47. PREDICTED EFFECT OF STRESS RELIEF AND STRESS RATIO ON 5083-O/5183 BUTT WELD FATIGUE LIFE.

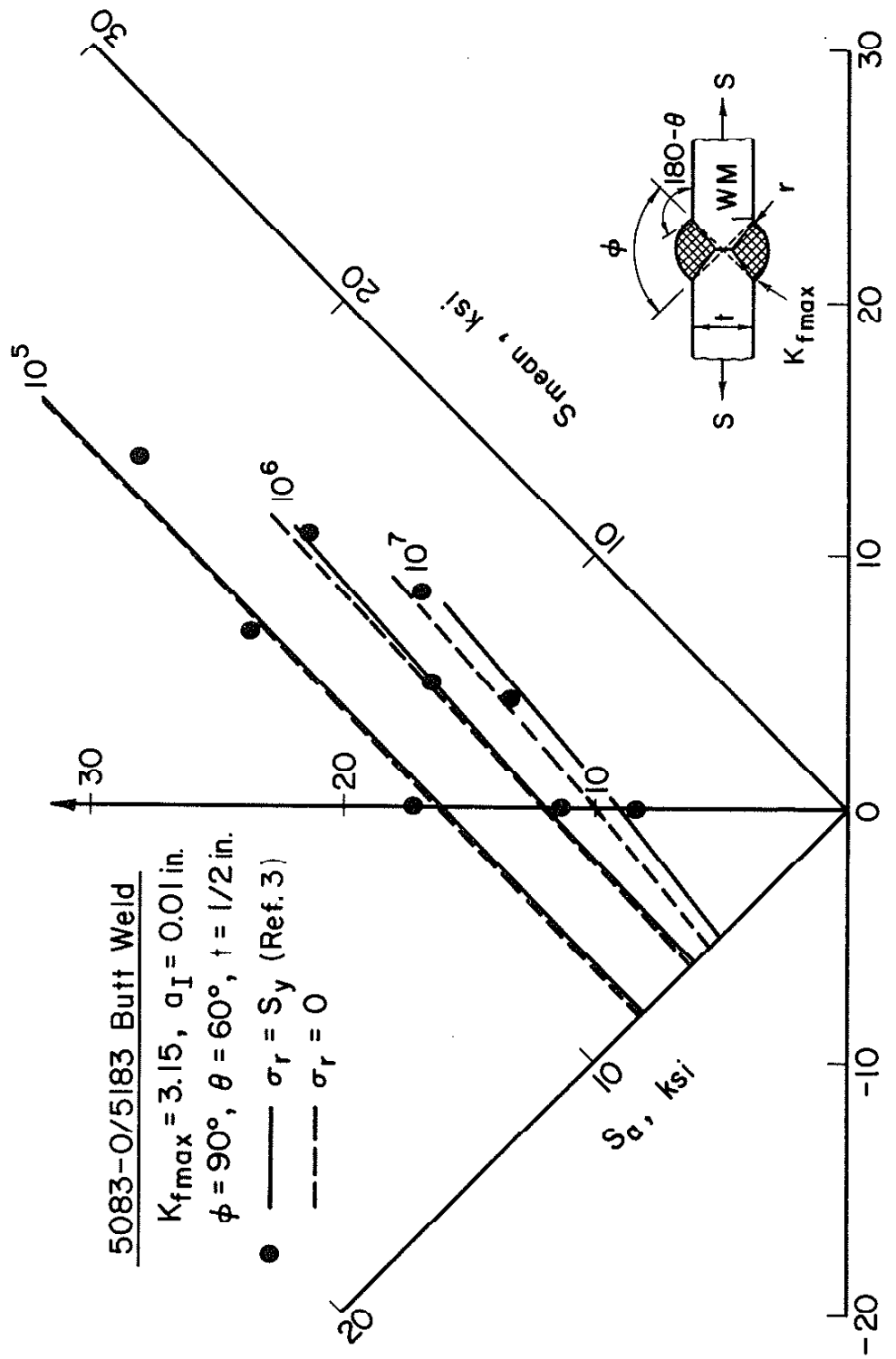

FIGURE 48. MODIFIED GOODMAN DIAGRAM FOR 5083-O/5183 BUTT WELDS IN THE AS-WELDED (TENSILE RESIDUAL STRESSES) AND STRESS RELIEVED CONDITIONS.

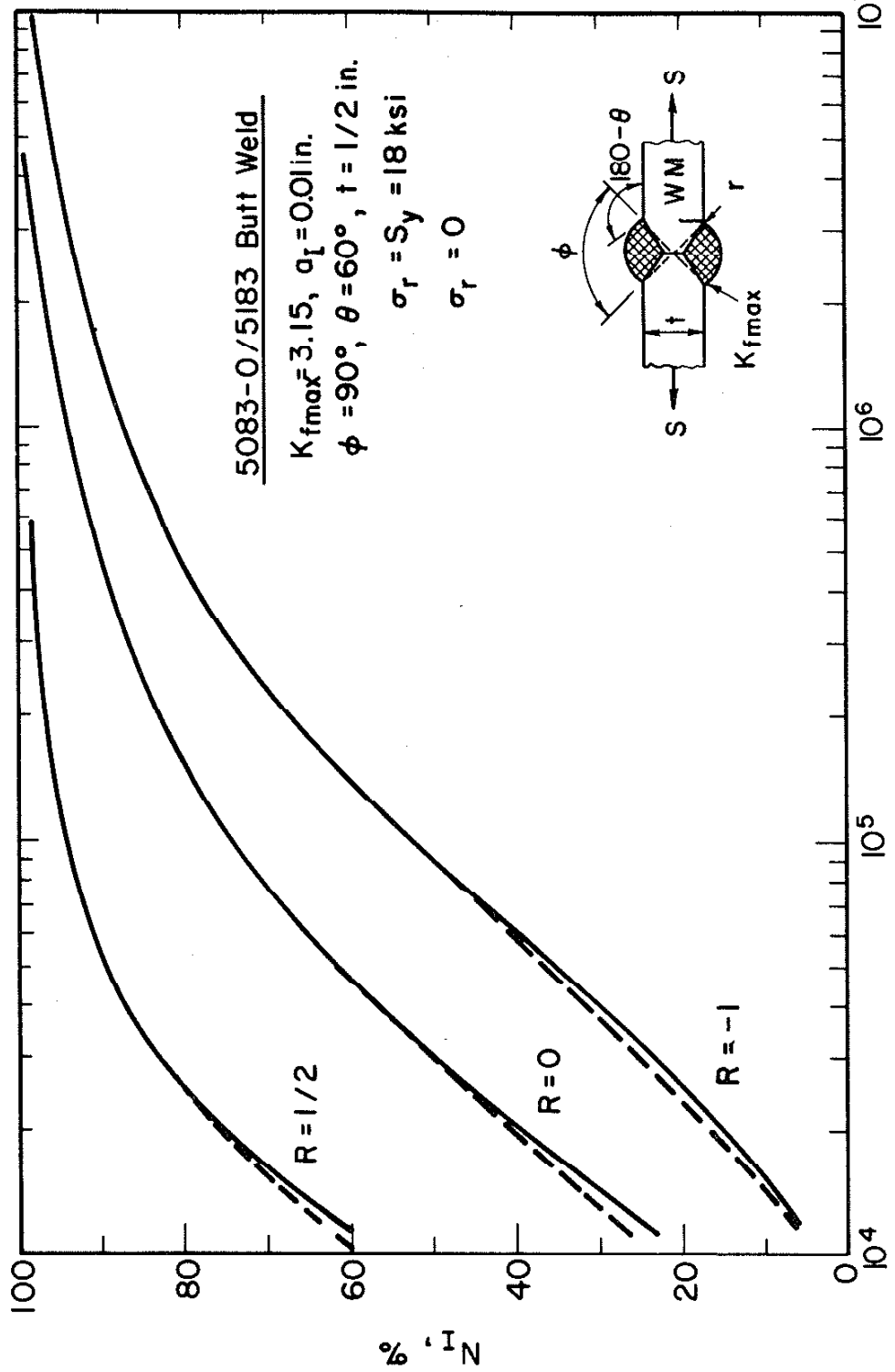

FIGURE 49. PREDICTED PARTITIONING OF THE CRACK INITIATION AND CRACK PROPAGATION LIFE OF 5083-O/5183 BUTT WELDS AS A FUNCTION OF THE TOTAL FATIGUE LIFE FOR TENSILE AND COMPRESSIVE RESIDUAL STRESSES AND VARIOUS STRESS RATIOS (R = -1, 0, 1/2).

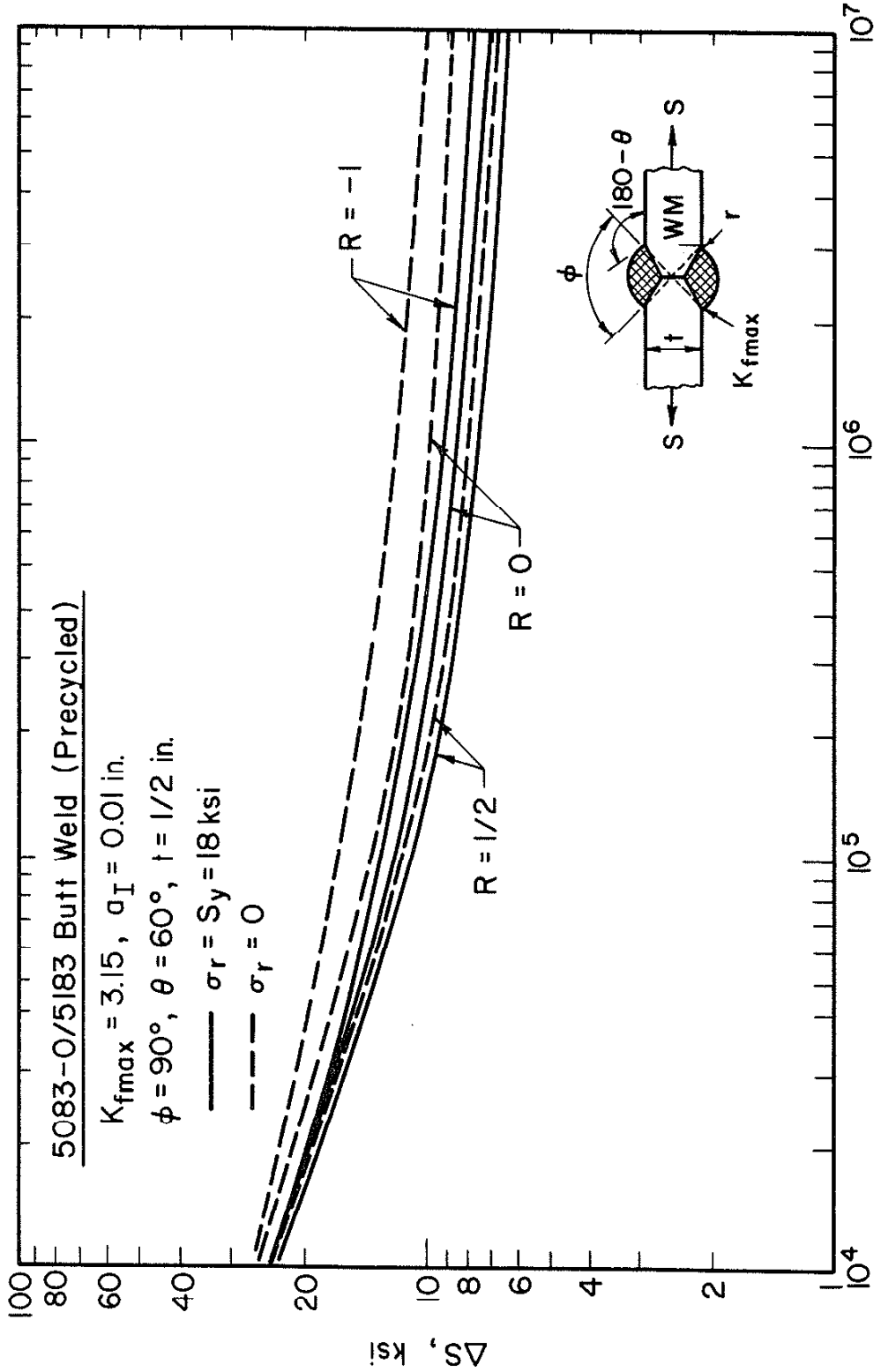

FIGURE 50. PREDICTED EFFECT OF STRESS RELIEF AND STRESS RATIO ON PRECYCLED 5083-O/5183 BUTT WELD FATIGUE LIFE.

APPENDIX

Contained in this appendix is a brief description, the directions for usage, and listing of the program used to simulate the set-up cycle and solve the damage integral (Eq. 27) for the fatigue crack initiation of a weld with residual stresses. An example problem is provided for user reference.

Program Description

The computer program discussed does the following: 1) simulates, using rheological modeling concepts (21, 36-38), the set-up cycle for a weld and thus establishes the initial mean stress ($\sigma_{o,i}$); and 2) solves the damage integral (Eq. 27) by a numerical technique for the fatigue crack initiation life (N_I). The computer program simulates the stress-strain response of A514, A36, or 5083-0 weld materials under Neuber control conditions with the hardening or softening behavior of these materials accounted for by the stress offset method of Jhansale (42). The damage integral is solved by expanding the integral (Eq. 27) as a power series and then integrating the series. The resulting integrated power series is then truncated as a 20th order polynomial in N_I which is solved by an interval halving method to find the root N_I. (The upper and lower bounds of the N_I interval are set by the life without mean stress damage and with "complete" mean stress damage, ie. no relaxation.) All necessary material properties are stored in the program in a matrix.

Program Usage

The input data is in the following form:

	INPUT VARIABLE	FORTRAN FORMAT
Program Control Card	Number of Problems (NTIMES) Number of Reversals (JREVER) Printing Code (IPRINT) 0 - Print all points of each reversal in logrithic increments of reversals 1 - Print summary of each reversal for logrithmic increments of reversal 2 - Print summary of each problem only	(3I10)
Problem Card	Material Number (NMATER) 1 to 10 - each number corresponds to a material as defined in the bending of the program listing	(I5, F5.2, 5F10.3)
	Fatigue Notch Factor (KF) Stress Range for Reversal 1 (SANN (1)) Stress Range for Reversal 2 (SANN (2)) Stress Range for Reversal 3 (SANN (3)) Stress Range for Reversal 4 (SANN (4)) Stress Range for Reversal 5 (SANN (5))	

The number of Problem Cards is simply determined by the user's requirements.

The output of the program varies from very detailed information to a generalized summary of loading, fatigue notch factor, material, and crack initiation life. The output detail is determined by the user, himself. A typical output is shown for the example problem where IPRINT = 2.

Example Problem

For user reference, an example of program application to the calculation of fatigue crack initiation life (N_I) for an A36 weld with a crack initiating in HAZ material is given. Both the condition of tensile residual stresses (σ_r) equal to the monotonic yield strength of the base metal (S_{yBM}) and no residual stresses (stress relieved) will be considered. The tensile residual stress problem will be solved first and the stress relieved problem solved second. The fatigue notch factor will be 3 ($K_f = 3$).

The program input in formated card form is given as:

```
123456789 123456789 123456789 123456789 123456789 123456789 123456789 123456789
                2           5           1
    8 3.0     42.0        30.0        30.0        30.0        30.0
    8 3.0     30.0        30.0        30.0        30.0        30.0
123456789 123456789 123456789 123456789 123456789 123456789 123456789 123456789
```

The output is:

```
FATIGUE CRACK INITIATION LIFE ANALYSIS - NEUBER CONTROL CONDITIONS

 MATERIAL IS       A36 HAZ

STRESS-STRAIN PROPERTIES

     ELASTIC MODULUS(KSI)................  27400.0
     PLASTIC STRAIN OFFSET.............. 0.000200

     MONOTONIC YIELDSTRENGTH(KSI)........  59.565
               STRENGTH COEFFICIENT(KSI).. 142.000
               STRAIN HARDENING EXPONENT...  0.1020

     CYCLIC    YEILD STRENGTH(KSI).......  34.608
               STRENGTH COEFFICIENT(KSI).. 216.000
               STRAIN HARDENING EXPONENT...  0.2150

FATIGUE PROPERTIES

     FATIGUE STRENGTH COEFFICIENT(KSI)..... 105.000
             DUCTILITY COEFFICIENT.........  0.2180
             STRENGHT EXPONENT.............  -0.066
             DUCTILITY EXPONENT........... -0.4920




  NEUBER PARAMETER =     0.29562
(KF)X(STRESS RANGE) =   -0.00000

          KF = 3.000S1= 42.000S2= 30.000S3= 30.000S4= 30.000S5= 30.000




          LIFE FOR FULL MEAN STRESS EFFECTS          3033
          LIFE FOR RELAXATION OF MEAN STRESS       212818
          LIFE WITH NO MEAN STRESS                1135304
             (LIVES GIVEN IN CYCLES)



  NEUBER PARAMETER =     0.29562
(KF)X(STRESS RANGE) =    90.00000

          KF = 3.000S1= 30.000S2= 30.000S3= 30.000S4= 30.000S5= 30.000



          LIFE FOR FULL MEAN STRESS EFFECTS          11832
          LIFE FOR RELAXATION OF MEAN STRESS       318102
          LIFE WITH NO MEAN STRESS                1135304
             (LIVES GIVEN IN CYCLES)
```

Program Listing

```
C                                                                       00100005
C THIS PROGRAM IS A COMPUTER SIMULATION OF A SMOOTH SPECIMEN            00100007
C      FATIGUED UNDER UNIAXIAL NEUBER CONTROL CONDITIONS.  THE          00100008
C      MATERIALS SIMULATED ARE :                                        00100009
C          1) ALUMINUM 5083-O        BASE METAL                         00100010
C          2) ALUMINUM 5183          WELD METAL                         00100011
C          3) ASTM A514 STEEL        BASE METAL                         00100012
C          4) ASTM A514 WELD         HEAT AFFECTED ZONE (HAZ)           00100013
C          5) ASTM A514 WELD         ONE-PASS WELD METAL                00100014
C          6) ASTM A514 WELD         TWO-PASS WELD METAL                00100015
C          7) ASTM A36 STEEL         BASE METAL                         00100016
C          8) ASTM A36 WELD          HEAT AFFECTED ZONE (HAZ)           00100017
C          9) ASTM A36 WELD          ONE-PASS WELD METAL                00100018
C         10) ASTM A36 WELD          TWO-PASS WELD METAL                00100019
C                                                                       00100020
C                                                                       00100021
      DIMENSION P(60),DELP(60),DS(2,60),DE(2,60),SLOCAL(60),ELOCAL(60), 00100022
     *   EPLOC(60),SGLOB(60),EGLOB(60),XK(2),XN(2),EPX(2),              00100023
     *   NPRINT(100),ANAME(3),R(3),SANN(20)                             00100024
      REAL*4 NEUBER,KF                                                  00100025
C                                                                       00100026
       DATA NPRINT/1,2,3,4,5,9,10,19,20,21,50,100,500,1000,1500,2000/   00100028
C
    1 FORMAT(3I10)
    2 FORMAT(I5,F5.2,5F10.3)
    3 FORMAT(16I5.2)
    4 FORMAT(1H1,///,T10,'FATIGUE CRACK INITIATION LIFE ANALYSIS - NEUBER00100029
     * CONTROL CONDITIONS',///,                T10,                      00100030
     *        ' MATERIAL IS       ',3A4,///,  T10,'STRESS-STRAIN PROPERT00100031
     *IES',//,T15,'ELASTIC MODULUS(KSI)..... ',F8.1,//,T15,             00100032
     *'PLASTIC STRAIN OFFSET.............',F9.6,//,T15,'MONOTONIC YIELD00100033
     *STRENGTH(KSI).......',F8.3,//,T26,'STRENGTH COEFFICIENT(KSI)..',  00100034
     *F8.3,//,T26,'STRAIN HARDENING EXPONENT...',F8.4,///)              00100035
    5 FORMAT(T15,'CYCLIC    YEILD STRENGTH(KSI).......',F8.3,//,T26,'STRE00100036
     *NGTH COEFFICIENT(KSI)..',F8.3,//,T26,'STRAIN HARDENING EXPONENT...'00100037
     *,F8.4,///,T10,'FATIGUE PROPERTIES',//,T15,'FATIGUE STRENGTH COEFFI00100038
     *CIENT(KSI).....',F8.3,//,T24,'DUCTILITY COEFFICIENT.........',F8.4,00100039
     */,T24,'STRENGHT EXPONENT...........',F8.3,//T24,'DUCTILITY EXPONE00100040
     *NT...........',F8.4,/////)                                        00100041
    6  FORMAT(/,T10,'NEUBER PARAMETER = ',F10.5,//,                     00100063
     *         T5,'(KF)X(STRESS RANGE) = ',F10.5,///,                  00100064
     *         T20,'KF = ',F5.3,'S1=',F7.3,'S2=',F7.3,                 00100065
     *         'S3=',F7.3,'S4=',F7.3,'S5=',F7.3,//)                    00100066
    7 FORMAT(T5,'REVERSAL(2N)=',I8,'   POINTS        STRAIN          STR00100042
     *ESS(KSI)     PLASTIC STRAIN     AVALIBILITY P(I)   CHANGE P(I)',/)00100043
    8 FORMAT(I32,T40,E11.4,T58,F8.3,T74,E11.4,T94,F8.5,T112,F8.5)       00100044
    9 FORMAT(/,T5,'SIGN(DS/DE)= ',F4.1,T26,'STRAIN AMPLITUDE =  ',E11.4,00100045
     *T61,'                                                ',          00100046
     *'STRESS AMPLITUDE =',T49,F8.3,T61,'                              00100047
     *                ',  /,T26,'MEAN STRESS       =',T49,F8.3,T61,    00100048
     *'                                                ',  /,T26,'PLASTIC 00100049
     *STRAIN AMP =',T49,E11.4,////)                                      00100050
   11 FORMAT(I12,T15,E10.3,T27,E10.3,T40,F7.2,T50,F7.2)                 00100068
   12 FORMAT(//,T20,'LIFE FOR FULL MEAN STRESS EFFECTS ',I15,/,         00100069
     *          T20,'LIFE FOR RELAXATION OF MEAN STRESS',I15,//,       00100070
     *          T20,'LIFE WITH NO MEAN STRESS          ',I15,//,       00100071
     *          T20,'  (LIVES GIVEN IN CYCLES)',///)                   00100072
C                                                                       00100073
      NMBEFR= 0                                                         00100076
      READ(5,1)NTIMES,JREVER,IPRINT
      DO 550 NOE=1,NTIMES
      READ(5,2)    NMATER,KF,SANN(1),SANN(2),SANN(3),SANN(4),SANN(5)
```

```
      CALL CURVE(NMATER,XK,XN,E,EPX,EF,SF,B,C,DE,DS,ANAMF)                00100080
      YSMON=XK(1)*(EPX(1))**XN(1)                                         00100081
      YSCYC=XK(2)*(EPX(2))**XN(2)                                         00100082
      IF( NMATER.EQ.NMBEFR) GO TO 25
      PRINT 4,ANAME(1),ANAME(2),ANAME(3),E,EPX(1),YSMON,XK(1),XN(1)       00100
      PRINT 5,YSCYC,XK(2),XN(2),SF,EF,B,C                                 00100085
   25 NMBEFR=NMATER
      NEUBER= (KF*SANN(5))**2.0/E                                         00100087
      PRINT   6, NEUBER,XAMP,KF,(SANN(L1),L1=1,5)
      XAMP=KF*SANN(5)                                                     00100088
C
C START SIMULATION AND CALCULATE AVALIBILITY MATRIX                       00100091
C                                                                         00100092
      DO 10 J=1,60                                                        00100094
      DELP(J)=0.0                                                         00100095
   10 P(J)=0.0                                                            00100096
      SGLOB(1)=0.0                                                        00100097
      EGLOB(1)=0.0                                                        00100098
      SLOCAL(1)=0.0                                                       00100099
      ELOCAL(1)=0.0                                                       00100100
      EPLOC(1)=0.0                                                        00100101
      SLAST=0.0                                                           00100102
      ELAST=0.0                                                           00100103
      TOTDAM=0.0                                                          00100104
      A=1.0                                                               00100105
      DMTOT=1.0                                                           00100106
      JCOUNT=1                                                            00100107
      EAMP=0.0                                                            00100108
      D=DS(2,1)                                                           00100109
      SIGN= -1.0                                                          00100110
      ICURVE=1                                                            00100115
C                                                                         00100116
C START REVERSALS AND INCREMENT STRESS-STRAIN PATH                        00100117
C                                                                         00100118
      DO 200 NREVER=1,JREVER                                              00100119
      NEUBER=CNTRL(NREVER,SANN,KF,E)                                      00100120
      IF(NREVER.GE.2) ICURVE=2                                            00100121
      REVDAM=1.0                                                          00100122
      SGLOB(1)=SLAST                                                      00100123
      EGLOB(1)=ELAST                                                      00100124
      I=0                                                                 00100125
C                                                                         00100126
C SET REVERSAL DIRECTION AND FIND HARDENING-SOFTENING OFFSET STRESS       00100127
C                                                                         00100128
      SIGN=-SIGN                                                          00100129
      IF(NREVER.GE.2)DS(2,1)=D + HARD(EAMP,NREVER,NMATER)                 00100130
      DE(2,1)=DS(2,1)/E                                                   00100131
   20 I=I + 1                                                             00100132
      DELP(I)=SIGN*P(I)                                                   00100133
      SLOCAL(I+1)=SLOCAL(I) + ABS(DELP(I))*DS(ICURVE,I)                   00100134
      ELOCAL(I+1)=ELOCAL(I) + ABS(DELP(I))*DE(ICURVE,I)                   00100135
      EGLOB(I+1)=ELAST + SIGN*ELOCAL(I+1)                                 00100136
      SGLOB(I+1)=SLAST + SIGN*SLOCAL(I+1)                                 00100137
      EPLOC(I+1)=SIGN*(ELOCAL(I+1)-SLOCAL(I+1)/E)                         00100138
C                                                                         00100139
C CHECK TO SEE IF CONTROL CONDITION EXCEEDED ON I-TH INCREMENT            00100140
C                                                                         00100141
      IF(NEUBER.LT.SLOCAL(I+1)*ELOCAL(I+1) ) GO TO 30                     00100142
      P(I)=P(I) + DELP(I)                                                 00100143
      GO TO 20                                                            00100144
C                                                                         00100145
C CALCULATED CONTROL CONDITION INTERSECTION POINT FOR I-TH INCREMENT      00100146
                                                                          00100147
```

```
C                                                                       00100148
   30 ALPHA=(SLOCAL(I)*DE(ICURVE,I) + ELOCAL(I)*DS(ICURVE,I))/(DE(ICURVE00100149
     *,I)*DS(ICURVE,I))                                                 00100150
      BETA=(SLOCAL(I)*ELOCAL(I) - NEUBER)/(DE(ICURVE,I)*DS(ICURVE,I))   00100151
      DELP(I)=-0.5*SIGN*(ALPHA-SQRT(ALPHA*ALPHA-4.0*BETA))              00100152
C                                                                       00100153
C COMPUTE THE LOCAL STRESS-STRAIN PATH END POINT AND                    00100154
C       CALCULATE GLOBAL STRESS-STRAIN PATH                             00100155
C                                                                       00100156
      SLOCAL(I+1)=SLOCAL(I) + ABS(DELP(I))*DS(ICURVE,I)                 00100157
      ELOCAL(I+1)=ELOCAL(I) + ABS(DELP(I))*DE(ICURVE,I)                 00100158
      SGLOB(I+1)=SLAST + SIGN*SLOCAL(I+1)                               00100159
      EGLOB(I+1)=ELAST + SIGN*ELOCAL(I+1)                               00100160
      EPLOC(I+1)=SIGN*(ELOCAL(I+1)-SLOCAL(I+1)/E)                       00100161
      P(I)=P(I) + DELP(I)                                               00100162
      SLAST=SGLOB(I+1)                                                  00100163
      ELAST=EGLOB(I+1)                                                  00100164
      EAMP= 0.5*ELOCAL(I+1)                                             00100165
      EPAMP=ABS(0.5*EPLOC(I+1))                                         00100166
      SAMP= 0.5*SLOCAL(I+1)                                             00100167
      SMEAN= 0.5*(SGLOB(I+1) + SGLOB(1))                                00100168
C                                                                       00100187
C PRINT STRESS-STRAIN PATH POINTS FOR SELECTED REVERSALS                00100188
C                                                                       00100189
      IF(NREVER.NE.NPRINT(JCOUNT))GO TO 200                             00100190
      JCOUNT=JCOUNT + 1                                                 00100191
      M=I+1                                                             00100192
      IF(IPRINT.NE.0.OR.IPRINT.NE.1) GO TO 200
      IF(IPRINT.EQ.1) GO TO 190
       PRINT    7, NREVER
       PRINT    8, (L,EGLOB(L),SGLOB(L),EPLOC(L),
     *    P(L),DELP(L),L=1,M)
      PRINT 9, SIGN,EAMP,SAMP,SMEAN,EPAMP                               00100196
       GO TO 200                                                        00100199
  190 PRINT  11, NREVER,EAMP,EPAMP,SAMP,SMEAN
  200 CONTINUE                                                          00100202
C                                                                       00100203
C COMPUTE FATIGUE LIFE AND OUTPUT                                       00100204
C                                                                       00100205
      ST2=SAMP                                                          00100211
      ET2=EAMP                                                          00100212
      CALL AMP(NEUBER,ST2,ET2,XK(2),XN(2),E)
      CALL XLIFE(B,C,SF,EF,E,ET2,ST2,SMEAN,NMATER,                      00100213
     *                LIFE1,LIFE2,LIFE3)                               00100214
      PRINT  12, LIFE1,LIFE2,LIFE3
  400 CONTINUE                                                          00100217
  550 CONTINUE
      STOP                                                              00100220
      END                                                               00100221
C                                                                       00100074
C SUBROUTINE GETS MATERIAL PROPERTIES FROM MATRIX                       00100218
C                                                                       00100222
      SUBROUTINE CURVE(NMATER,XK,XN,E,EPX,EF,SF,B,C,DE,DS,ANAME)        00100219
C                                                                       00100223
      REAL*4 K,N,XK(2),XN(2),EPX(2),DS(2,60),DE(2,60)                   00100224
      DIMENSION XANAME(40),XEF(20),XSF(20),XB(20),XC(20),XXX(40),XNX(40)00100225
      DIMENSION  XE(20),ANAME(3),XEPX(20)                               00100226
      DATA XANAME/2AL 52,2083 2,2 WM 2,2AL 52,2183 2, 2 WM 2,2A5142,2 BM00100227
     * 2,2    2,2A5142,2 HAZ2,2    2,2A5142,2 WM(2,21P) 2,2A5142,2 WM(2,00100228
     *22P) 2,2A36 2,2BM  2,2    2,2A36 2,2HAZ 2,2    2,2A36 2,2WM(12,2P)00100229
     *  2,2A36 2,2WM(22,2P)  2/                                        00100230
      DATA XEF/.405,.581,.975,.783,.848,.595,.271,.218,.607,.602/
```

```
      DATA XSF/105.,92.5,189.,290.,274.,204.,147.,105.,131.,149./          00100231
      DATA XC/-.692,-.89,-.699,-.713,-.734,-.59,-.451,-.492, -.548,        00100232
     *   -.567/                                                            00100233
      DATA XB/-0.122,-0.107,-.079,-.087,-.115,-.079,-.132,-.066,-.075,     00100234
     *   -0.090/                                                           00100235
      DATA XEPX/.0002,.0002,.0002,.0002,.0002,.0002,.0002,.0002,.0002,     00100236
     *   0.0002/                                                           00100237
      DATA XKX/45.5,45.5,172.,306.,215.,210.,113.,142.,143.,123.,73.5,     00100238
     *   73.5,158.,375.,292.,250.,159.,216.,146.,179./                     00100239
      DATA XNX/0.133,0.133,0.060,0.092,0.092,0.092,0.085,0.102,0.0146,     00100240
     *   0.098,0.13,0.0719,0.0719,0.092,0.1667,0.1667,0.1667,0.215,        00100241
     *   0.155,0.197/                                                      00100242
      DATA XE/10300.0,10300.0,30300.0,30300.0,30300.0,30300.0,27500.0,     00100243
     *   27400.0,27400.0,27400.0,27400.0/                                  00100244
      E=XE(NMATER)                                                         00100245
      ANAME(1)=XANAME(3*(NMATER-1) + 1)                                    00100246
      ANAME(2)=XANAME(3*(NMATER-1) + 2)                                    00100247
      ANAME(3)=XANAME(3*(NMATER-1) + 3)                                    00100248
      EF=XEF(NMATER)                                                       00100249
      SF=XSF(NMATER)                                                       00100250
      B=XB(NMATER)                                                         00100251
      C=XC(NMATER)                                                         00100252
      EPX(1)=XEPX(NMATER)                                                  00100253
      EPX(2)=EPX(1)                                                        00100254
      XK(1)=XKX(NMATER)                                                    00100255
      XK(2)=XKX(10+NMATER)                                                 00100256
      XN(1)=XNX(NMATER)                                                    00100257
      XN(2)=XNX(10+NMATER)                                                 00100258
      L=1                                                                  00100259
      M=51                                                                 00100260
      EPUP=0.200                                                           00100261
      DO 30 I=1,2                                                          00100262
      K=XK(I)                                                              00100263
      EPY=EPX(I)                                                           00100264
      N=XN(I)                                                              00100265
      DO 10 J=1,L                                                          00100266
      DS(I,J)=(1.0/(1.0*L))*K*(EPY)**N                                     00100267
   10 DE(I,J)=DS(I,J)/E                                                    00100268
      DSLAST=K*(EPY)**N                                                    00100269
      DELAST=DSLAST/E                                                      00100270
      DELEP2=(ALOG10(EPUP)-ALOG10(EPY))/(1.0*(M-L))                        00100271
      L1=L+1                                                               00100272
      DO 20 J=L1,M                                                         00100273
      EP2= 10.0**(ALOG10(EPY) + (J-L)*DELEP2)                              00100274
      S2=K*(EP2)**N                                                        00100275
      ET2=S2/E + EP2                                                       00100276
      DE(I,J)=ET2 - DELAST                                                 00100277
      DS(I,J)=S2 - DSLAST                                                  00100278
      DELAST=ET2                                                           00100279
   20 DSLAST=S2                                                            00100280
   30 CONTINUE                                                             00100281
      RETURN                                                               00100282
      END                                                                  00100283
C                                                                          00100093
C
C THIS SUBROUTINE COMPUTES THE NEUBER PARAMETER USED FOR CONTROL
C
      FUNCTION CNTRL(N,S,KF,E)                                             00100284
C                                                                          00100090
      REAL*4 KF,S(20)                                                      00100285
      I=N                                                                  00100286
      IF(N.GT.5) I=5                                                       00100287
```

```
      CNTRL= (KF*S(I))**2.0/E                                          00100288
      RETURN                                                           00100289
      END                                                              00100290
C
      FUNCTION HARD(ET2,I,J)                                           00100291
C                                                                      00100111
      DIMENSION  A1(10),A2(10),B1(10),B2(10),C1(10)                    00100292
      DATA A1/-1000.,-1000.,0.,990.,490.,1800.,0.,1470.,500.,1470./    00100293
      DATA A2/50.0,50.0,0.00,70.8,27.7,20.0,0.0,23.25,20.,20./         00100294
      DATA B1/20.28,20.28,0.0,8.7,2.5,20.0,0.0,1.0,1.0,1.0/            00100295
      DATA B2/0.022,0.022,0.00,0.00,0.00,0.00,0.00,0.00,0.00,0./       00100296
      DATA C1/ 0.0, 0.0, 0.0, 0.0, 29.0,30.0, 0.0, 0.0,25.,25./        00100297
      IF(J.EQ.6) J=3
      HARD=0.0                                                         00100298
      IF(I.EQ.1) RETURN                                                00100299
      SSAT=A1(J)*ET2 + A2(J)                                           00100300
      C=B1(J)*ET2 + B2(J)                                              00100301
      IF(I.EQ.2) S1=0.0                                                00100302
      S2=C*(SSAT-S1) + S1                                              00100303
      HARD=-0.5*(S1 + SSAT) + C1(J)                                    00100304
      IF(J.EQ.1.OR.J.EQ.2) HARD=0.5*(S1 - SSAT)                        00100305
      IF(J.EQ.8) HARD=-0.5*(S1-SSAT)                                   00100306
      S1=S2                                                            00100307
      RETURN                                                           00100308
      END                                                              00100309
C                                                                      00100114
C THIS SUBROUTINE SOLVES FOR THE FATIGUE LIFE FROM THE DAMAGE INTERAL
C
      SUBROUTINE XLIFE(B,C,SF,EF,E,ET2,ST2,SMEAN2,NMATER,              00100445
C                                                                      00100328
     *           LIFE1,LIFE2,LIFE3)
      REAL*4 K                                                         00100329
      K= FUNK(ET2,NMATER)                                              00100330
      ICAL=0                                                           00100331
      S1=0.0                                                           00100332
      LIFE1=INT((ST2/(SF-SMEAN2))**(1.0/B))/2                          00100333
      LIFE2= LIFE(ST2,SMEAN2,SF,B,K)/2                                 00100334
      LIFE3=INT((ST2/SF)**(1.0/B))/2                                   00100335
C                                                                      00100336
      RETURN                                                           00100337
      END                                                              00100338
C                                                                      00100339
C                                                                      00100340
C THIS FUNCTION ESTIMATES LIFE AS THE MEAN STRESS RELAXES              00100341
C      BY APPROXIMATION OF A DAMAGE INTERGRAL EQUATION AS              00100342
C      A TRUNCATED SERIS EXPANSION                                     00100343
C                                                                      00100344
C                                                                      00100345
                                                                       00100346
      FUNCTION LIFE(ST2,SMEAN,SF,B,K)                                  00100347
C                                                                      00100348
      REAL*4 K                                                         00100349
C                                                                      00100350
C THE FOLLOWING IS A ROOT FINDER FOR  N  IN F(N) WHICH IS              00100351
C     EXPRESSED AS A TRUNCATED SERIS EXPANSION                         00100352
C                                                                      00100353
C DEFINE INITIAL PARAMETERS                                            00100354
C                                                                      00100355
      BETA=1.0/B                                                       00100356
      ALPHA=-SMEAN/SF                                                  00100357
      IF(ABS(ALPHA).GE. 1.0 ) GO TO 50                                 00100358
      DSTAR=(ST2/(SF))**(-1.0/B)                                       00100359
      DMEAN=(ST2/(SF-SMEAN))**(-1.0/B)                                 00100360
```

```
      ITERMS=20                                                          00100361
      XLEFT=1.0/DMEAN                                                    00100362
      XRIGHT=1.0/DSTAR                                                   00100363
      IF(XRIGHT.EQ.XLEFT) GO TO 30                                       00100364
      IF(XLEFT.GT.XRIGHT) XRIGHT=1.0/DMEAN                               00100365
      IF(XRIGHT.EQ.XLEFT) XLEFT=1.0/DSTAR                                00100366
      IF(K.GE. 0.0 ) GO TO 60                                            00100367
      IF(ALPHA.EQ. 0.0 ) GO TO 70                                        00100368
C                                                                        00100369
C DETERMINE THE NUMBER OF ITERATIONS NEEDED TO FIND  N                   00100370
C                                                                        00100371
      ITER=INT(ALOG(XRIGHT-XLEFT)/ALOG(2.0)) + 1                         00100372
C                                                                        00100373
C                                                                        00100374
      FLEFT=POLY(XLEFT,K,ALPHA,DSTAR,BETA,ITERMS)                        00100375
C                                                                        00100376
C BEGIN HALF-INTERVAL ITERATIONS                                         00100377
C                                                                        00100378
      DO 20 I=1,ITER                                                     00100379
      XHALF=(XRIGHT + XLEFT)/2.0                                         00100380
      FHALF=POLY(XHALF,K,ALPHA,DSTAR,BETA,ITERMS)                        00100381
C                                                                        00100382
C CHOOSE THE SUB-INTERVAL CONTAINING THE ROOT                            00100383
C                                                                        00100384
      IF(FHALF*FLEFT.LE.0.0) GO TO 10                                    00100385
      XLEFT=XHALF                                                        00100386
      FLEFT=FHALF                                                        00100387
      GO TO 20                                                           00100388
   10 XRIGHT=XHALF                                                       00100389
   20 CONTINUE                                                           00100390
C                                                                        00100391
C COMPUTE THE FINAL ROOT OF THE INTERGRAL EXPANSION                      00100392
C                                                                        00100393
   30 LIFE=INT((XLEFT+XRIGHT)/2.0)                                       00100394
      IF(LIFE.LE.0) LIFE=1                                               00100395
      RETURN                                                             00100396
   50 LIFE=2                                                             00100397
      RETURN                                                             00100398
   60 LIFE= INT(1.0/DMEAN)                                               00100399
      IF(LIFE.LE.0) LIFE=3                                               00100400
      RETURN                                                             00100401
   70 LIFE= INT(1.0/DSTAR)                                               00100402
      IF(LIFE.LE.0) LIFE=4                                               00100403
C                                                                        00100404
      RETURN                                                             00100405
      END                                                                00100406
C                                                                        00100408
C THIS FUNCTION COMPUTES THE COEFFICIENTS AND SUM OF                     00100409
C     THE TRUNCATED SERIS EXPANSION USED TO REPRESENT                    00100410
C     THE DAMAGE INTERGRAL                                               00100411
C                                                                        00100413
      FUNCTION POLY(N,K,ALPHA,DSTAR,BETA,ITERMS)                         00100414
C                                                                        00100415
      REAL*4 N,K,GAMA(50)                                                00100416
C                                                                        00100417
C COMPUTE POLYNUMIAL COEFFICIENTS FOR SERIS EXPANSION                    00100418
C                                                                        00100419
      DO 20 I=1,ITERMS                                                   00100420
      X=1.0                                                              00100421
      CALL UNDERZ(20FF20)                                                00100422
      DO 10 J=1,I                                                        00100423
      X=X*(BETA-J+1)/J                                                   00100424
```

```
   10 CONTINUE                                                          00100425
      GAMA(I)=X*(ALPHA**I)/(I*K+1.0)                                    00100426
   20 CONTINUE                                                          00100427
      CALL UNDERZ(ZONEZ)                                                00100428
C                                                                       00100429
C SUM THE TRUNCATED SERIS                                               00100430
C                                                                       00100431
      SUM=1.0                                                           00100432
      CALL UNDERZ(ZOFFZ)                                                00100433
      DO 30 I=1,ITERMS                                                  00100434
      SUM=SUM + GAMA(I)*N**(I*K)                                        00100435
   30 CONTINUE                                                          00100436
      CALL UNDERZ(ZONEZ)                                                00100437
C                                                                       00100438
C                                                                       00100440
C COMPUTE  F(N)= DAMAGE*N*SUM - 1.0 = 0.0                               00100439
      POLY= DSTAR*N*SUM - 1.0                                           00100441
C                                                                       00100442
      RETURN                                                            00100443
      END                                                               00100444
C                                                                       00100447
C THIS FUNCTION COMPUTES THE RELAXATION RATE  K  FOR THE                00100448
C      MEAN STRESS ESTABLISHED FOR A SPECIFIC MATERIAL                  00100449
C                                                                       00100450
      FUNCTION FUNK(ET2,N)                                              00100451
      REAL*4 A(10),B(10),C(10),D(10)                                    00100452
      DATA A/.187,.187,.000889,.000889,.014444,.000889,0.0,
     *   .001667,.001667,.001667/
      DATA B/-93.3,-93.3,2.22,2.22,-3.88,2.22,0.0,15.0,15.0,15.0/
      DATA C/.0,.0,-3111.1,-3111.1,-5555.5,-3111.1,0.0,-36666.6,
     *   -36666.6,-36666.6/
C                                                                       00100457
      FUNK= A(N) + B(N)*ET2 + C(N)*ET2*ET2                              00100460
C                                                                       00100461
      IF(FUNK.GE.0.0) FUNK=0.0
C                                                                       00100463
      RETURN                                                            00100464
      END                                                               00100465
C
C THIS SUBROUTINE SOLVES FOR THE STABALIZED VALUES OF STRAIN AND STRESS AMPLITUD
C
      SUBROUTINE AMP(NEUBER,S,EAMP,K,N,E)
C
      REAL*4 N,K,NEUBER
      A=1.0/E
      B=(1.0/N + 1.0)*(1.0/K)**(1.0/N)
      S=SQRT(NEUBER*E)
   10 CONTINUE
      F=4.0*A*S*S + 4.0*S*(S/K)**(1.0/N) - NEUBER
      FP=  8.0*A*S + 4.0*B*S**(1.0/N)
      S=S -F/FP
      IF(ABS(F).LE. 1.0E-06) GO TO 20
      GO TO 10
   20 EAMP= S/E +(S/K)**(1.0/N)
      RETURN
      END
```